A GRAVITY STUDY OF BIG HAND AND COLUMBUS-NIAGARAN REEF FIELDS IN ST. CLAIR COUNTY, MICHIGAN

Thesis for the Degree of M. S.

MICHIGAN STATE UNIVERSITY

WARREN E. KEITH

1967

ABSTRACT

A GRAVITY STUDY OF BIG HAND AND COLUMBUS-NIAGARAN REEF FIELDS IN ST. CLAIR COUNTY, MICHIGAN

By Warren E. Keith

The gravity method is one of the principal exploration techniques utilized in the search for petroleum reservoirs associated with Niagaran reef structures in southeastern Michigan. However, not all reef structures have obvious gravity anomalies. The Big Hand oil and Columbus gas fields, which are separated by only two miles are an excellent illustration of two nearby reef structures which appear to give different gravitational results.

A gravitational study of these two reefs shows that the Columbus reef has an associated +0.27 mgal anomaly, while no anomaly is correlated with the Big Hand reef. Theoretical gravity anomalies computed from geological information indicate the gravity anomaly associated with the Big Hand reef is cancelled out by a negative anomaly originating from a structure in the overlying F-salt. These calculations also show that structural relief on the A-2 carbonate and the A-1 carbonate and reef body contrasting with the A-2 salt accounts for the major portion of the gravity anomalies associated with the reefs.

A GRAVITY STUDY OF BIG HAND AND COLUMBUS-NIAGARAN REEF FIELDS IN ST. CLAIR COUNTY, MICHIGAN

By

Warren E. Keith

A THESIS

Submitted to
Michigan State University
in partial fulfillment of the requirements
for the degree of

MASTER OF SCIENCE

Department of Geology

1967

ACKNOWLEDGMENTS

The author wishes to sincerely thank Dr. William J. Hinze for his invaluable guidance and genuine interest during the preparation of this study. Acknowledgment is also made to Dr. H. F. Bennett and Chairman C. E. Prouty for their suggestions and helpful criticism pertaining to this study.

Thanks is also expressed to the Department of Geology, Michigan State University, for the use of their World Wide gravimeter and to Michigan State University for the use of the CDC 3600 computer.

TABLE OF CONTENTS

LIST OF TABLES

LIST OF FIGURES

LIST OF APPENDICES

CHAPTER I

INTRODUCTION

Purpose of Study

The purpose of this investigation is to determine the applicability and geological significance of the gravity method in the study of the Columbus gas and the Big Hand oil pool.

The Columbus and Big Hand fields produce from Niagaran reef structures. Many similar reef structures in southeastern Michigan have been found by the gravity method. However, the Big Hand reef does not exhibit an obvious gravity anomaly and therefore was not found by the gravity method. The primary objective was to determine if the gravity method could have been used to detect the presence of this reef.

The Columbus gas field has a well-defined gravity anomaly associated with it. The main purpose of studying and defining this anomaly is to compare it with the nearby Big Hand reef.

A geological study of the reef structures was made and calculations were performed to determine the gravity effect of these structures. The objective of this portion of the study was to delineate the geological factors which produce or negate an observable gravity anomaly.

Location of Area

The area of investigation lies entirely in T5N, R15 and 16E. This places it in the political townships of Columbus and St. Clair, St. Clair County, Michigan. The location of the study area is indicated in Figure 1.

Physiography of Area

The area of investigation is extremely flat lying. Only in the vicinity of the Belle River and Rattle Run stream channels is there appreciable topographic relief and there it is limited to approximately 50 feet. There is, however, a gradual increase in elevation from 635 feet above sea level in the southeast to 740 feet in the northwest.

The area lies in the Erie-Huron Lowland and is covered with glacial drift which varies in thickness from 120 to 210 feet. The drift has been described as composed of glacial lake clay and lake bed sand.

Rich topsoil has developed in the glacial drift. This topsoil and level topography make the area very suitable for farming. As a result, predominately agricultural communities have developed in this region.

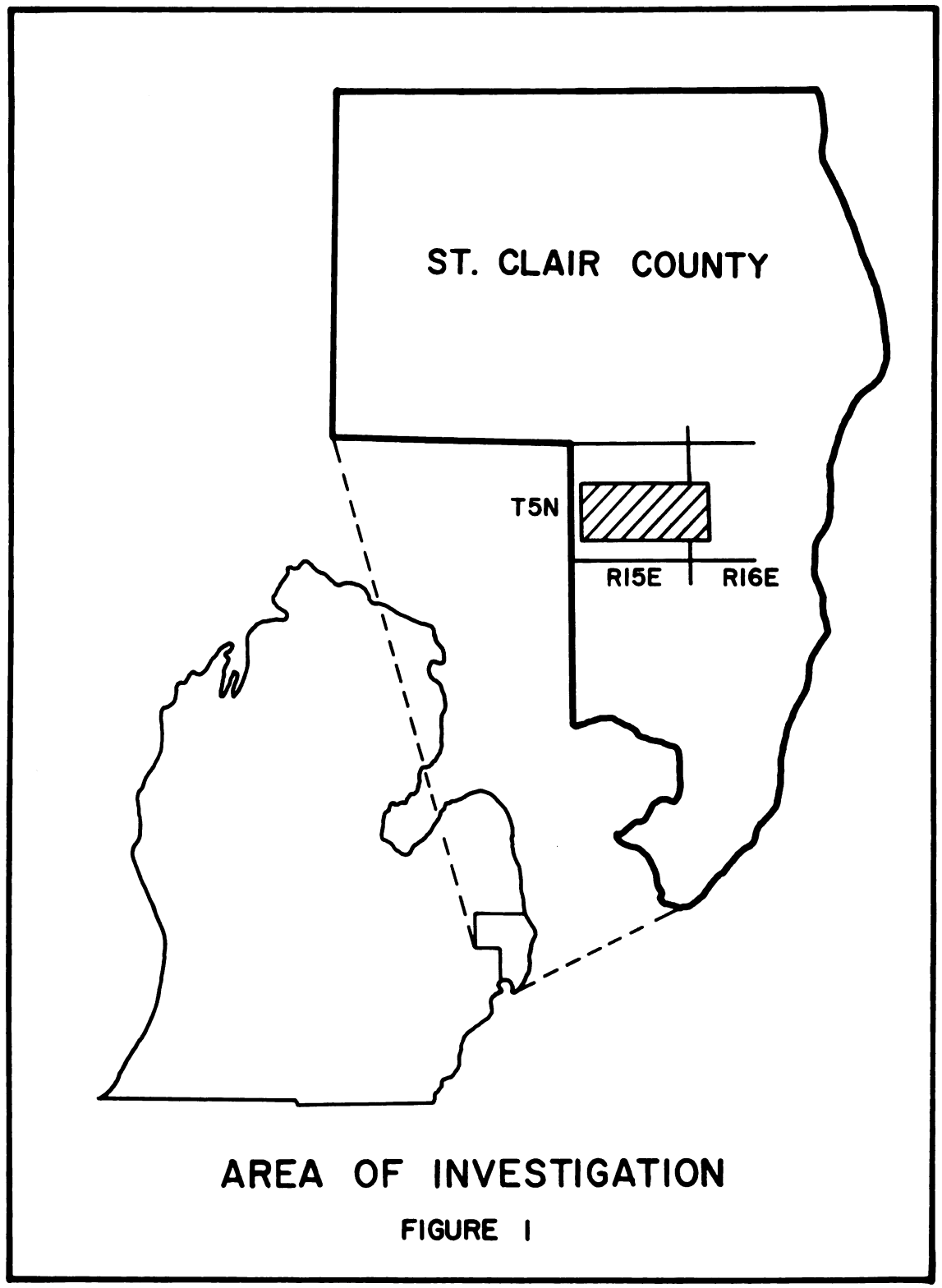

AREA OF INVESTIGATION

FIGURE 1

CHAPTER II

GEOLOGY

Regional Geology of Michigan Basin

The Michigan Basin underlies the entire southern Peninsula and the eastern part of the northern Peninsula of Michigan. It also extends into the portions of Ontario bordering on Lake Huron, Lake St. Clair, and Lake Erie, as well as the northwestern part of Ohio, northern Indiana, northeastern Illinois, and eastern Wisconsin.

The Michigan Basin has been structurally described as an intracratonic, sedimentary basin. The rocks subcrop beneath the Pleistocene glacial drift in a roughly circular pattern, centered in the southern Peninsula of Michigan. Proceeding from the rim to the center of the Basin, the rocks become younger and generally thicker.

The Basin is rimmed by tectonically positive features. Figure 2 illustrates the location of these features. On the north, northeast and northwest, the crystalline Precambrian rocks of the craton form the outer limits of the Basin. The southern boundary is formed by the two prongs of the bifurcated Cincinnati Arch, the prong to the northeast is the Findlay Arch and the northwest prong is the Kankakee Arch. The Algonquin Arch, which is an extension of the Findlay Arch,

forms the eastern border of the Michigan Basin and the Wisconsin Arch is the western limit.

In Cambrian time the Michigan Basin was low relative to the Canadian Shield to the north and the Wisconsin Arch to the west. An isopach map (Cohee in U.S.G.S. Prelim., Chart 33) of the Cambrian and the Canadian series (early Ordovician) shows a general thickening in the southern Peninsula of Michigan, but the greatest thickness occurs in northeastern Illinois. Thus, it appears that Michigan was part of a much larger basin. Thinning of the Paleozoic sediments in Ontario indicates that the Algonquin Arch also was present at this time.

Wide spread structural changes, evidenced in a major erosional unconformity, occurred at the end of Canadian time. The Findlay and Kankakee Arches may have developed as a result of these changes. However, an isopach map of the upper Ordovician rocks does not indicate the exist of these Arches.

During the Silurian period the Basin continued to develop. However, the rocks of the early and middle Silurian period are thickest around the edge of the Basin and become thinner toward the center of the Basin. Some geologists have interpreted this as evidence of a positive feature in the center of the Basin. Other feel it is simply a case of nondeposition because of a lack of sediments.

During Salina (late Silurian) time the Michigan Basin began to subside rapidly. The area of greatest subsidence coinciding with the present center of the Basin. By this time, the Basin had become very restricted. As a result, great thicknesses of evaporites were deposited, as much as 2500 feet in the center of the Basin.

During the Devonian, the Basin continued to subside. The center of greatest subsidence shifted eastward from where it had been in the late Silurian.

Throughout the Mississippian and Pensylvannian periods, the Michigan Basin retained the general shape that it had acquired during the late Silurian and Devonian. However, after the Devonian, there was very little subsidence and the Basin filled in with Mississippian and Pennsylvannian sediments.

The previous summary is derived from detailed discussions by Pirtle (1932), Cohee (1948), Ver Wiebe (1952), Landes (1956), and Ehlers and Kesling (1962).

Stratigraphy

General Stratigraphy of Michigan Basin

The generalized stratigraphy of the Michigan Basin is given in Figure 3. This geological column has been prepared by the Michigan Department of Conservation, Geological Survey Division.

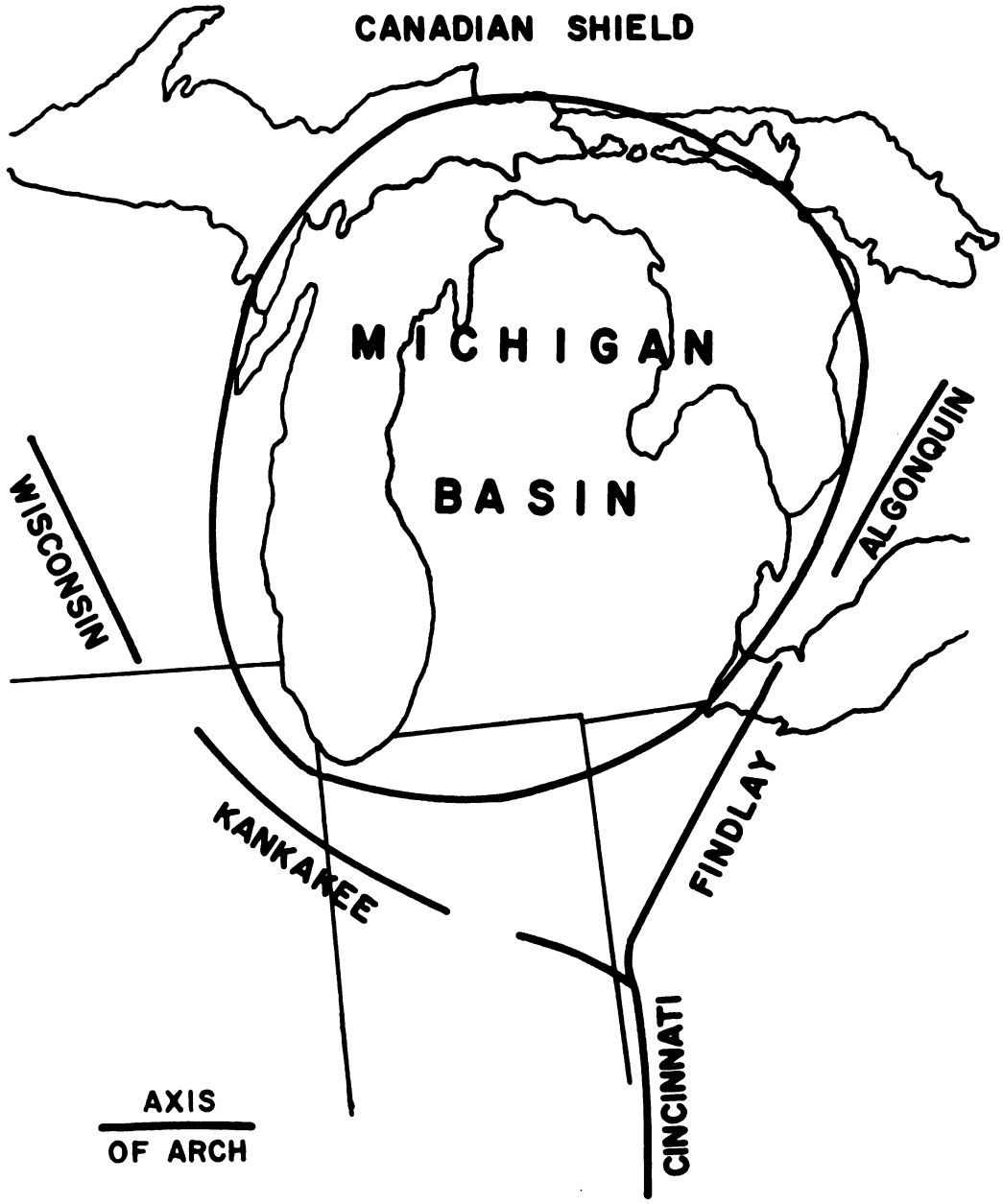

REGIONAL TECTONIC FEATURES

FIGURE 2

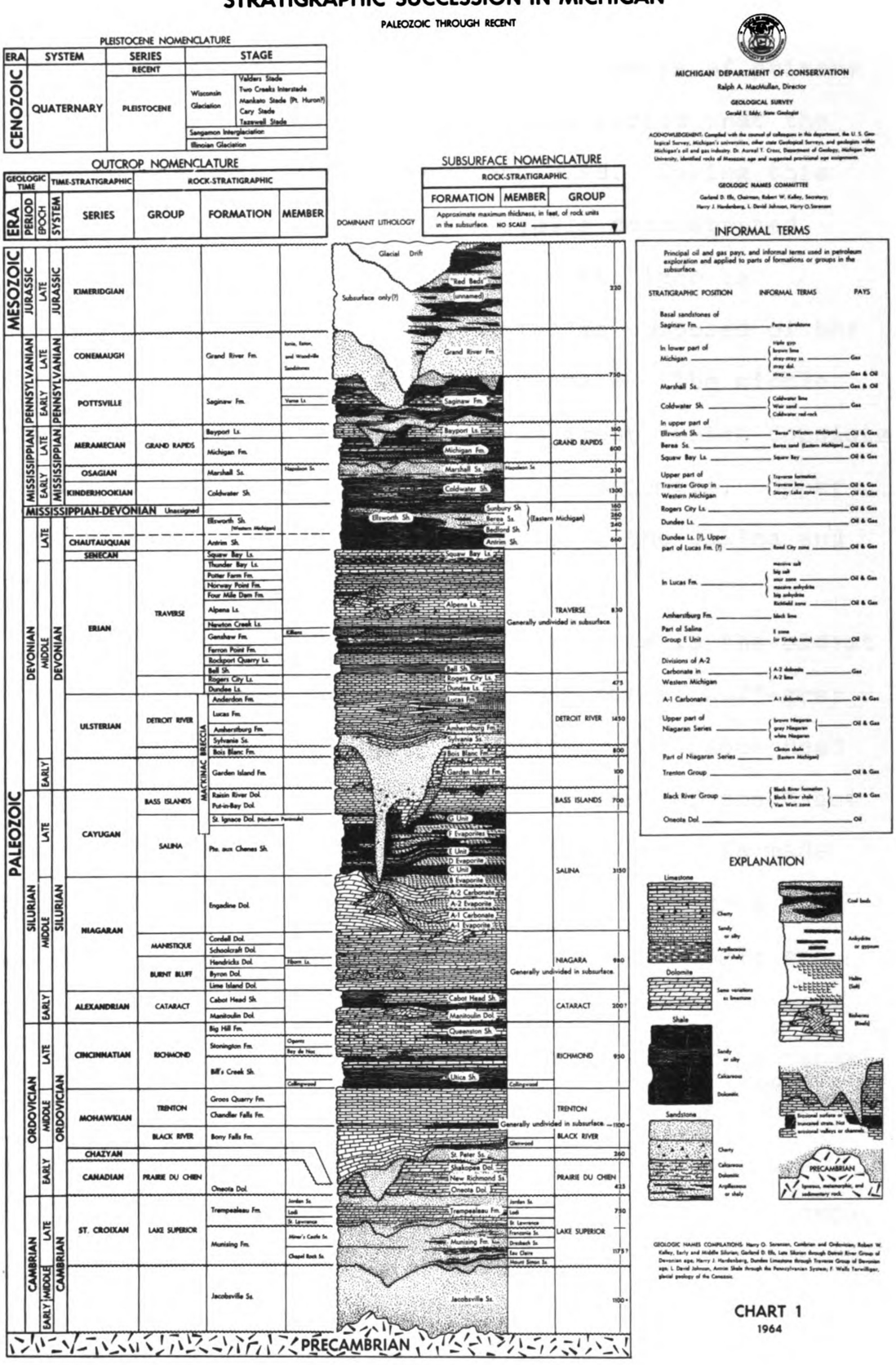
STRATIGRAPHIC SUCCESSION IN MICHIGAN
PALEOZOIC THROUGH RECENT
PLEISTOCENE NOMENCLATURE
ERA
SYSTEM
SERIES
STAGE
CENOZOIC
QUATERNARY
RECENT
PLEISTOCENE
Wisconsin Glaciation
Valders Stade
Two Creeks Interstade
Mankato Stade (Ft. Huron?)
Cary Stade
Tazewell Stade
Sangamon Interglaciation
Illinoian Glaciation
OUTCROP NOMENCLATURE
GEOLOGIC TIME
TIME-STRATIGRAPHIC
ROCK-STRATIGRAPHIC
ERA
PERIOD
EPOCH
SYSTEM
SERIES
GROUP
FORMATION
MEMBER
SUBSURFACE NOMENCLATURE
ROCK-STRATIGRAPHIC
FORMATION
MEMBER
GROUP
Approximate maximum thickness, in feet, of rock units in the subsurface. NO SCALE
DOMINANT LITHOLOGY
MESOZOIC
PALEOZOIC
JURASSIC
KIMERIDGIAN
PENNSYLVANIAN
CONEMAUGH
Grand River Fm.
POTTSVILLE
Saginaw Fm.
MISSISSIPPIAN
MERAMECIAN
GRAND RAPIDS
Bayport Ls.
Michigan Fm.
OSAGIAN
Marshall Ss.
Napoleon Ss.
KINDERHOOKIAN
Coldwater Sh.
MISSISSIPPIAN-DEVONIAN Unassigned
Ellsworth Sh. (Western Michigan)
DEVONIAN
CHAUTAUQUAN
Antrim Sh.
SENECAN
ERIAN
TRAVERSE
Squaw Bay Ls.
Thunder Bay Ls.
Potter Farm Fm.
Norway Point Fm.
Four Mile Dam Fm.
Alpena Ls.
Newton Creek Ls.
Genshaw Fm.
Ferron Point Fm.
Rockport Quarry Ls.
Bell Sh.
Rogers City Ls.
Dundee Ls.
ULSTERIAN
DETROIT RIVER
Anderdon Fm.
Lucas Fm.
Amherstburg Fm.
Sylvania Ss.
Bois Blanc Fm.
MACKINAC BRECCIA
Garden Island Fm.
SILURIAN
BASS ISLANDS
Raisin River Dol.
Put-in-Bay Dol.
St. Ignace Dol. (Northern Peninsula)
CAYUGAN
SALINA
Pte. aux Chenes Sh.
NIAGARAN
Engadine Dol.
MANISTIQUE
Cordell Dol.
Schoolcraft Dol.
BURNT BLUFF
Hendricks Dol.
Byron Dol.
Lime Island Dol.
Thorn Ls.
ALEXANDRIAN
CATARACT
Cabot Head Sh.
Manitoulin Dol.
ORDOVICIAN
CINCINNATIAN
RICHMOND
Big Hill Fm.
Stonington Fm.
Bill's Creek Sh.
Opeongo
Bay de Noc
Collingwood
MOHAWKIAN
TRENTON
Groos Quarry Fm.
Chandler Falls Fm.
BLACK RIVER
Bony Falls Fm.
CHAZYAN
CANADIAN
PRAIRIE DU CHIEN
Oneota Dol.
CAMBRIAN
ST. CROIXAN
LAKE SUPERIOR
Trempealeau Fm.
Munising Fm.
Jordan Ss.
Lodi
St. Lawrence
Miner's Castle Ss.
Chapel Rock Ss.
Jacobsville Ss.
PRECAMBRIAN
Glacial Drift
Subsurface only(?)
"Red Beds" (unnamed)
Grand River Fm.
Saginaw Fm.
Bayport Ls.
Michigan Fm.
Marshall Ss.
Napoleon Ss.
Coldwater Sh.
Sunbury Sh.
Berea Ss.
Bedford Sh.
Antrim Sh.
(Eastern Michigan)
GRAND RAPIDS
Squaw Bay Ls.
Alpena Ls.
Generally undivided in subsurface.
TRAVERSE
Bell Sh.
Rogers City Ls.
Dundee Ls.
Lucas Fm.
Amherstburg Fm.
Sylvania Ss.
Bois Blanc Fm.
Garden Island Fm.
DETROIT RIVER
BASS ISLANDS
G Unit
F Evaporite
E Unit
D Evaporite
C Unit
B Evaporite
A-2 Carbonate
A-2 Evaporite
A-1 Carbonate
A-1 Evaporite
SALINA
Generally undivided in subsurface.
NIAGARA
Cabot Head Sh.
Manitoulin Dol.
CATARACT
Queenston Sh.
RICHMOND
Utica Sh.
Collingwood
Generally undivided in subsurface.
TRENTON
BLACK RIVER
Glenwood
St. Peter Ss.
Shakopee Dol.
New Richmond Ss.
Oneota Dol.
PRAIRIE DU CHIEN
Jordan Ss.
Lodi
St. Lawrence
Franconia Ss.
Dresbach Ss.
Eau Claire
Mount Simon Ss.
Trempealeau Fm.
Munising Fm.
LAKE SUPERIOR
Jacobsville Ss.
PRECAMBRIAN
MICHIGAN DEPARTMENT OF CONSERVATION
Ralph A. MacMullan, Director
GEOLOGICAL SURVEY
Gerald E. Eddy, State Geologist
ACKNOWLEDGEMENT. Compiled with the counsel of colleagues in this department, the U. S. Geological Survey, Michigan's universities, other state Geological Surveys, and geologists within Michigan's oil and gas industry. Dr. Aureal T. Cross, Department of Geology, Michigan State University, identified rocks of Mesozoic age and suggested provisional age assignments.
GEOLOGIC NAMES COMMITTEE
Garland D. Ells, Chairman, Robert W. Kelley, Secretary; Harry J. Hardenbergh, L. Daniel Johnson, Harry O. Sorensen
INFORMAL TERMS
Principal oil and gas pays, and informal terms used in petroleum exploration and applied to parts of formations or groups in the subsurface.
STRATIGRAPHIC POSITION
INFORMAL TERMS
PAYS
Basal sandstones of Saginaw Fm. — Parma sandstone
In lower part of Michigan — triple gas, brown lime, stray-sandy zs., stray dol., stray zs. — Gas
Marshall Ss. — Gas & Oil
Coldwater Sh. — Coldwater lime, Weir sand, Coldwater red-rock — Gas
In upper part of Ellsworth Sh. — "Berea" (Western Michigan) — Oil & Gas
Berea Ss. — Berea sand (Eastern Michigan) — Oil & Gas
Squaw Bay Ls. — Squaw Bay — Oil & Gas
Upper part of Traverse Group in Western Michigan — Traverse formation, Traverse lime, Stoney Lake zone — Oil & Gas
Rogers City Ls. — Oil & Gas
Dundee Ls. — Oil & Gas
Dundee Ls. (?), Upper part of Lucas Fm. (?) — Reed City zone — Oil & Gas
In Lucas Fm. — massive salt, big salt, stray zone, massive anhydrite, big anhydrite, Richfield zone — Oil & Gas
Amherstburg Fm. — black lime
Part of Salina Group E Unit — E zone (or Kinsigh zone) — Oil
Divisions of A-2 Carbonate in Western Michigan — A-2 dolomite, A-2 lime — Gas
A-1 Carbonate — A-1 dolomite — Oil & Gas
Upper part of Niagaran Series — brown Niagaran, gray Niagaran, white Niagaran — Oil & Gas
Part of Niagaran Series — Clinton shale (Eastern Michigan)
Trenton Group — Oil & Gas
Black River Group — Black River formation, Black River shale, Van Wert zone — Oil & Gas
Oneota Dol. — Oil
EXPLANATION
Limestone
Cherty
Sandy or silty
Argillaceous or shaly
Dolomite
Some variations as limestone
Shale
Sandy or silty
Calcareous
Dolomitic
Sandstone
Cherty
Calcareous
Dolomitic
Argillaceous or shaly
Coal beds
Anhydrite or gypsum
Halite (Salt)
Reduction (Breaks)
Basinal outline or truncated strata. Not occasional valleys or channels.
PRECAMBRIAN
Igneous, metamorphic, and sedimentary rock.
GEOLOGIC NAMES COMPILATIONS. Harry O. Sorensen, Cambrian and Ordovician; Robert W. Kelley, Early and Middle Silurian; Garland D. Ells, Late Silurian through Detroit River Group of Devonian age; Harry J. Hardenbergh, Dundee Limestone through Traverse Group of Devonian age; L. Daniel Johnson, Antrim Shale through the Pennsylvanian System; F. Wells Terwilliger, glacial geology of the Canozoic.
CHART 1
1964

FIGURE 3

Silurian Stratigraphy

The stratigraphy of the Silurian system is of primary importance to this study. It was in this period that the reef structures began, flourished, and died. During this time their influence was most dramatically demonstrated.

The lower Silurian in southeastern Michigan is represented by the Cataract group, which is composed of the Manitoulin dolomite and the Cabot Head shale. The middle Silurian is represented by the Niagaran group, which consists of the Clinton formation and the Lookport dolomite. Upper Silurian rocks are divided into two groups, the Salina and Bass Island.

Cataract Group.--The Manitoulin dolomite is the oldest Silurian formation in the Basin. It consists of buff-gray to gray, thin bedded, and cherty dolomite. The Cabot Head shale overlies the Manitoulin. The lower part of the Cabot Head is an argillaceous dolomite. The upper half is made up of interbedded green shale and thin layers of gray argillaceous dolomite, as well as layers of red shale and gypsum.

Niagaran Group.--The Clinton shale overlies the Cabot Head. It has been described as a gray to greenish-gray, dolomitic shale. The overlying Lockport and Salina have been exhaustively studied by Landes (1945) and Evans (1950). Their classification is shown in Table 1.

Table 1.--Salina and Niagaran Strata in the Subsurface of St. Clair County.

Formation	Unit	Description
Salina	G	DOLOMITE: brown, finely crystalline; shaly dolomite; some anhydrite.
	F	SALT: in thick beds separated by beds of shale, shaly dolomite, gray and buff, and brown, crystalline dolomite; anhydrite nearly always present.
	E	SHALE: with argillaceous, gray and buff dolomite.
	D	SALT: nearly pure; thin partings of buff dolomite.
	C	SHALE: gray, dolomitic.
	B	SALT: thick salt beds with thin dolomite layers.
	A-2	DOLOMITE: brown, brown gray, gray and dark gray, finely crystalline; some dark bituminous shale.
	A-2	SALT: where salt is absent the base of A-2 is marked by anhydrite.
	A-1	DOLOMITE: buff, brown, brown gray and dark gray, dense to medium crystalline; some dark bituminous shale.
	A-1	ANHYDRITE: at base.
Niagaran Group	Guelph-Lockport or Niagaran	DOLOMITE: tan, gray brown and brown, very finely to coarsely crystalline and vugular; often finel laminated near top.
		DOLOMITE: light and dark gray mottled, finely crystalline.
		DOLOMITE: light to blue gray, finely to coarsely crystallin.

Bass Island Group.--The youngest strata in the Silurian is the Bass Island group. It represents the closing phase of the evaporite cycle. It is characterized by a clean dolomite.

This summary of Silurian stratigraphy is a resume of literature published by Newcombe (1928), Landes (1945), Evans (1950), Ehlers and Kesling (1962), and Alguire (1962).

Geology of Reef Structures

Niagaran Reef Structures

During the Niagaran epoch (middle Silurian), reef structures flourished and developed into what Lowenstam (1957) has described as a reef archipelago. The Michigan Basin occupied the southwestern part of the archipelago.

The reefs within the archipelago were isolated structures with varying densities of distribution through space and time. The structures range in areal extent from a few feet to several miles, and in height from 10 feet to nearly 1000 feet. Although they existed as individual units, the reefs greatly influenced the overall environment of the Silurian sea. They acted as a large-scale sediment trap. It has been estimated that the inter-reef beds may be as much as twice the thickness of equivalent beds in reef-free areas. The reef archipelago probably acted as a barrier to circulation, which resulted in the saline conditions occurring in the Cayugan epoch.

The two reefs studied in this investigation, the Columbus and Big Hand, are part of the reef archipelago which presumably developed along the Findlay-Algonquin Arch. They were positioned in that part of the Basin which was

subsiding rapidly, as a consequence, the reefs had to grow rapidly upwards in order to remain near sea level. Thus, they developed into pinnacle reefs.

The Columbus and Big Hand reefs are typical of fully developed reef structures. A typical reef consists of two structural components--the reef core and reef flank. The reef core is a massive build up of high-purity carbonates. Genetically, the core is the growth center of the reef. It is composed of the skeletal framework of the reef builders, with the interstitial spaces of the framework filled with bioclastic detritus of the niche dwellers and some terrigenous clastics (Lowenstam, 1957).

The reef flank borders the reef core and dips away from it at varying angles. The reef flank is genetically made up of reef-building organisms, coarse to clay-size and intertonguing inter-reef deposits. The reef flank, in contrast to the reef core, is well stratified.

This, then, is the setting and development of the reefs structures which were studied in this investigation.

Geology of Columbus and Big Hand Reef

Structure contour and isopach maps of selected formations have been prepared in this study. The formations which were structure contoured are the Niagaran formation, the A-1 carbonate unit, the A-2 carbonate unit, the B- salt unit, the C unit, the F- salt unit, the Dundee formation

and the Traverse lime formation. The structure contour maps are presented in Figures 4 through 11 in ascending order according to age and stratigraphic position. They are presented in this order to show the decreasing influence of the reefs structure on the subsequent formations.

Isopach maps have been prepared for the A-1 anhydrite and the A-2 evaporite to show the relationship between the reef structures and the lateral variations in thickness of these units.

A structure contour map of the Niagaran formation, Figure 4, shows the location and configuration of the Columbus and Big Hand reefs. The Columbus reef is centered between sections 21 and 22 of T5N, R15E, and trends approximately north-south. The base of the reef is at an elevation of -2400 feet and the highest control contour places the top of the reef at -2100 feet. Thus, the reef has a relief of at least 300 feet. The reef is approximately 0.75 miles wide and 1.5 miles in length.

The Big Hand reef, located entirely in the eastern half of section 24 of T5N, R15E, lies two miles east of Columbus. This reef is positioned 100 feet up-dip from the Columbus reef. Its lateral dimensions are only about half as large as those of the Columbus structure--the width is 0.5 miles and the length is 0.75 miles. However, it has a relief of nearly 275 feet.

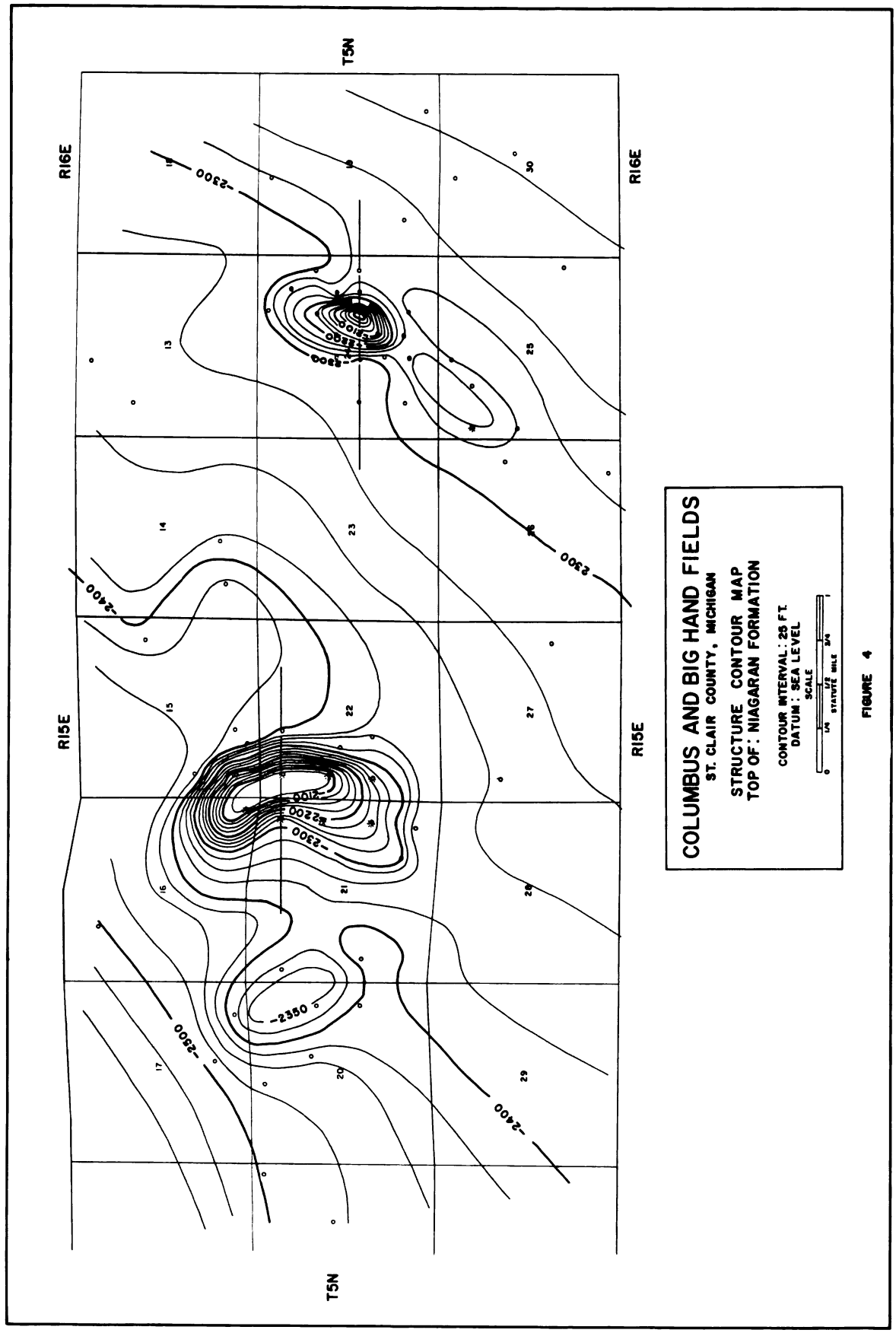
T5N
R16E
R15E
T5N
-2300
-2400
-2350
-2100
-2200
COLUMBUS AND BIG HAND FIELDS
ST. CLAIR COUNTY, MICHIGAN
STRUCTURE CONTOUR MAP
TOP OF: NIAGARAN FORMATION
CONTOUR INTERVAL: 25 FT.
DATUM: SEA LEVEL
SCALE
STATUTE MILE

FIGURE 4

Figure 5 is a structure contour map of the A-1 carbonate unit. This unit is about 100 feet above the Niagaran formation. On this unit there is still 200 feet of closure above both the Columbus and Big Hand reefs. In both cases, the configuration of the structure conforms closely with that of the reef itself.

Proceeding upward in the column, Figure 6 shows a structure contour map of the A-2 carbonate unit. At this elevation the structural influence of the reefs has decreased. However, there is still 50 feet of closure centered over the Columbus reef, with a negative closure of 25 feet to the northeast. Above the Big Hand reef there is 50 feet of positive closure and 50 feet of negative closure to the northwest of the reef. The negative features, associated with the Columbus and Big Hand reefs, may be explained by either salt flowage, or by salt solution in the A-2 evaporite which lies directly below the A-2 carbonate.

The top of the B-salt, which is about 750 feet above the Niagaran formation, has been contoured and is shown in Figure 7. There is still 10 feet of closure above both reefs at this elevation. The center of the closure, above the Columbus reef, has shifted to the south. The structure above the Big Hand reef has extended in length, but it is still positioned above the reef.

Figure 8 is a structure contour map of the C-unit. There is 10 feet of closure above the Columbus reef. The -1450 foot contour line nearly closes above the Big Hand reef.

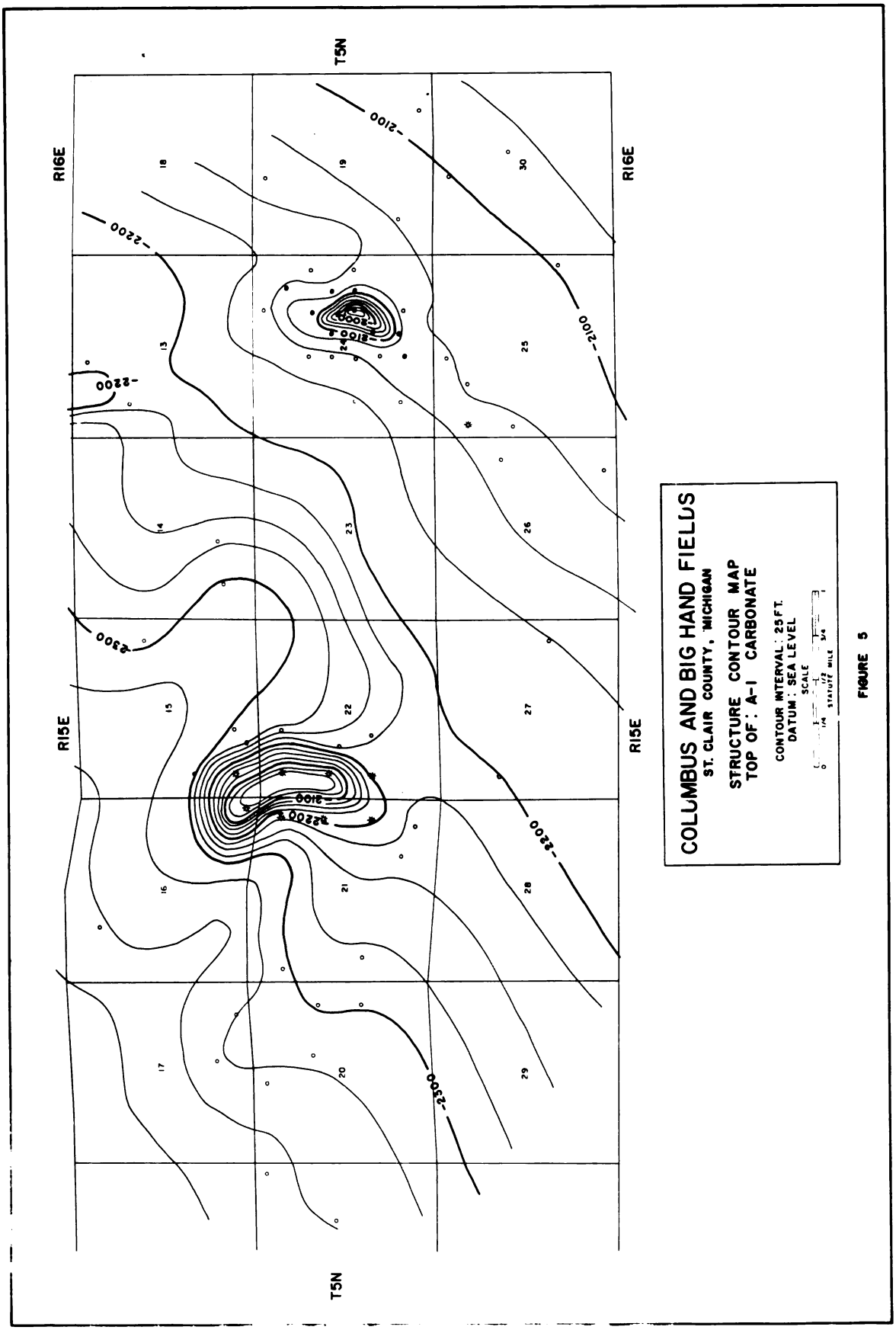
T5N
R16E
R15E
T5N
R16E
R15E
-2200
-2100
-2300
-2400
-2500
-2600
-2700
-2800
-2900
-3000
-3100
-3200
COLUMBUS AND BIG HAND FIELDS
ST. CLAIR COUNTY, MICHIGAN
STRUCTURE CONTOUR MAP
TOP OF: A-1 CARBONATE
CONTOUR INTERVAL: 25 FT.
DATUM: SEA LEVEL
SCALE
STATUTE MILE

FIGURE 5

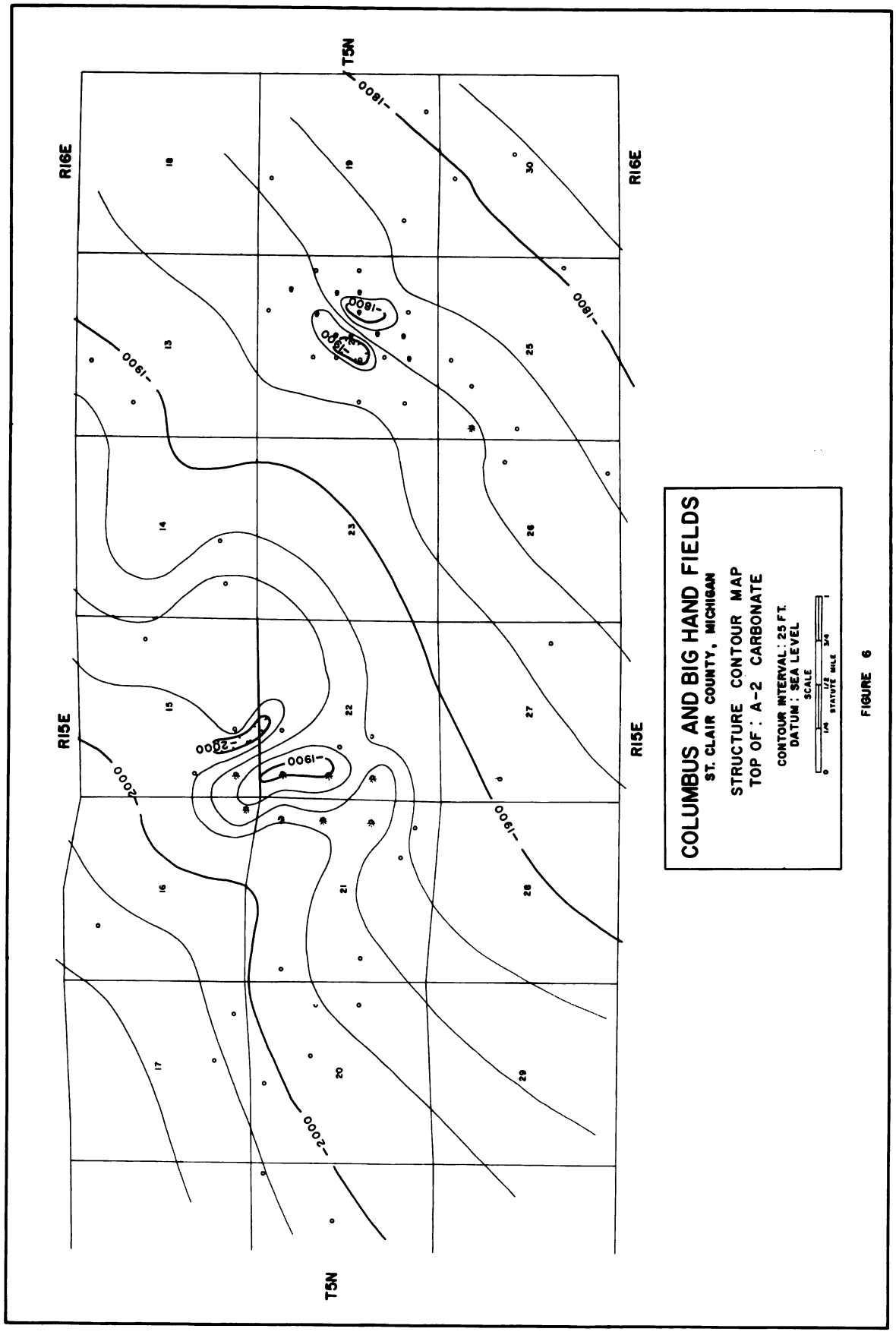
T5N
R16E
R15E
T4N
-1800
-1900
-2000
COLUMBUS AND BIG HAND FIELDS
ST. CLAIR COUNTY, MICHIGAN
STRUCTURE CONTOUR MAP
TOP OF : A-2 CARBONATE
CONTOUR INTERVAL: 25 FT.
DATUM : SEA LEVEL
SCALE
0
1/4
1/2
3/4
1
STATUTE MILE

FIGURE 6

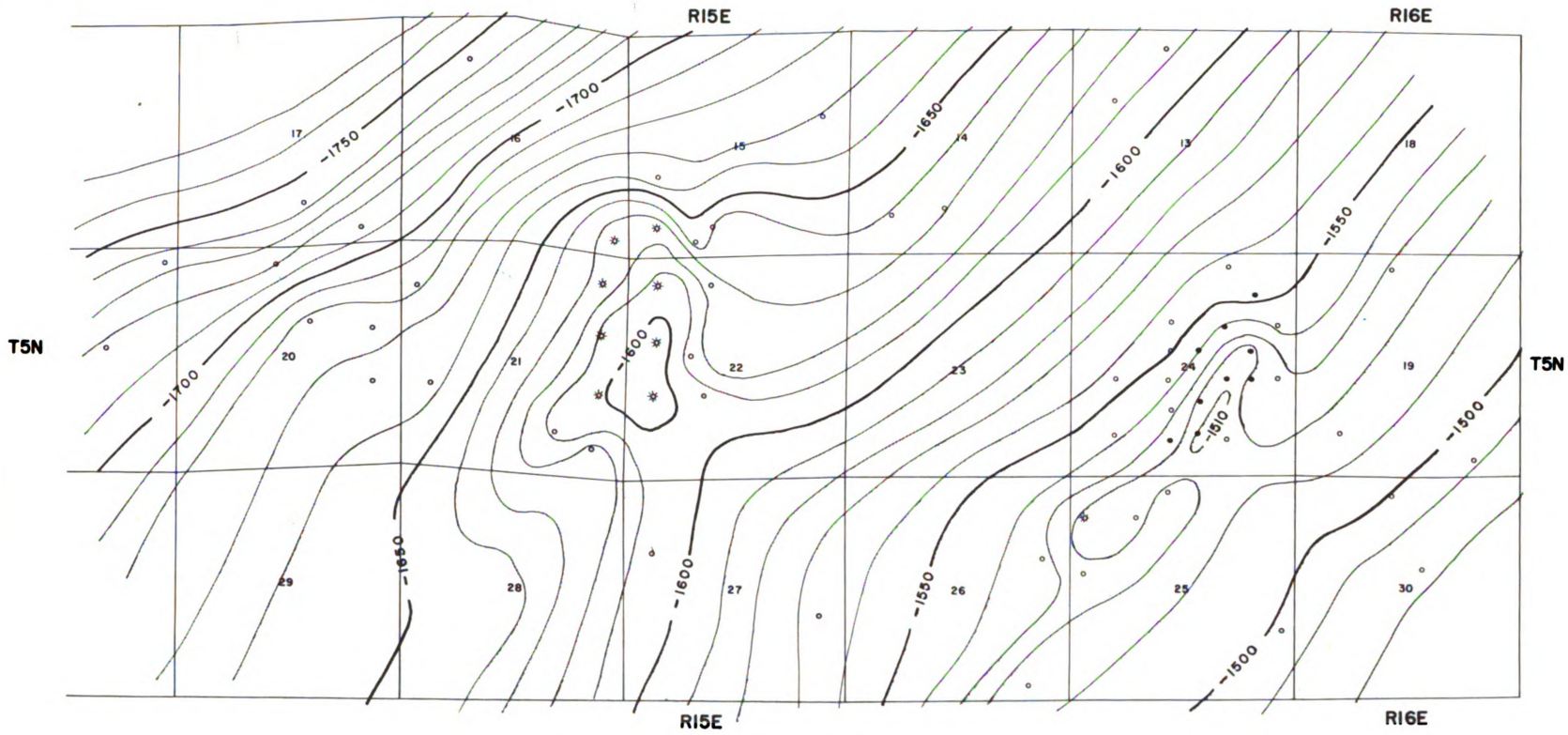

COLUMBUS AND BIG HAND FIELDS

ST. CLAIR COUNTY, MICHIGAN

STRUCTURE CONTOUR MAP
TOP OF : B-SALT UNIT

CONTOUR INTERVAL : 10 FT.
DATUM : SEA LEVEL

SCALE

0 1/4 1/2 3/4 1
STATUTE MILE

FIGURE 7

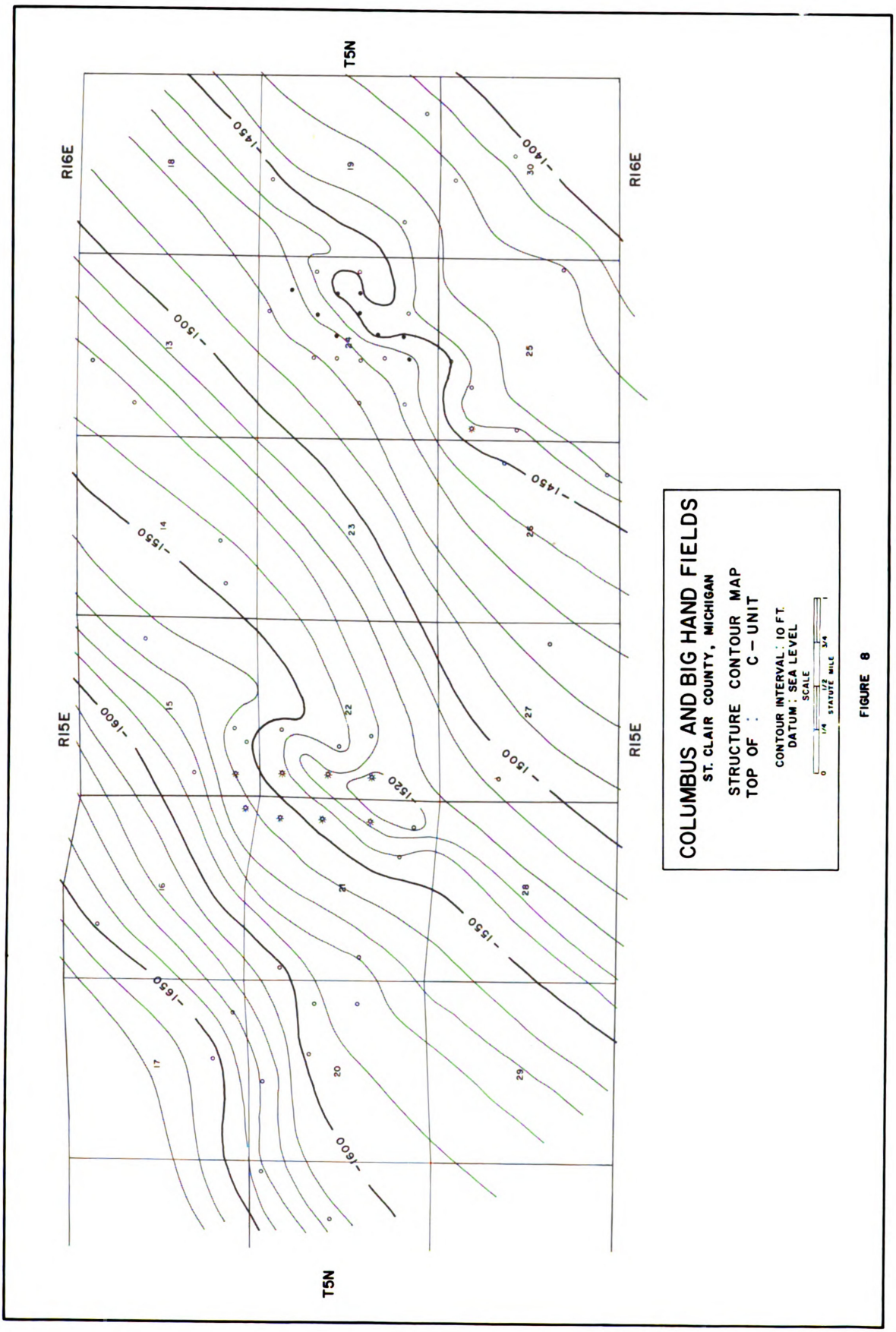
T5N
R16E
R15E
T5N
-1450
-1500
-1550
-1600
-1650
-1400
-1520
-1500
-1450
-1550
-1600
-1500
-1550
-1600
COLUMBUS AND BIG HAND FIELDS
ST. CLAIR COUNTY, MICHIGAN
STRUCTURE CONTOUR MAP
TOP OF : C – UNIT
CONTOUR INTERVAL : 10 FT.
DATUM : SEA LEVEL
SCALE
0
1/4
1/2
3/4
STATUTE MILE

FIGURE 8

Figure 9 shows the structure on top of the F-salt unit. This formation is approximately 1300 feet above the Niagaran surface. As illustrated in this figure, there is no structural reflection associated with the Columbus reef. However, there is a large structural high, with 40 feet of closure, located to the south southwest of the Big Hand reef. This structure is too large, both in areal extent and relief, to be directly related to the reef structure. Salt flowage may be the explanation of this structure, but in order to develop such a large structure due to salt flowage, it seems necessary to postulate a fracture zone in this area. The fracture zone could have provided an avenue into which the salt migrated. There are other possible explanations for the development of this positive structural feature. Uniform deposition of the salt and subsequent removal of the salt from adjacent areas by solution may be one explanation. Another posibility is that local conditions near the reef structure were such that more salt was deposited originally. This structure could be instrumental in explaining the gravity picture associated with the Big Hand reef.

Figure 10 and 11 are structure contour maps on the Dundee lime and the Traverse lime. There are no apparent structures, either on the Dundee or the Traverse maps which are associated with the Columbus reef. The structure maps on the Traverse and Dundee above the Big Hand reef show 10 feet of negative closure to the northwest of the reef

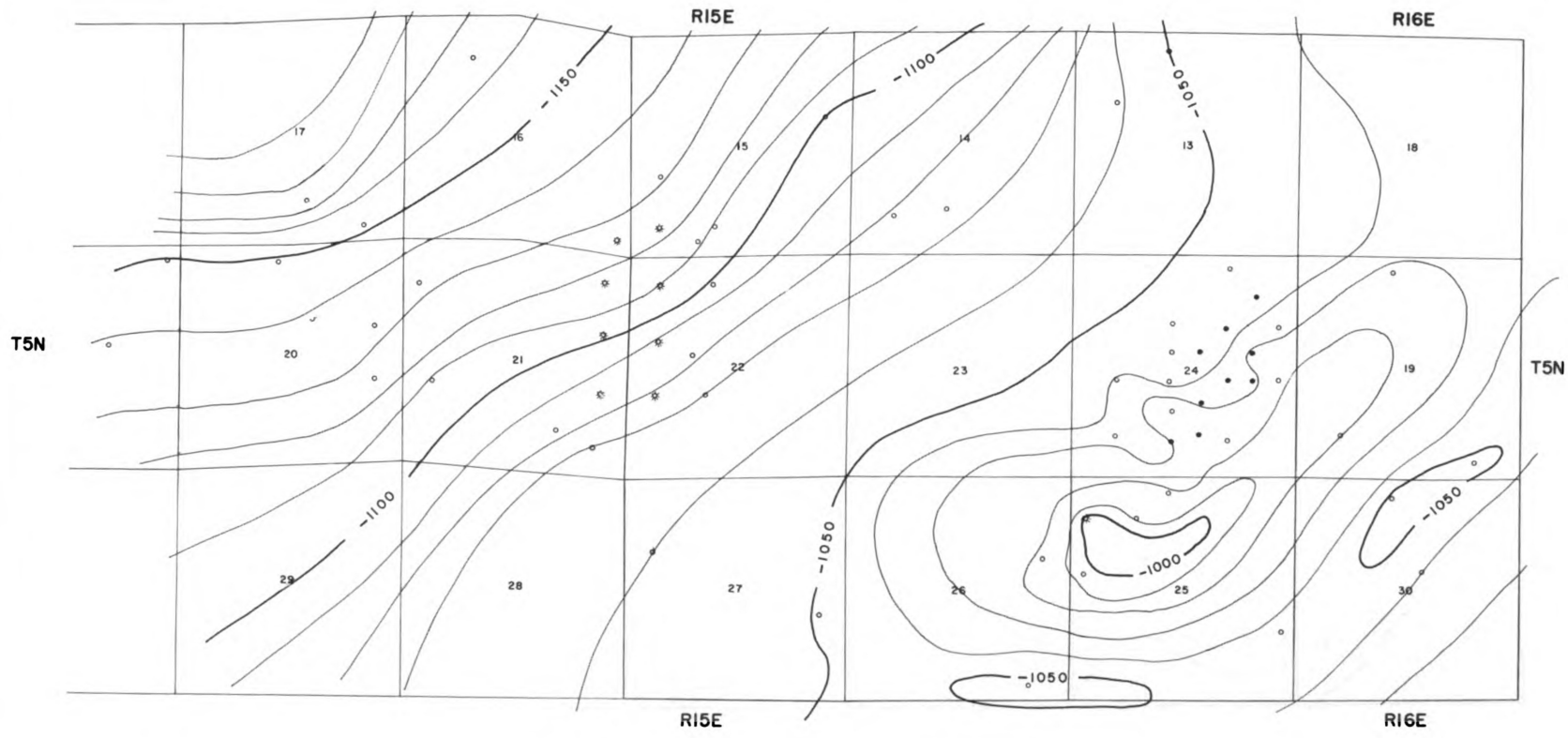

COLUMBUS AND BIG HAND FIELDS

ST. CLAIR COUNTY, MICHIGAN

STRUCTURE CONTOUR MAP
TOP OF : F-SALT UNIT

CONTOUR INTERVAL : 10 FT.
DATUM : SEA LEVEL

SCALE

0 1/4 1/2 3/4 1
STATUTE MILE

FIGURE 9

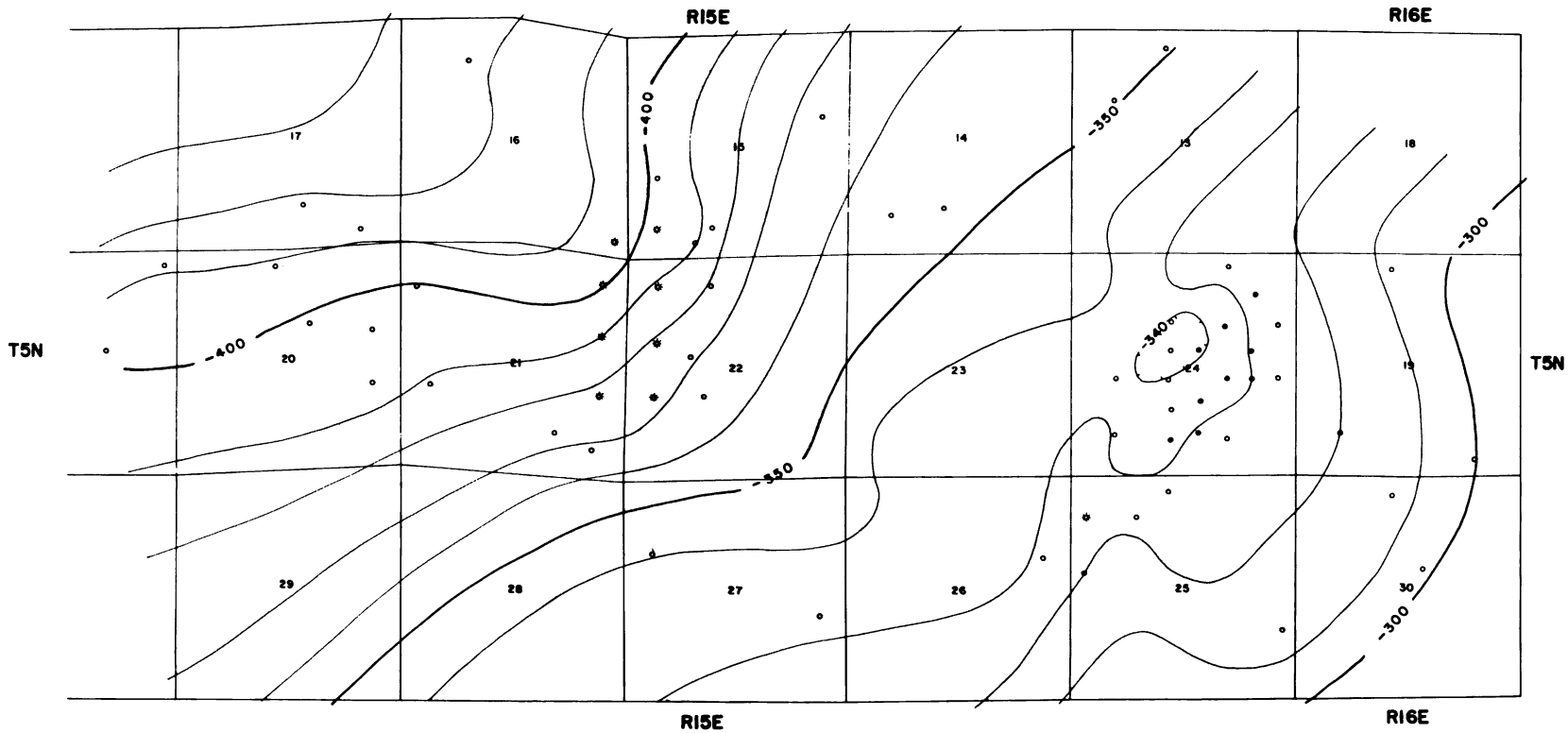

COLUMBUS AND BIG HAND FIELDS

ST. CLAIR COUNTY, MICHIGAN

STRUCTURE CONTOUR MAP
TOP OF : DUNDEE LIME

CONTOUR INTERVAL : 10 FT.
DATUM : SEA LEVEL

SCALE

0 1/4 1/2 3/4 1
STATUTE MILE

FIGURE 10

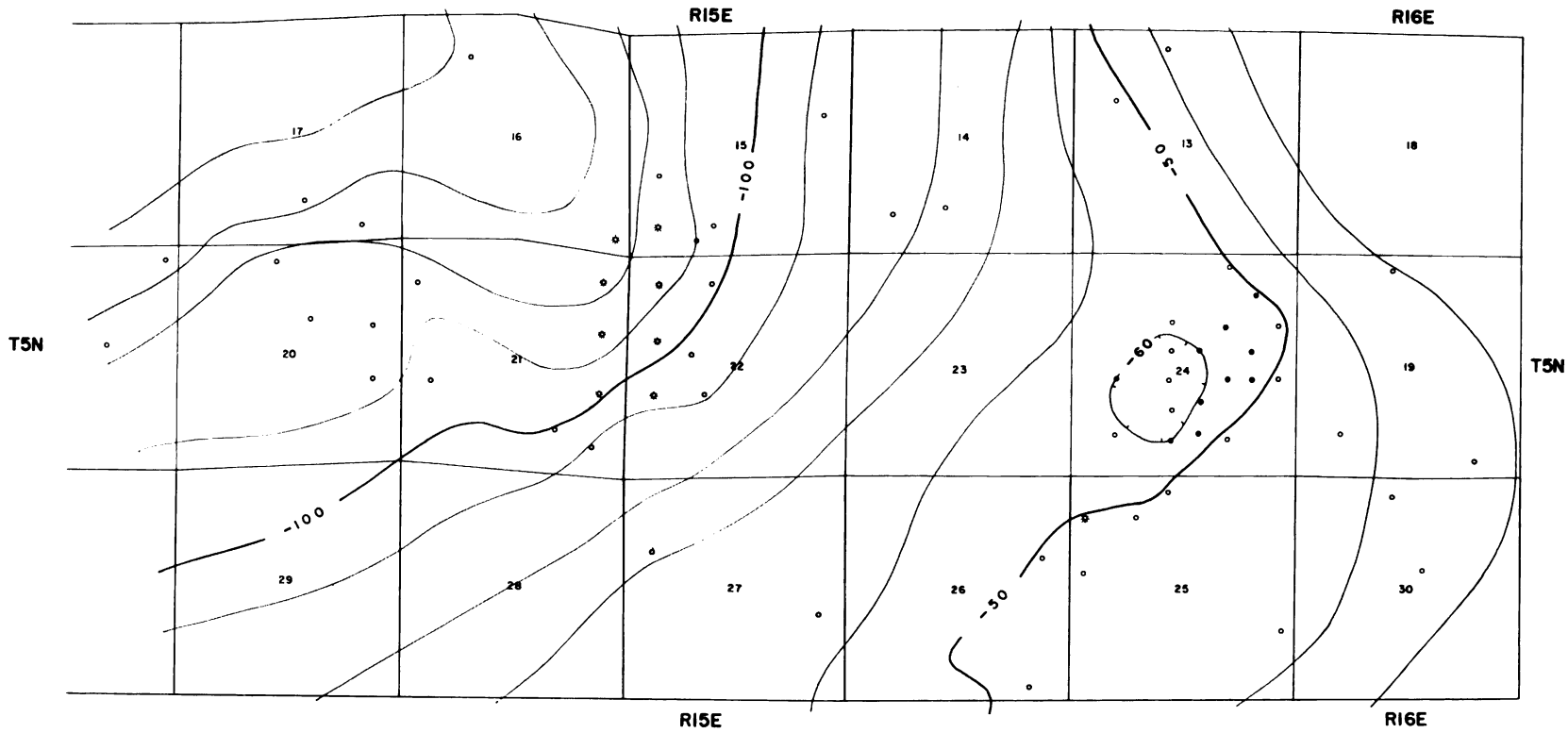

COLUMBUS AND BIG HAND FIELDS
ST. CLAIR COUNTY, MICHIGAN

STRUCTURE CONTOUR MAP
TOP OF: TRAVERSE LIME

CONTOUR INTERVAL: 10 FT.
DATUM: SEA LEVEL

SCALE
0 1/4 1/2 3/4 1
STATUTE MILE

FIGURE 11

structure. The closure on both formations is small, but the position and shape of both features are too similar to discredit them as insignificant. These structures could be the results of slumping along the postulated fracture zone which was put forth as an explanation for the structure on the F-salt unit. However, they also give supporting evidence to the other explanations of this positive feature.

Figure 12 is an isopach map of the A-1 anhydrite, which lies directly above the Niagaran formation. The A-1 anhydrite thins from 20 to zero feet as it pinches out against the reefs. This thinning is a characteristic behavior of the A-1 anhydrite.

An isopach map of the A-2 evaporite is shown in Figure 13. Over the Columbus reef, this unit thins 150 feet, while over the Big Hand reef it thins a total of 100 feet. The A-2 evaporite unit consists mostly of salt, with approximately 25 feet of anhydrite at the top of the unit. The anhydrite layer continues across the top of both reefs, but the thick salt layer wedges out against the reef flanks. Other units and formations thin over the reef structures, but because of the close stratigraphic position and plastic nature of these two units, they thin more drastically.

Figures 14 and 15 are cross-sections of the Columbus and Big Hand reefs, respectively. They illustrate the structural and stratigraphic relationship of the formations and units which were structure contoured, and isopached.

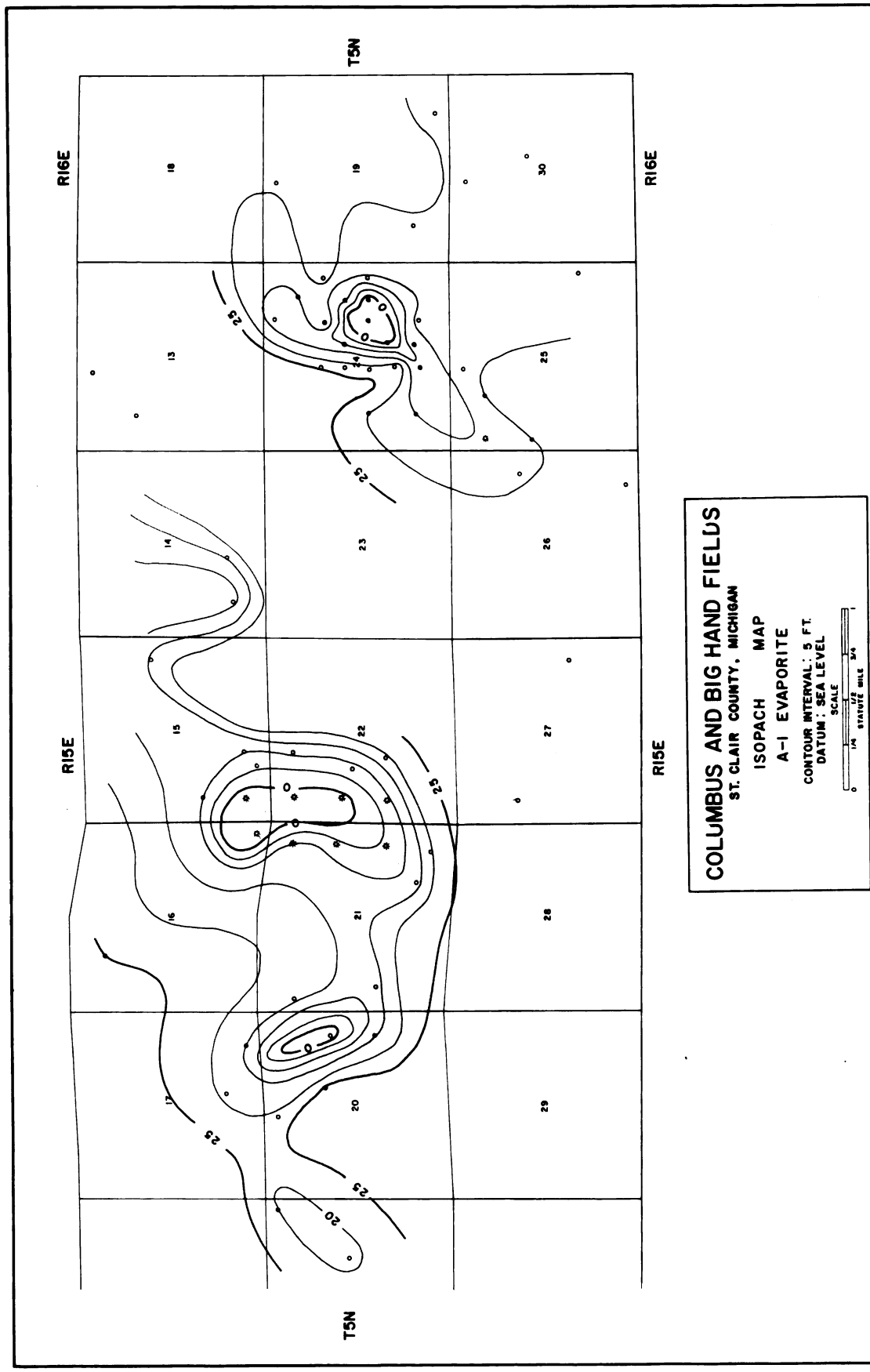
T5N
R16E
R15E
T5N
COLUMBUS AND BIG HAND FIELDS
ST. CLAIR COUNTY, MICHIGAN
ISOPACH MAP
A-1 EVAPORITE
CONTOUR INTERVAL: 5 FT.
DATUM: SEA LEVEL
SCALE
0
1/4
1/2
STATUTE MILE
3/4
1
25
25
25
20

FIGURE 12

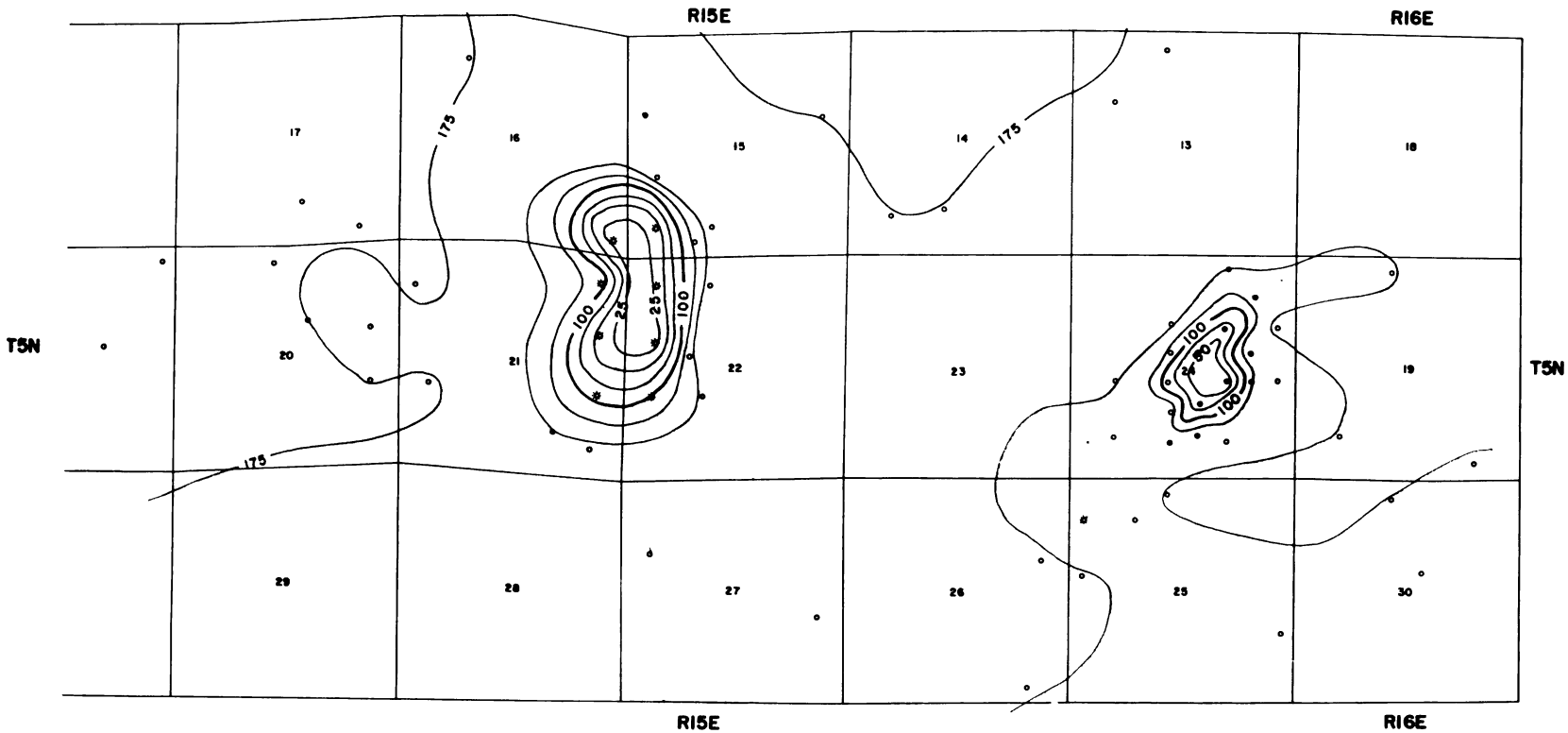

COLUMBUS AND BIG HAND FIELDS

ST. CLAIR COUNTY, MICHIGAN

ISOPACH MAP

A-2 EVAPORITE

CONTOUR INTERVAL: 25 FT.
DATUM: SEA LEVEL

SCALE

0 1/4 1/2 3/4 1
STATUTE MILE

FIGURE 13

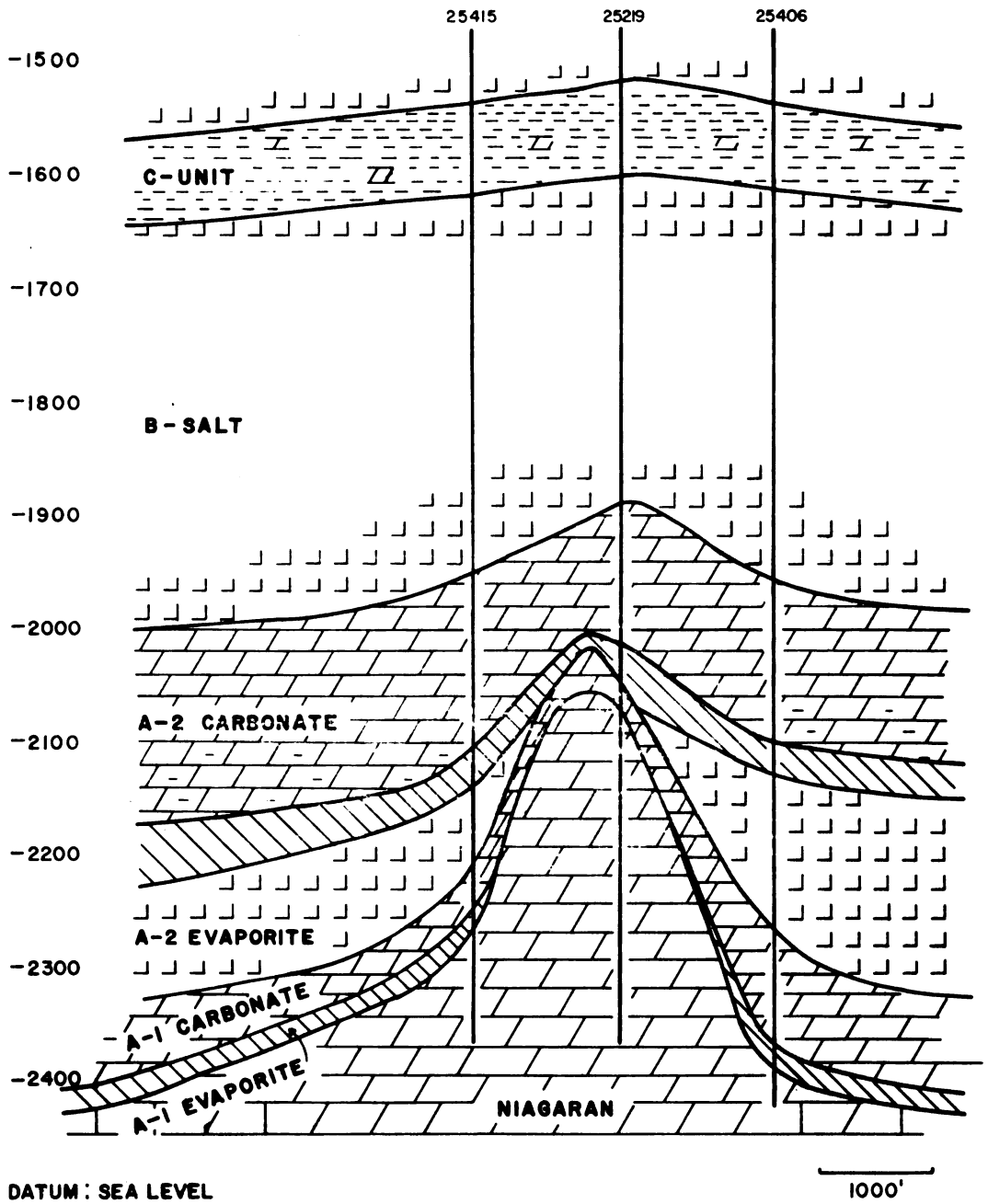

GEOLOGIC CROSS-SECTION

COLUMBUS REEF

FIGURE 14

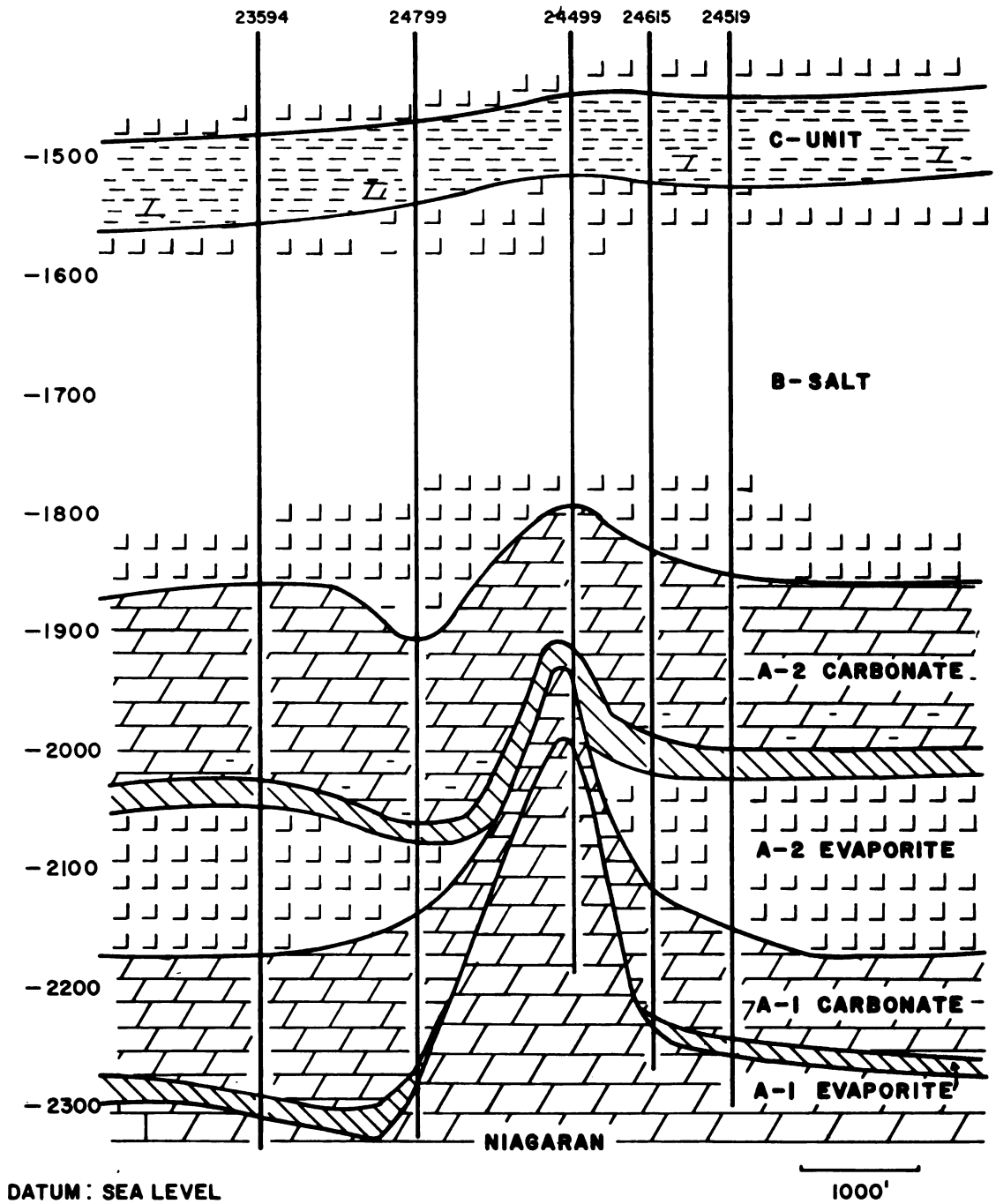

GEOLOGIC CROSS-SECTION

BIG HAND REEF

FIGURE 15

Figure 16 demonstrates the relationship of the F-salt structure to the Big Hand reef structure. The location of the profiles are shown on the structure contour of the Niagaran formation, Figure 4.

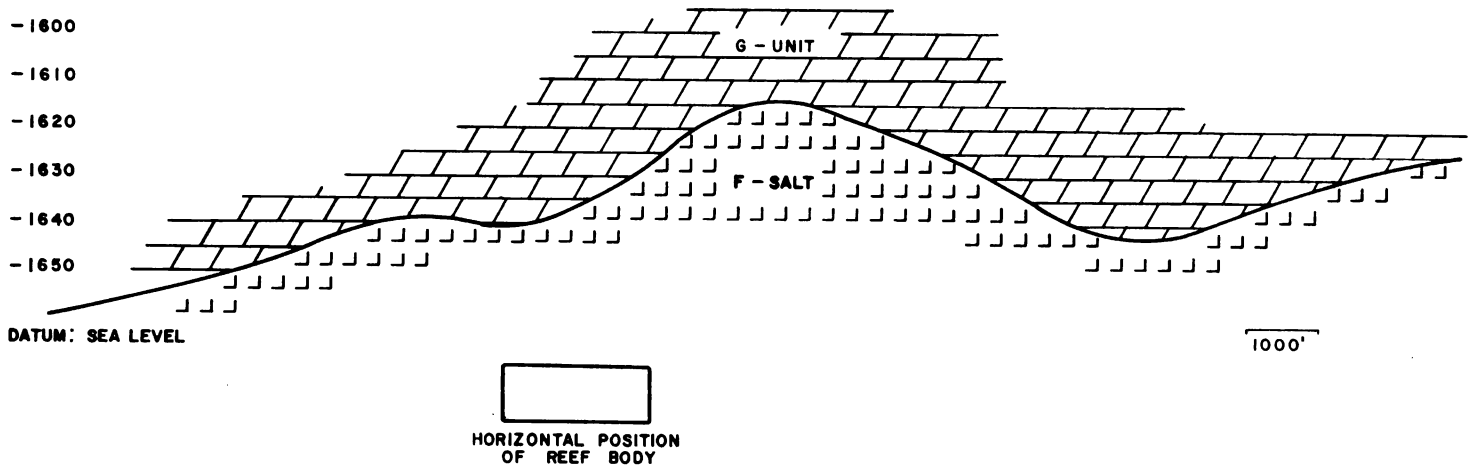

RELATIONSHIP OF F-SALT STRUCTURE TO BIG HAND REEF

FIGURE 16

CHAPTER III

GRAVITY STUDY

History of Reef Studies by the Gravity Method

The gravity method has been widely used in the exploration for reef structures of varying ages. It has met with success in many areas, but fundamental questions regarding the application of the method and the geological significance of the gravity anomalies still remain unanswered. Therefore, a review of pertinent previous studies is necessary for a discussion of the results and conclusions of this investigation.

Yungul (1961) reviewed the existing literature on gravity investigations of reef structures and summarized the predominant thoughts which were derived from these studies. His summary is as follows:

1. Reefs frequently show recognizable gravity anomalies which may be (a) a simple high, (b) a high with a negative rim around it, (c) a low with a positive tendency in the center, or (d) a simple low. Most frequently it is a high with a negative rim around it, like a 'sombreo.'

2. When the anomaly is of the sombrero type or a simple high, its intensity is of the order of +0.5 mg. This is greater than an allowable density contrast between the reef mass and the enclosing sediments could produce. What is more, a gravity high may be present even when the reef density is less than that of the enclosing sediments. Clayton (1951) reports

that at North Snyder the cores show the reef is less dense than the surrounding shales. Yet, the anomaly is +0.6 mg.

3. The existence of a negative rim has so far not been satisfactorily explained.

4. The gravity highs are too narrow to be generated by masses at specified reef depths.

5. When the anomaly is of the sombrero type, the width of the positive is of the order of the width of the reef, irrespective of the reef depth.

6. The local (residual) anomalies are frequently located near the apexes of regional gravity highs.

7. As far as west Texas is concerned, the reef bottoms are local positive reliefs. We have no such data for the other regions.

8. Thinning and draping in the shales over and around the reefs are more than that indicated by conventional calculations of differential compaction.

9. Either because of certain underlying causes, or merely because of world-wide abundance of shales, the surrounding regional formations are shales in most cases.

10. The equivalent porosities in the reefs are estimated to be of the order of 12 per cent. The main constituent of most reefs is calcium carbonate. Consequently, the density is about 2.5.

11. The reef heights are from about one hundred to about eight hundred feet, widths 1/2 to 3 miles, and the known depths 2,000 to 7,000 ft. The slopes on the flanks may be up to 40 degrees.

12. In view of the wide ranges of the observed reef geometries and anomaly types, it seems, at present, that there is no direct, evident relation between the reef mass specifications (depth, height, extent, density) and the gravity anomaly specifications (type, intensity, extent). Consequently, certain factors other than the reef mass play the major role.

Yungul then tried to explain the prevailing facts concerning observed gravity anomalies associated with reef structures. Of course, a density contrast must exist in order for a gravity anomaly to be produced. Any approach to explaining gravity anomalies must be directed toward explaining the existing density contrast and determining how these contrast were created. Yungul believed that the reef structures greatly influenced the sedimentary environment. This influence resulted in high concentrations of sand vertically above the reef bodies as opposed to lower concentrations in the off-reef facies. This then created the existing density contrast. He concludes:

1. Reefs of the isolated type frequently show positive gravity anomalies in the order of 0.5 mg, with a true negative rim around it and the zero anomaly contour is usually close to the reef outline.

2. No evident direct relation between reef specifications and gravity anomaly specifications can be expected.

3. The main contribution of the reef to the anomaly is not the mass of the reef itself, but it is the influence of the reef on subsequent geological processes.

4. The anomaly depends largely on what has happened after the reef was covered, and to some extent on the lithology of pre-reef formations.

5. The major cause of the gravity anomaly is probably the lateral variations of sand content in shales around and above the reef.

Two gravity case histories, one by Pohly (1954) of the Dawn No. 156 Pool in southwestern Ontario and one by Servos (1965) of the Marine City, Berlin and Belle River Mills fields, are of particular interest to this investigation. They are in the same geological province and general area as the Columbus and Big Hand reef structures.

Pohly concludes:

1. Reefs can be detected because of their shallow depth of burial and the sharp density contrast between salt and reef limestone.

2. Gravity anomalies can be caused by local thinning of salt and by local concentrations of dense gravels or boulders in the glacial drift. These gravity anomalies can be confused with anomalies caused by reef structures.

Servos summarizes his findings as follows:

1. The gravity anomalies over reefs are positive with magnitudes of about +0.20 mg.

2. The width of the isolated anomalies varied with the isolation method. The anomalies isolated by the least squares method are about twice as wide as the reef mass. The downward continuation of an upward continued surface method gives a ratio of about 1.3 to 1 for the width of the anomaly to the width of the reef. The second derivative method gives a ratio from 1.3 to 1 for the 2500' upward continued surface up to 1.6 to 1 for the 5000' upward continued surface. The cross profile method on the Marine City reef gives a ratio of 2:1. The graphical and statistical methods of isolation indicate a larger anomaly width to reef width ratio than do the analytical methods. These results are consistent for the Marine City, Belle River Mills, and Berlin reefs.

3. The reef anomalies have adjacent parallel to sub-parallel negative anomalies associated with the positive anomalies. These can be accounted

for by theoretical calculation of bedrock topographic effects, however, the coincidence of the negative anomalies indicate they are not fortuitous but may be controlled by structure in the sediments or they are coming from a deeper source.

4. The reef anomalies are not associated with any regional gravity pattern.

5. The source of the anomalies observed over reefs in the Michigan Basin are not the reef mass, but the conditions created after reef development. The probable source of the anomalies is the lateral variation in density overlying the reef. In the Michigan Basin these density contrasts are between dolomite and limestone and dolomite and salt.

All of the studies thus far conducted, generally conclude that there is a gravity anomaly associated with carbonaceous reef structures. There is, however, disagreement as to the exact cause of the anomalies and the relationship of the reef structures to the observed anomaly. Indeed, some disagreement should be expected for the geological factors are not the same in all cases.

Gravity Maps

Now that the geological setting of the Columbus and Big Hand reef structures has been established and previous reef studies have been discussed, the observed and residual gravity maps which are presented in this section will have more meaning and geological significance.

Various isolation techniques have been used to determine if some methods would give better results and also to observe if changes in the characteristics of the anomalies obtained

from the different techniques would give a clue to the source of the anomalies.

The field methods and reduction of data are discussed in Appendix A and B, respectively. Appendix C is devoted to the discussion of the isolation techniques utilized in this study.

The location of the Columbus and Big Hand reefs is shown on the gravity maps by the parallel line pattern. The Columbus reef is located on the west and the Big Hand reef is on the east. The small circles indicate gravity points.

Bouguer Gravity Map

The Bouger gravity map of the study area is shown in Figure 17. As can be seen from the map, there is an anomalous area in the vicinity of the Columbus reef, but there is no apparent anomaly present in the vicinity of the Big Hand reef. The regional gradient in the northwest portion is about 1.0 mgals/mile and the contours trend northwest-southeast. In the southeast portion of the area, the contours generally trend in the same direction, however, the contour lines begin to spread out. The regional gravity picture agrees with the regional map prepared by Hinze (1963). A portion of this map is shown in Figure 18 where the rectangle denotes the study area.

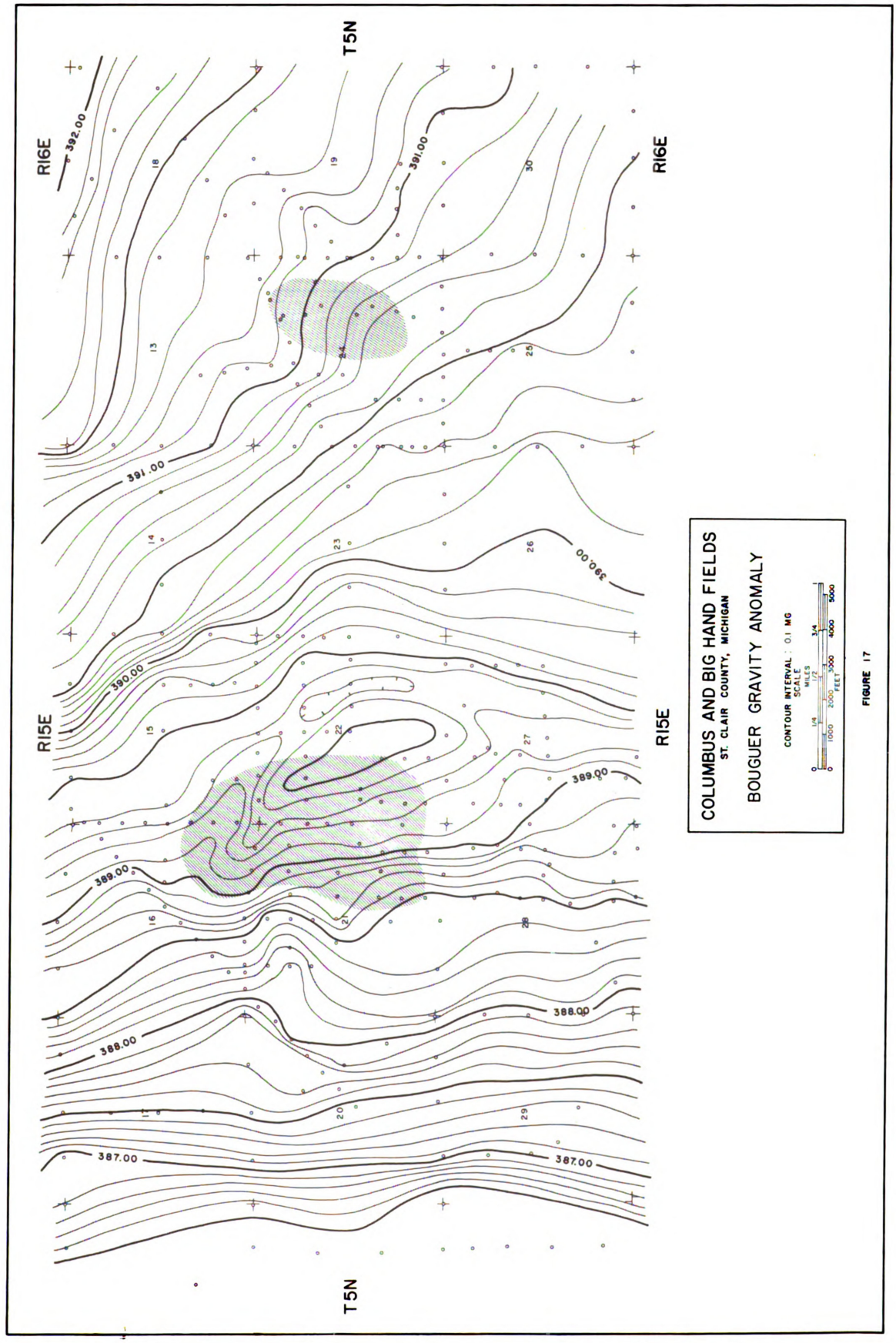
T5N
R16E
R15E
392.00
391.00
390.00
389.00
388.00
387.00
COLUMBUS AND BIG HAND FIELDS
ST. CLAIR COUNTY, MICHIGAN
BOUGUER GRAVITY ANOMALY
CONTOUR INTERVAL : 0.1 MG
SCALE
MILES
FEET
1000
2000
3000
4000
5000

FIGURE 17

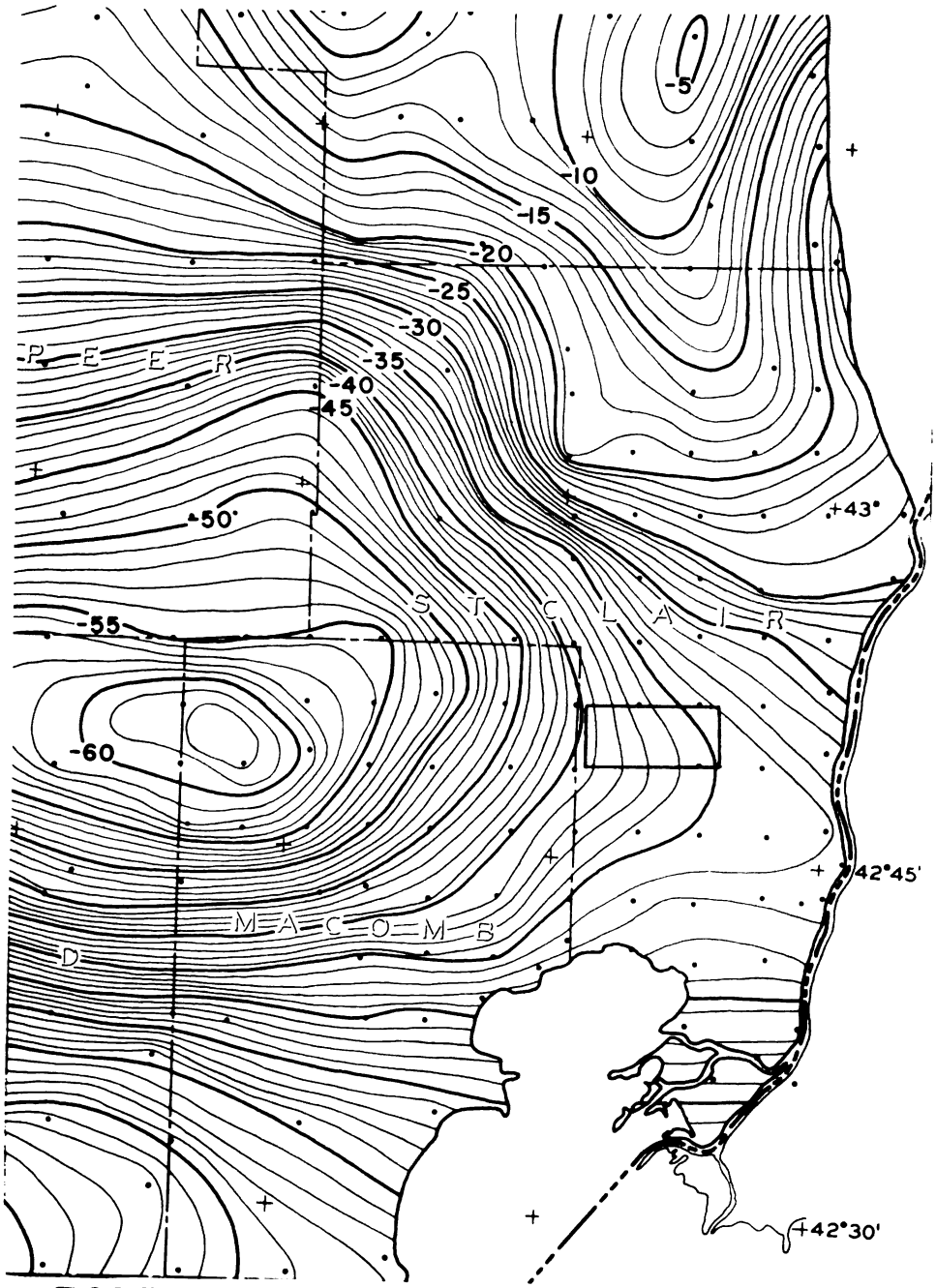

PORTION OF REGIONAL GRAVITY MAP OF MICHIGAN

FIGURE 18

(after HINZE, 1963)

Cross-Profiles Map

Figure 19 is the residual gravity map prepared by the cross-profile method. A positive anomaly of 0.3 mgals is located almost directly over the Columbus reef. The Columbus reef is flanked on the east and west by negative anomolies of 0.2 mgals amplitude. In section 20 and in the west part of section 21 there is another positive anomoly with a 0.2 mgals magnitude.

There are no isolated anomolies in the vicinity of the Big Hand reef, in fact, the gravity values tend to decrease over the reef structure. To the northwest of the reef, the gravity values increase. These values are enclosed in the +0.1 mgals contour lines. The +0.1 contour lines trend north and tie in with an anomoly associated with the Smiley reef.

Least Squares Residual Maps

The least squares technique also was used to isolate the residual gravity anomolies. The observed Bouguer anomaly surface minus the 2nd degree approximation, and the observed Bouguer anomaly surface minus the 4th degree approximation, are shown in Figures 20 and 21 respectively. The same anomolies are present on these maps that are present on the cross-profile residual map. The positive anomaly in section 20 and 21 has increased 0.1 mgal in magnitude to +0.3 mgal the negative anomoly on the east side

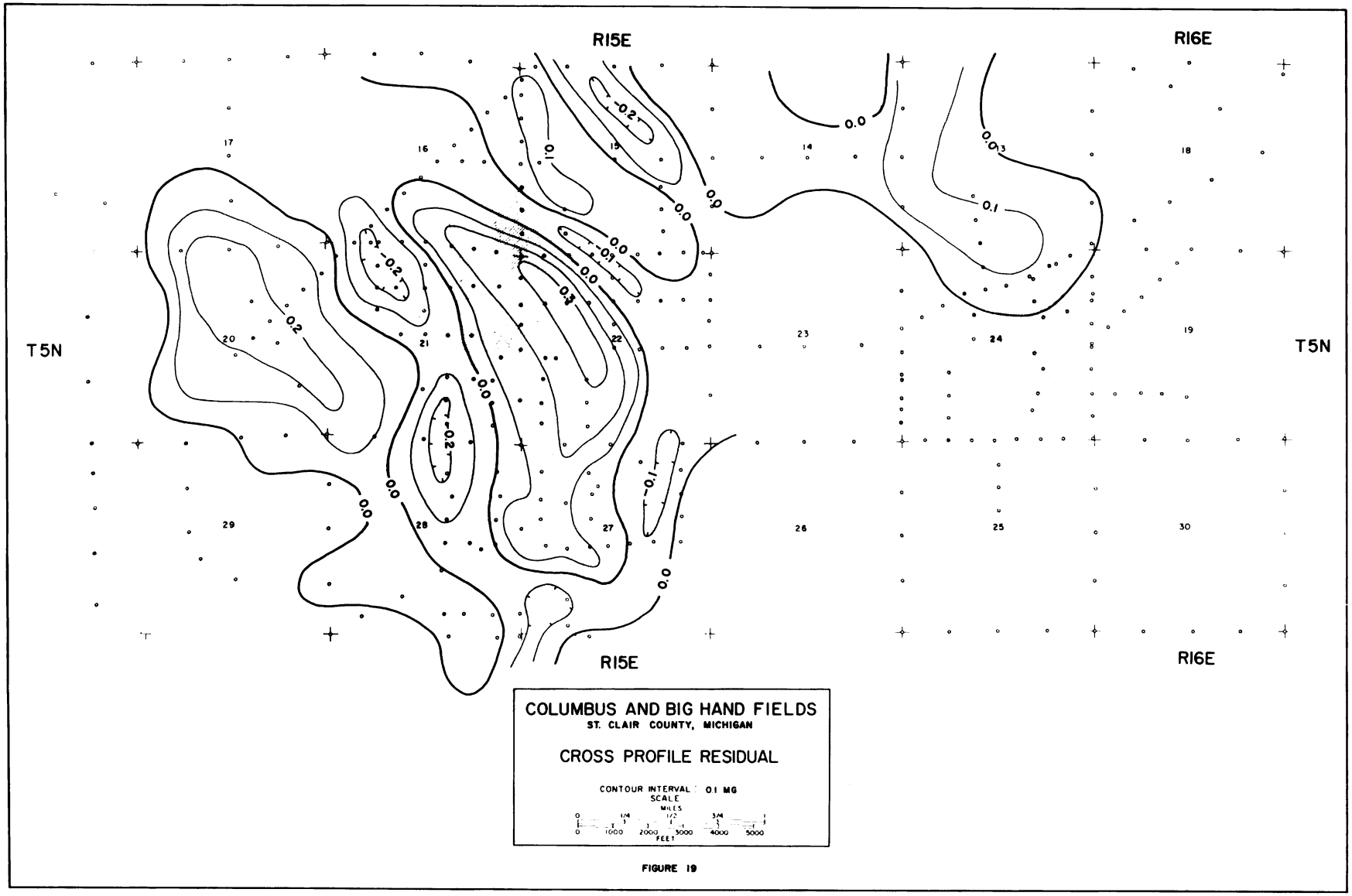
R15E
R16E
T5N
T5N
R15E
R16E
COLUMBUS AND BIG HAND FIELDS
ST. CLAIR COUNTY, MICHIGAN
CROSS PROFILE RESIDUAL
CONTOUR INTERVAL : 01 MG
SCALE
MILES
FEET

FIGURE 19

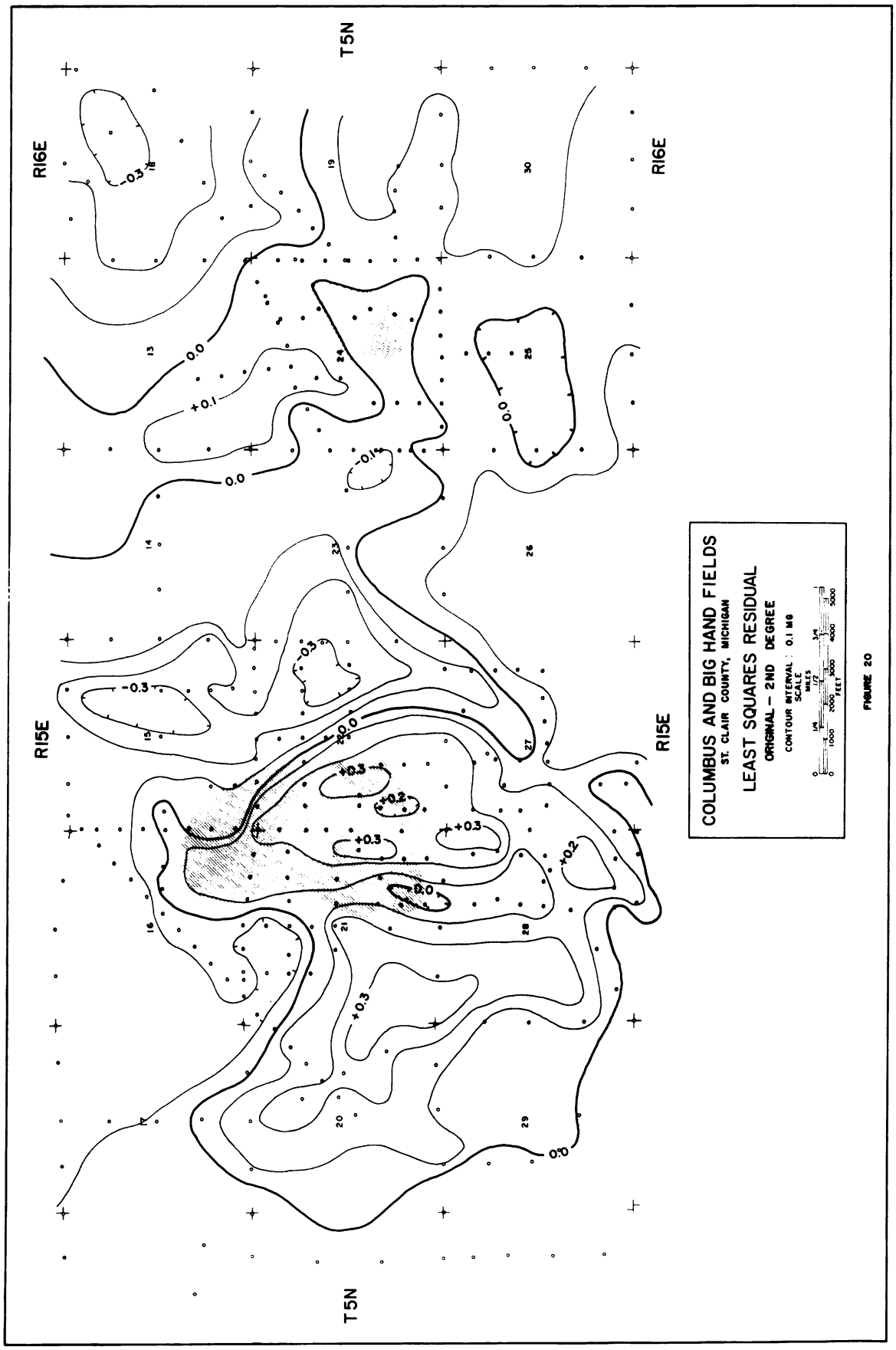
T5N
R16E
R15E
T5N
COLUMBUS AND BIG HAND FIELDS
ST. CLAIR COUNTY, MICHIGAN
LEAST SQUARES RESIDUAL
ORIGINAL – 2ND DEGREE
CONTOUR INTERVAL: 0.1 MG
SCALE
MILES
FEET

FIGURE 20

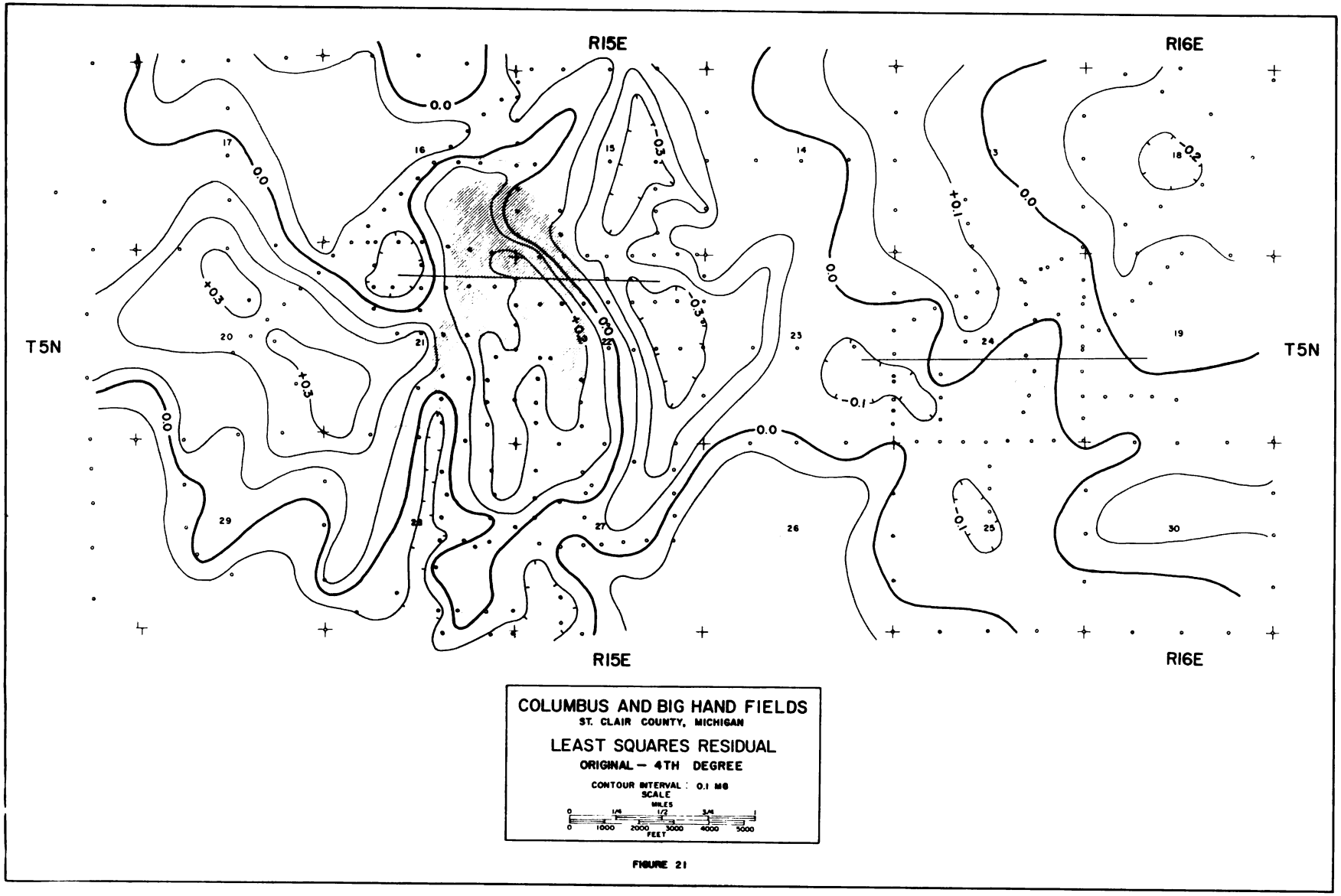

COLUMBUS AND BIG HAND FIELDS
ST. CLAIR COUNTY, MICHIGAN
LEAST SQUARES RESIDUAL
ORIGINAL — 4TH DEGREE
CONTOUR INTERVAL : 0.1 MG
SCALE
MILES
0 1/4 1/2 3/4
0 1000 2000 3000 4000 5000
FEET

FIGURE 21

of the Columbus reef has increased in amplitude to -0.3 mgal.

The observed minus the 4th degree and the observed minus 2nd degree show essentially the same results. However, the observed minus the 4th degree isolates the anomalies better and for this reason it is felt that the 4th degree polynominal best approximates the regional gravity trend.

Upward and Downward Continued Maps

In order to perform the isolation techniques of upward and downward continuations and second derivatives, the Bouguer values must be in a square grid pattern. To obtain a grid pattern, gravity values were interpolated between the original randomly spaced data. To obtain the interpolated value at a point, all of the gravity values that occur within a radius of 2700 feet of the point were fitted with a 3rd degree polynomial equation. The gravity value at the point was then obtained from the polynomial equation. This entire operation was performed on the digital computer. The interpolated Bouguer gravity map is shown in Figure 22. It is the same as the Bouguer gravity map except that the contour lines have been somewhat smoothed out.

Initially, a grid interval of 500 feet was used in the upward and downward continuation and second derivative calculations but it was found that this interval caused the values to oscillate and resulted in many small isolated

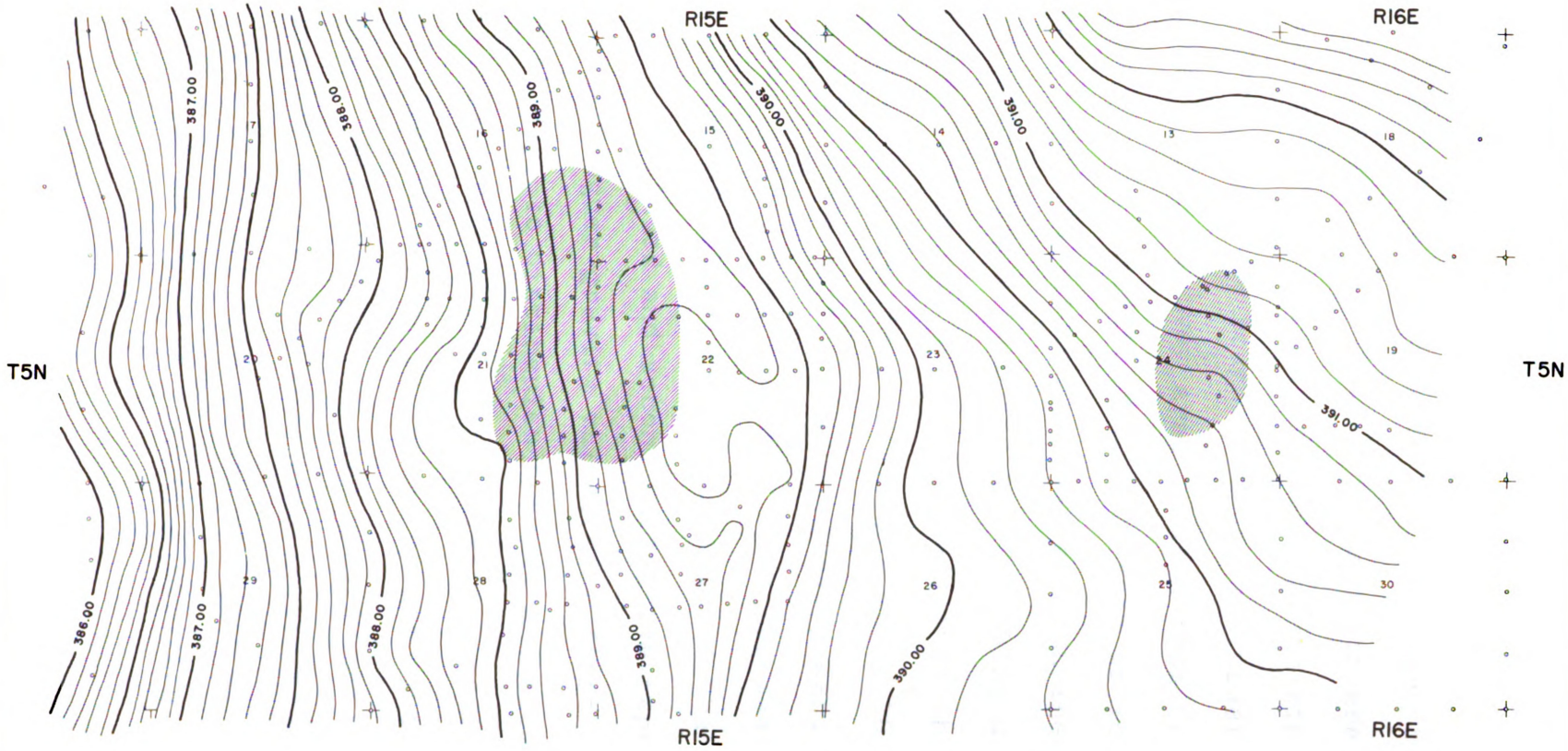
R15E
R16E
T5N
T5N
R15E
R16E
386.00
387.00
388.00
389.00
390.00
391.00
COLUMBUS AND BIG HAND FIELDS
ST. CLAIR COUNTY, MICHIGAN
INTERPOLATED BOUGUER
GRAVITY ANOMALY
CONTOUR INTERVAL : 0.1 MG
SCALE
MILES
0 1/4 1/2 3/4 1
0 1000 2000 3000 4000 5000
FEET

FIGURE 22

anomolies. Therefore, a grid interval of 1000 feet was used. This interval gave much better results. Because of the limited regional data it was necessary to use only 6 rings instead of the full 10 rings which are suggested by Henderson (1960). The radius of the 6th ring is 5000 feet. Therefore, when the Bouguer values are upward continued, 5000 feet of the survey area is lost from the edges of the original map. An additional 5000 feet is lost when the upward continued values are downward contined (Servos, 1965). The original Bouguer map and the following upward and downward continued and second derivative maps show the same areal coverage. Regional data covering a strip 10,000 feet wide around the edges of the Bouguer gravity map, was used but is not shown on the maps because it was necessary only for the calculation of values around the edge of the upward and downward continued and second derivative maps.

The Bouguer gravity values were first upward continued in an attempt to distinguish between anomalies caused by near surface features and anomalies caused by features at greater depth. Figure 23 is the upward continued gravity surface. This surface has been upward continued 2000 feet. The gravity values have been greatly smoothed by this process. The large anomalous area in the vicinity of the Columbus reef is indicated on this map only by a widening of the contour lines.

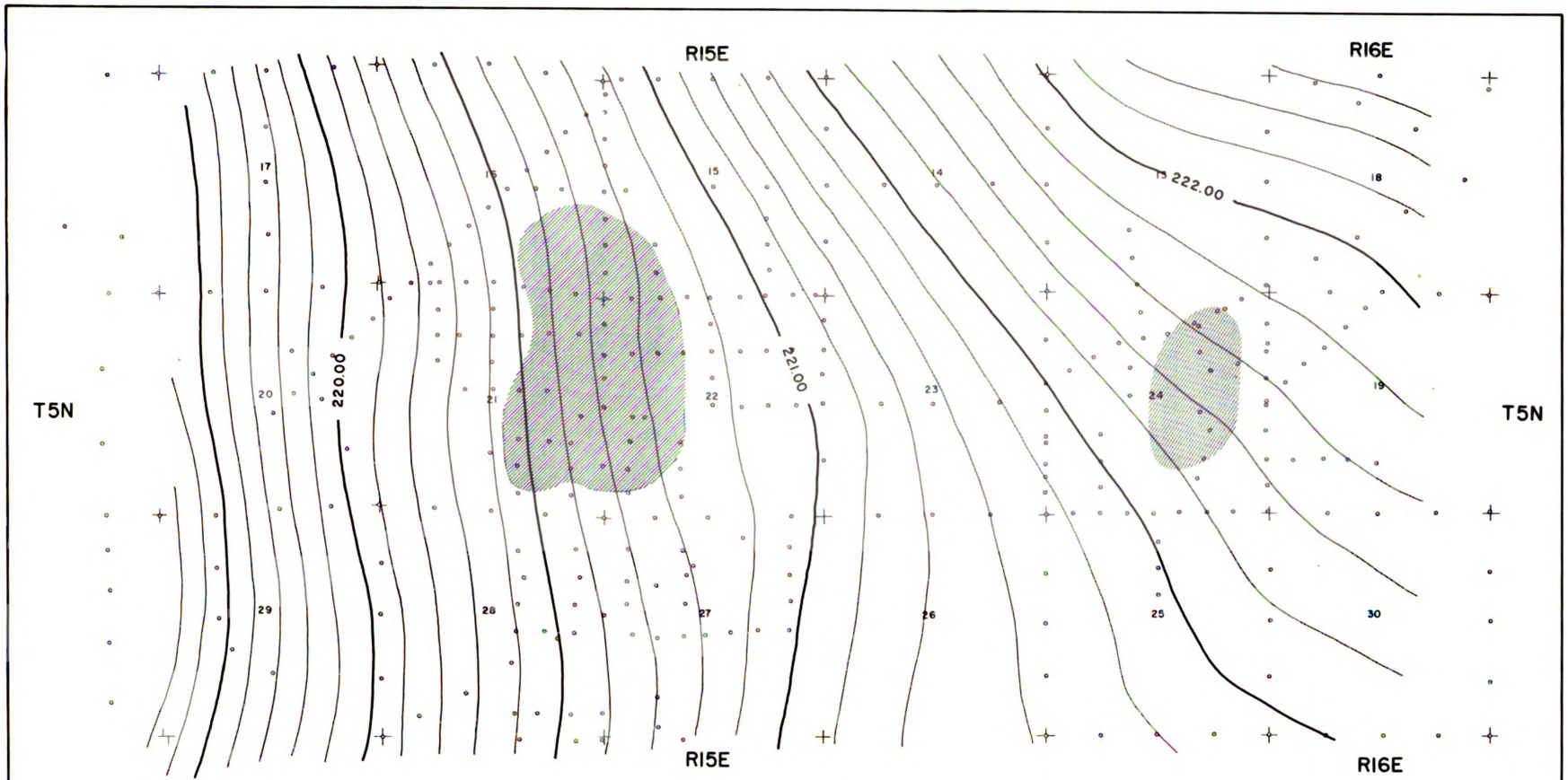

COLUMBUS AND BIG HAND FIELDS
ST. CLAIR COUNTY, MICHIGAN
BOUGUER GRAVITY ANOMALY
UPWARD CONTINUED 2000 FT.

CONTOUR INTERVAL : 0.1 MG
SCALE
MILES
0 1/4 1/2 3/4 1
0 1000 2000 3000 4000 5000
FEET

FIGURE 23

After the Bouguer surface was upward continued, it was then downward continued to bring out the anomalous features. Figure 24 is a map of the 3000 feet downward continued surface. The anomaly associated with the Columbus reef was isolated. The closure on the anomaly is +0.5 mgals. The positive anomaly in sections 20 and 21 is present on this map. The negative anomalies on the east and west side of the Columbus reef have diminished somewhat in relation to the positive anomalies. However, they are still present. This can mean one of two things. The source of the anomalies is deeply buried, or the source of the anomalies is near surface, but the character of the anomalies is such that it resembles a deep source and therefore this method cannot distinguish between the two.

Directly to the northwest, and partly overlapping the Big Hand reef, there is a slight increase in the gravity values. However, there is no positive closure on this map that is associated with this reef.

The same upward continued surface was then downward continued an additional 1000 feet. The resulting map is shown in Figure 25. The same anomalous features that were present in Figure 24 have been isolated on this map. The isolated gravity low, which occurs in sections 25 and 26, is correlativity with the structural high on the F-salt (Figure 9).

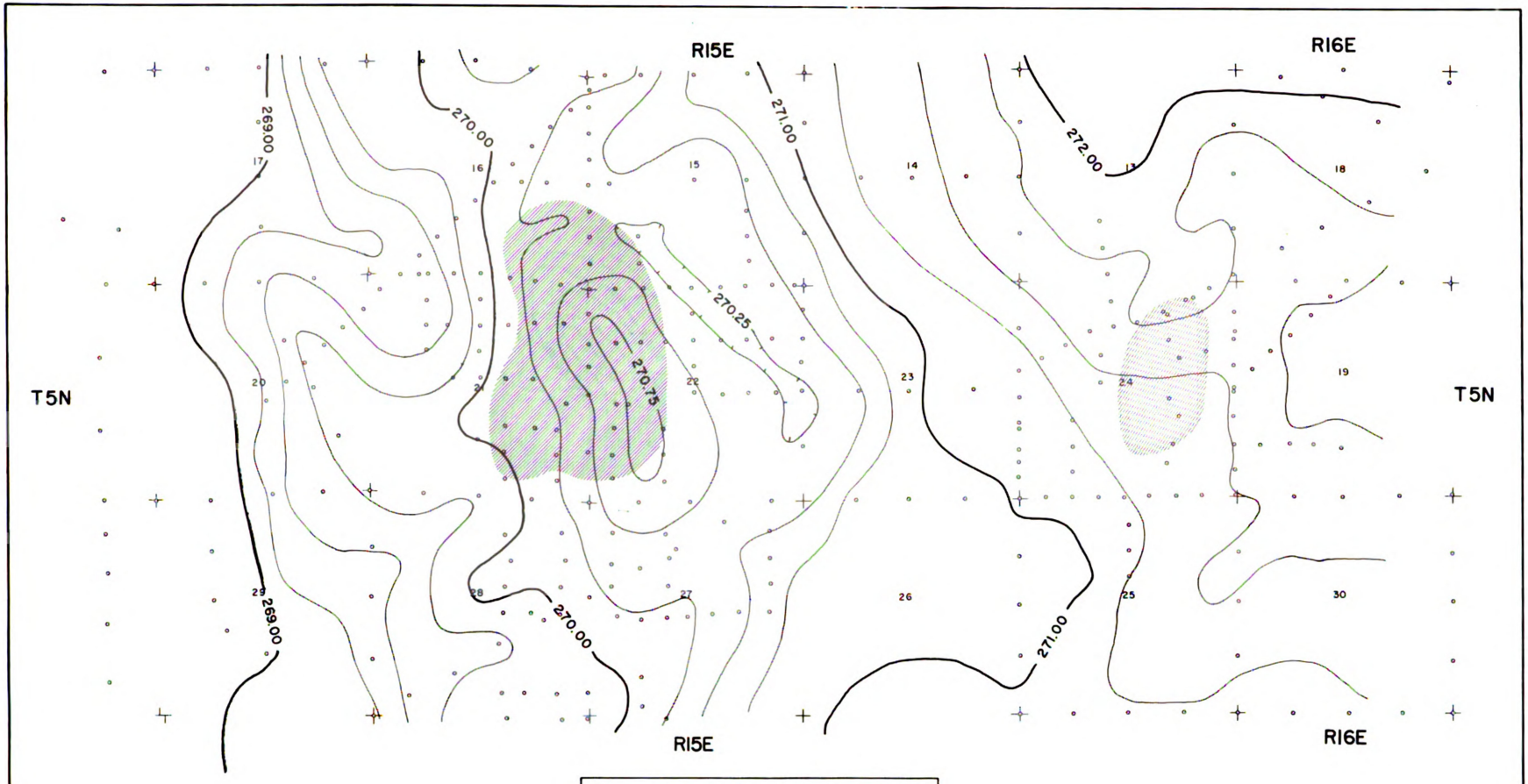
RI5E
RI6E
T5N
T5N
RI5E
RI6E
269.00
270.00
271.00
272.00
270.25
270.75
269.00
270.00
271.00
17
16
15
14
18
20
21
22
23
24
19
29
28
27
26
25
30
COLUMBUS AND BIG HAND FIELDS
ST. CLAIR COUNTY, MICHIGAN
BOUGUER GRAVITY ANOMALY
UPWARD CONTINUED 2000 FT.
AND DOWNWARD CONTINUED 3000 FT.
CONTOUR INTERVAL : 0.25 MG
SCALE
MILES
0
1/4
1/2
3/4
1
FEET
0
1000
2000
3000
4000
5000

FIGURE 24

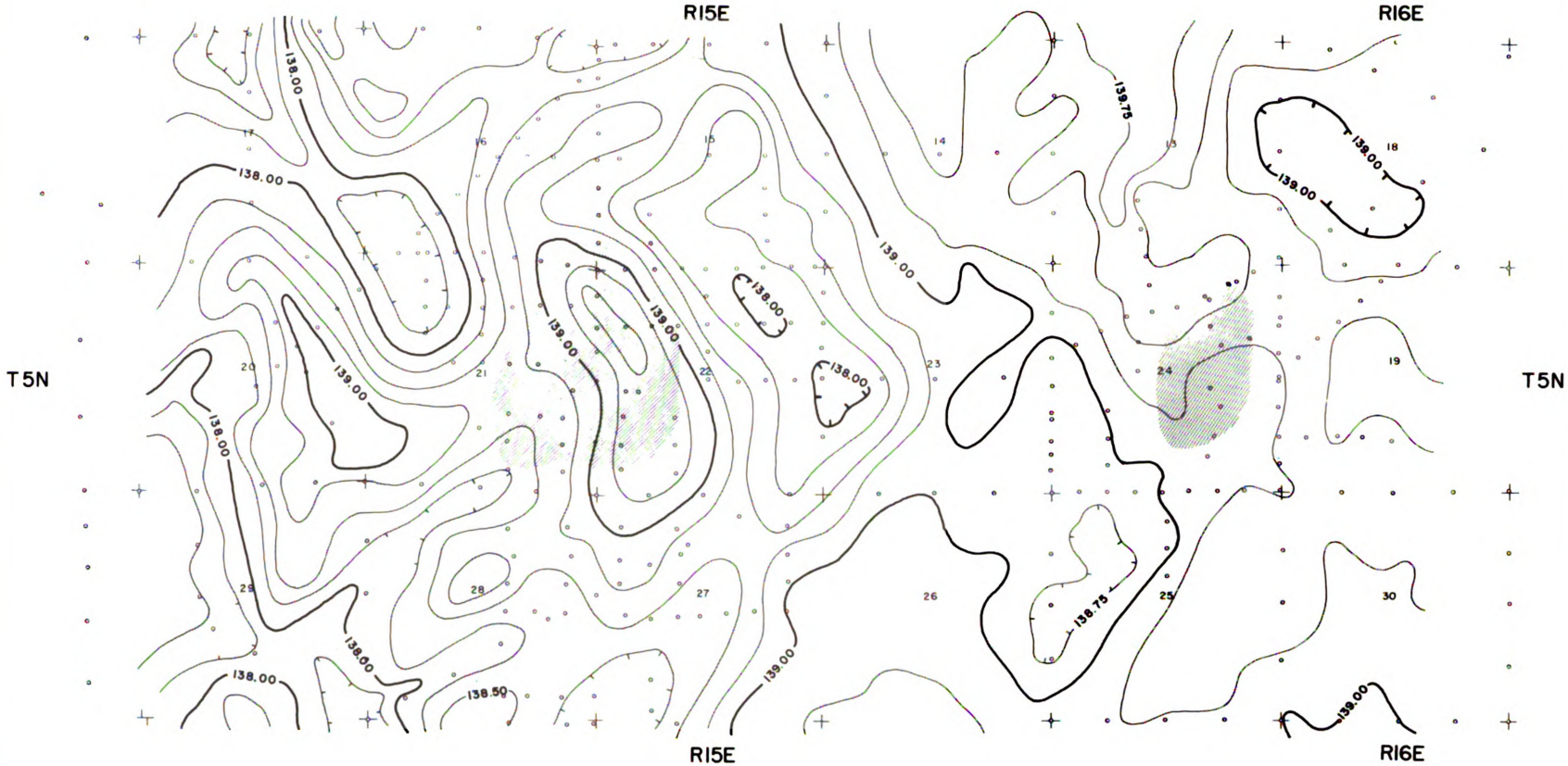

COLUMBUS AND BIG HAND FIELDS
ST. CLAIR COUNTY, MICHIGAN
BOUGUER GRAVITY ANOMALY
UPWARD CONTINUED 2000 FT.
AND DOWNWARD CONTINUED 4000 FT.
CONTOUR INTERVAL : 0.25 MG
SCALE
MILES
0 1/4 1/2 3/4 1
0 1000 2000 3000 4000 5000
FEET

FIGURE 25

Second Derivative Maps

Figure 26 is a map of the second derivative of the interpolated Bouguer gravity surface. The negative anomalies on the east and west side of the Columbus reef are easily recognized. The positive features, which are shown on the other maps, are not very well defined. The 2nd derivative method tends to accentuate near surface features and slight inaccuracies in the data. For this reason, better results are obtained if the second derivative is calculated on the upward continued surface rather than on the original surface.

This was done and the resulting map is shown in Figure 27. The anomolous features that were isolated by the other techniques also have been resolved by this method.

Interpretation

The gravity maps exhibit several distinct gravity anomalies. This immediately raises questions as to the source of these anomalies. Is the large positive anomaly associated with the Columbus field a product of the reef structure? If it is, then what parts of the reef structure contribute the most to this anomaly? Do the negative anomalies which flank the Columbus reef on the east and west originate with the reef structure? What is the origin of the large positive anomaly to the west of Columbus? Why is there no apparent gravity anomaly in the vicinity of the Big Hand reef?

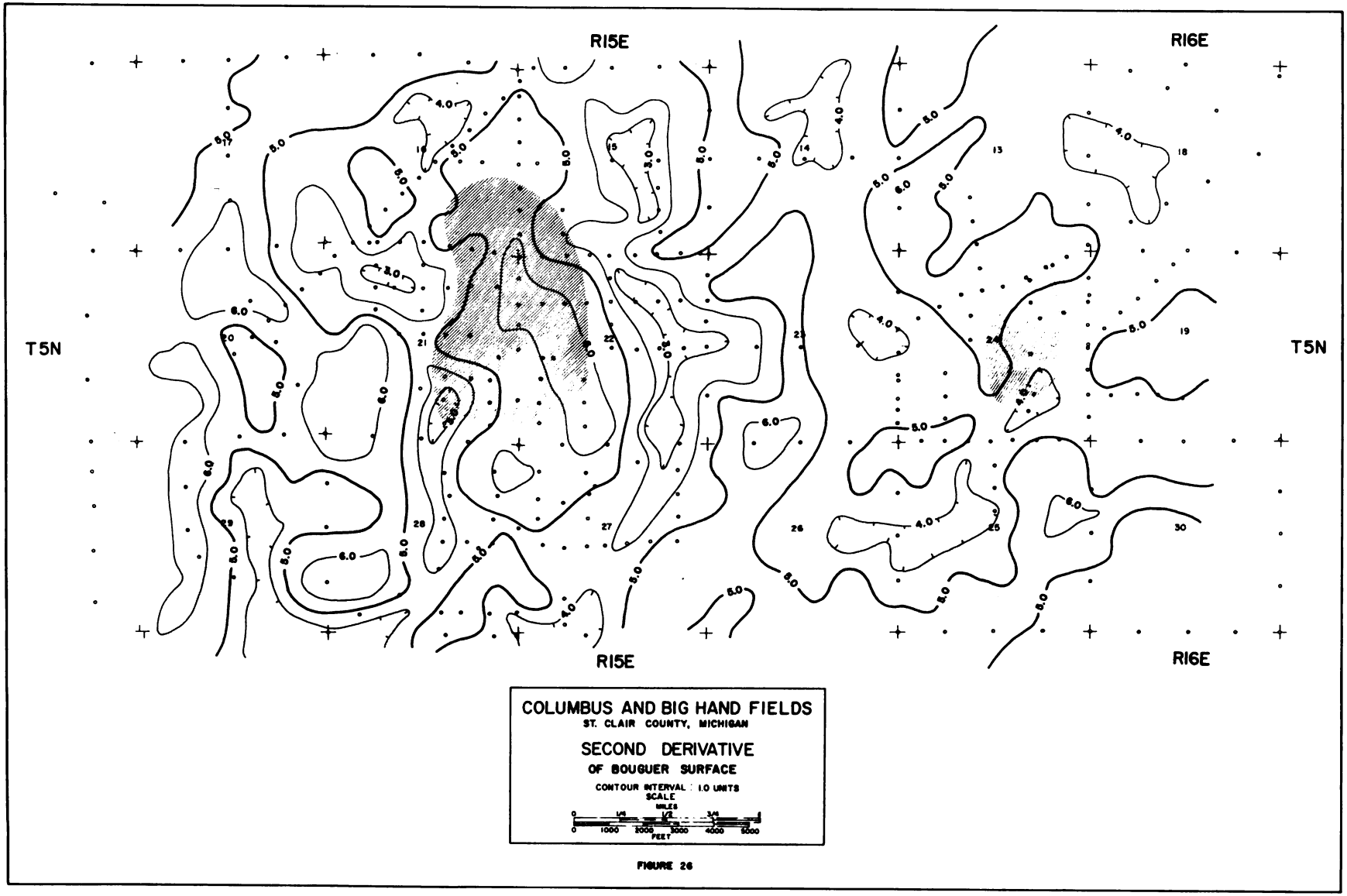
R15E
R16E
T5N
T5N
R15E
R16E
COLUMBUS AND BIG HAND FIELDS
ST. CLAIR COUNTY, MICHIGAN
SECOND DERIVATIVE
OF BOUGUER SURFACE
CONTOUR INTERVAL : 1.0 UNITS
SCALE
MILES
0 1/4 1/2 3/4 1
0 1000 2000 3000 4000 5000
FEET

FIGURE 26

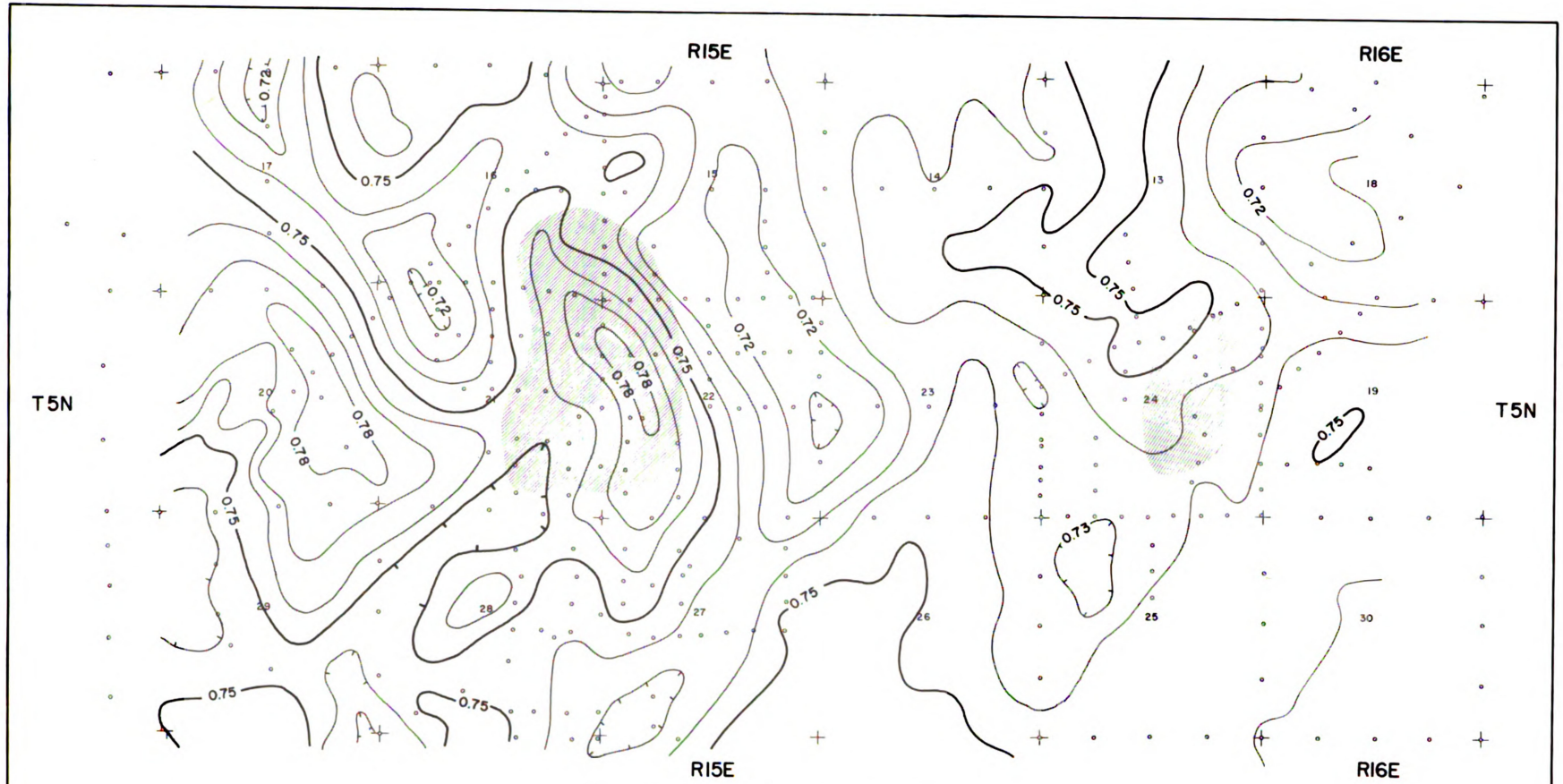
R15E
R16E
T5N
T5N
R15E
R16E
0.72
0.75
0.78
0.73
17
18
19
20
21
22
23
24
25
26
27
28
29
30
COLUMBUS AND BIG HAND FIELDS
ST. CLAIR COUNTY, MICHIGAN
SECOND DERIVATIVE
OF 2000 FT. UPWARD
CONTINUED SURFACE
CONTOUR INTERVAL 0.01 UNITS
SCALE
MILES
0
1/4
1/2
3/4
1
FEET
0
1000
2000
3000
4000
5000

FIGURE 27

Theoretical gravity studies of the Columbus and Big Hand reef structures and bedrock river channels map help to answer these questions.

Theoretical Gravity Study of Reef Structures

A theoretical gravity study was carried out on the Columbus and Big Hand reef structures. This was done in an attempt to determine if these reef structures produce a gravity anomaly. And, if an anomaly is produced, what is its magnitude and what parts of the reef structure contribute most to the anomaly.

The two-dimensional gravity computation method was used to calculate the gravity effect of these reefs (Talwani, Worzel, Lamar, and Landisman, 1959). The two-dimensional geologic sections used in these calculations are shown in Figure 14 and 15.

Gravity anomalies are, of course, caused by lateral variations in density. In this computation method, bodies of the same density contrast are approximated by polygons. The polygons used in this study and their density contrasts are shown in Figures 29 and 31. The resultant anomaly due to these structures is shown at the top of the figures. The gravity anomalies resulting from each individual body are shown in Figures 30, 32 and the anomaly resulting from combining these individual anomalies is shown at the top of the figure.

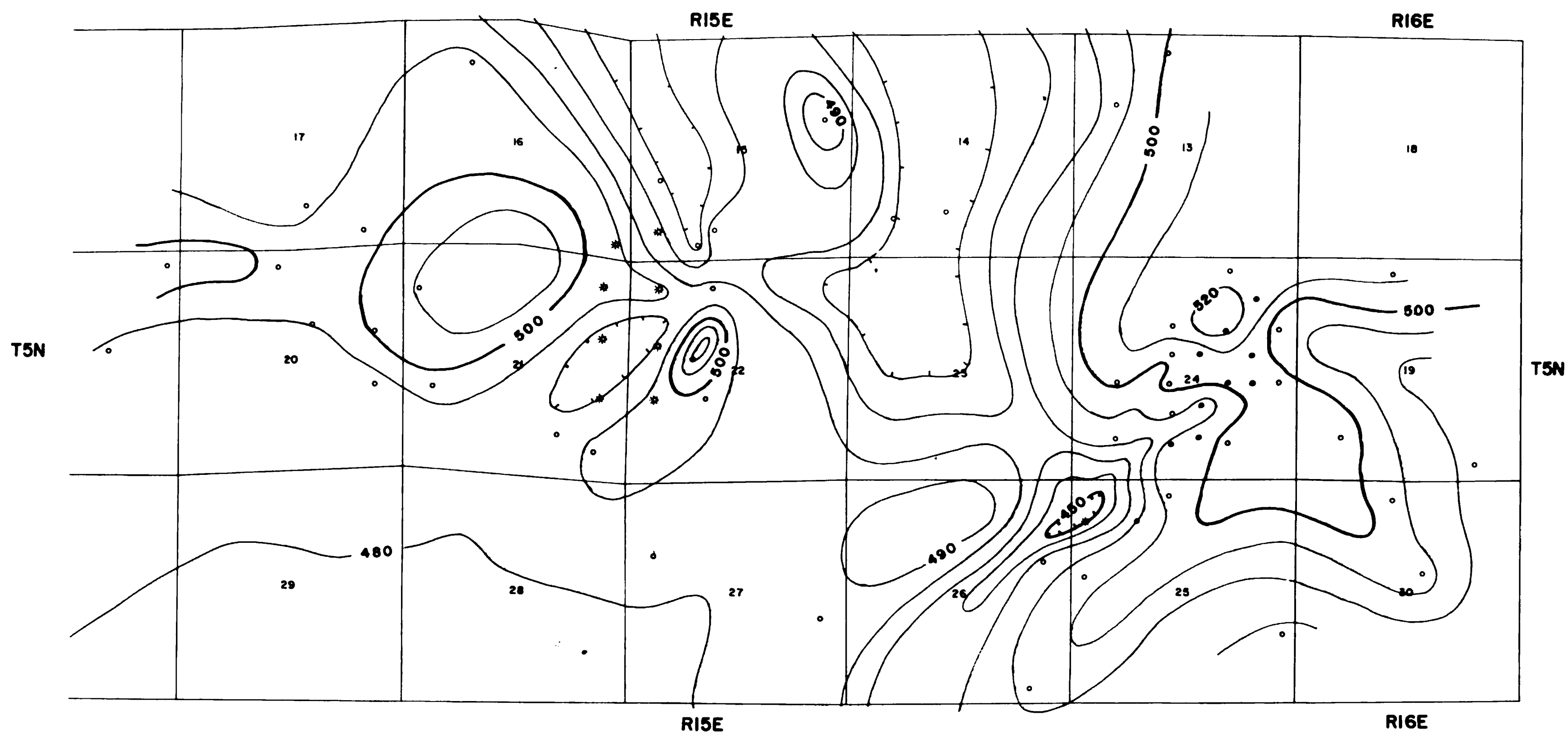

COLUMBUS AND BIG HAND FIELDS
ST. CLAIR COUNTY, MICHIGAN

BEDROCK ELEVATION MAP

CONTOUR INTERVAL: 10 FT.
DATUM: SEA LEVEL
SCALE
0 1/4 1/2 3/4 1
STATUTE MILE

FIGURE 28

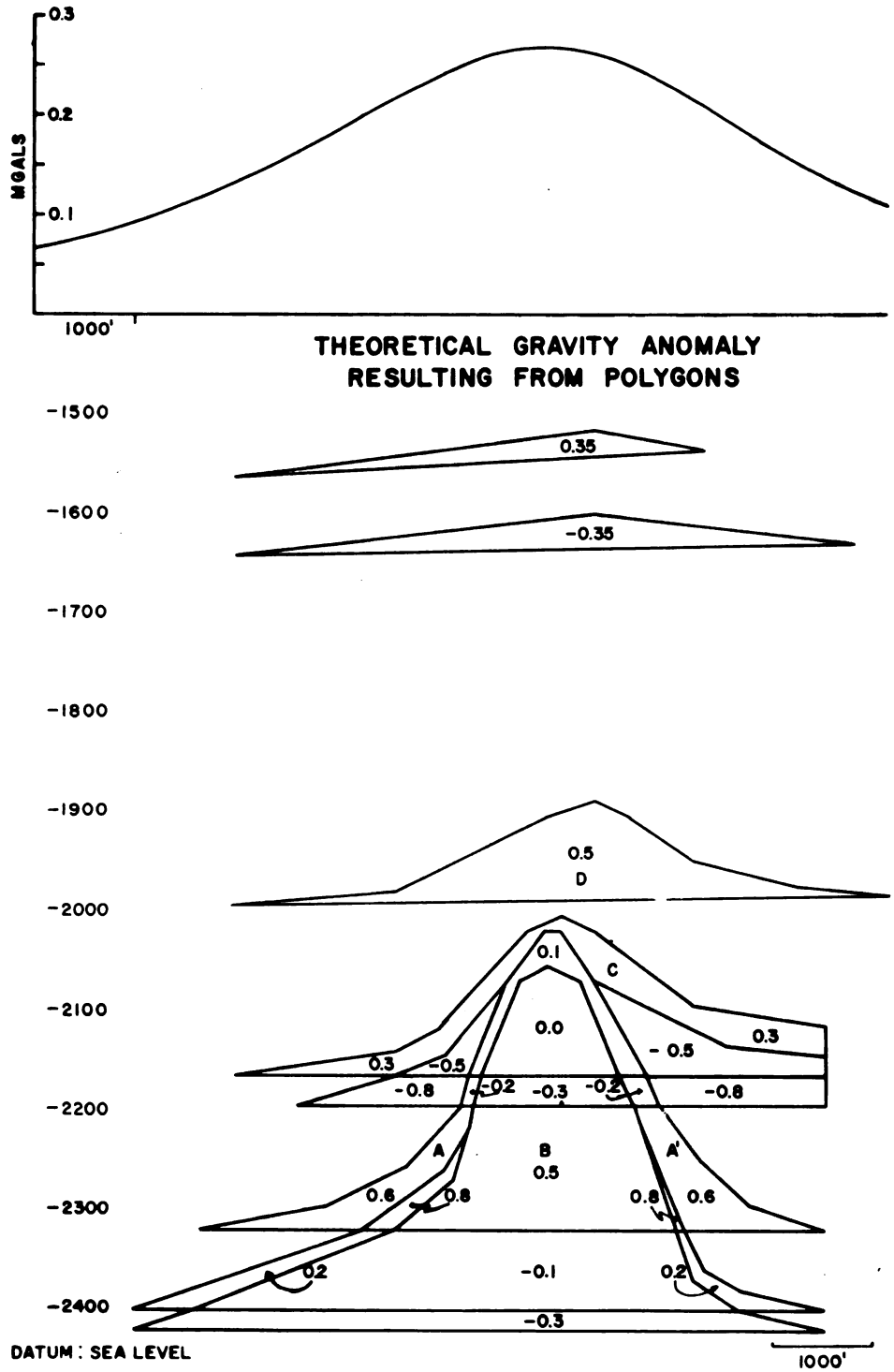
0.3
0.2
0.1
MGALS
1000'
THEORETICAL GRAVITY ANOMALY
RESULTING FROM POLYGONS
-1500
-1600
-1700
-1800
-1900
-2000
-2100
-2200
-2300
-2400
0.35
-0.35
0.5
D
0.1
C
0.0
0.3
-0.5
-0.8
-0.2
-0.3
A
B
A'
0.6
0.8
0.2
-0.1
-0.3
DATUM : SEA LEVEL
1000'
APPROXIMATION POLYGONS
FOR COLUMBUS REEF STRUCTURE
FIGURE 29

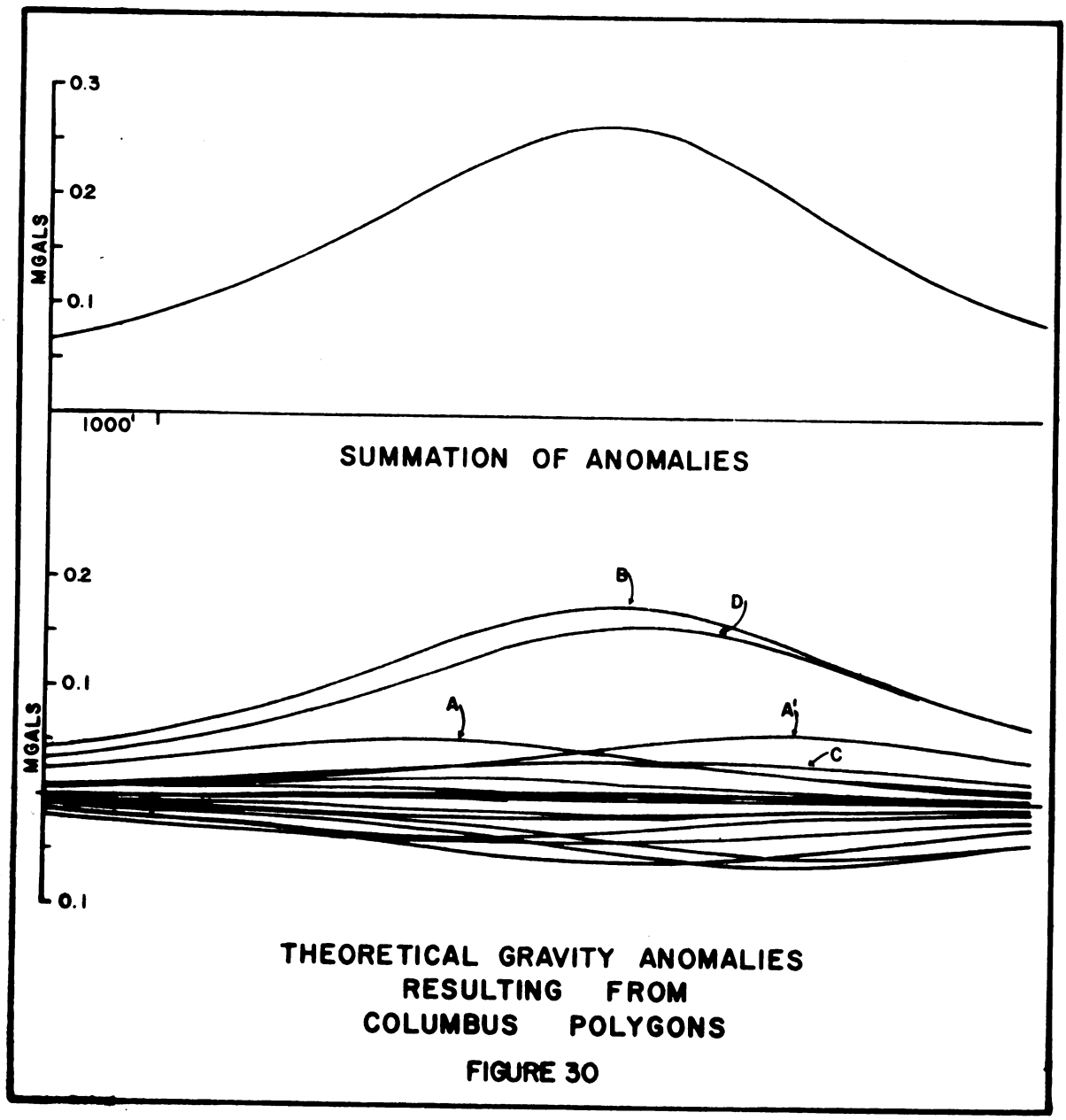

THEORETICAL GRAVITY ANOMALIES
RESULTING FROM
COLUMBUS POLYGONS

FIGURE 30

Approximation Polygons for Columbus Reef Structure

Polygon	Strata	Constrasts with
A	A-1 carbonate	A-2 salt
A'	A-1 carbonate	A-2 salt
B	reef body	A-2 salt
C	A-2 anhydrite	A-2 carbonate
D	A-2 carbonate	B-salt

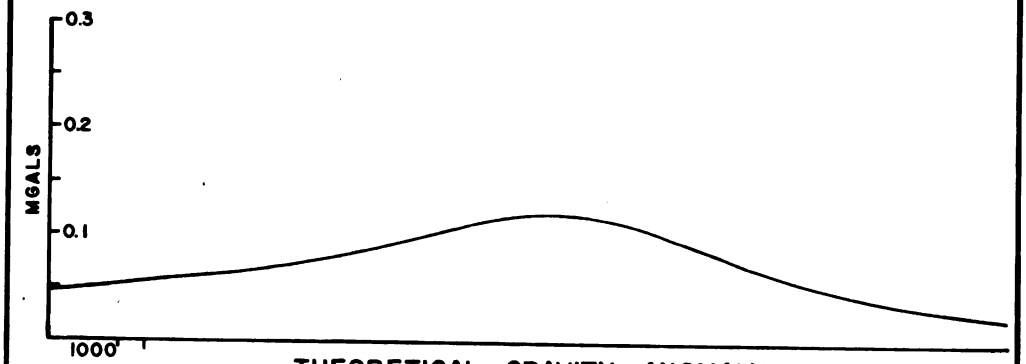

THEORETICAL GRAVITY ANOMALY
RESULTING FROM POLYGONS

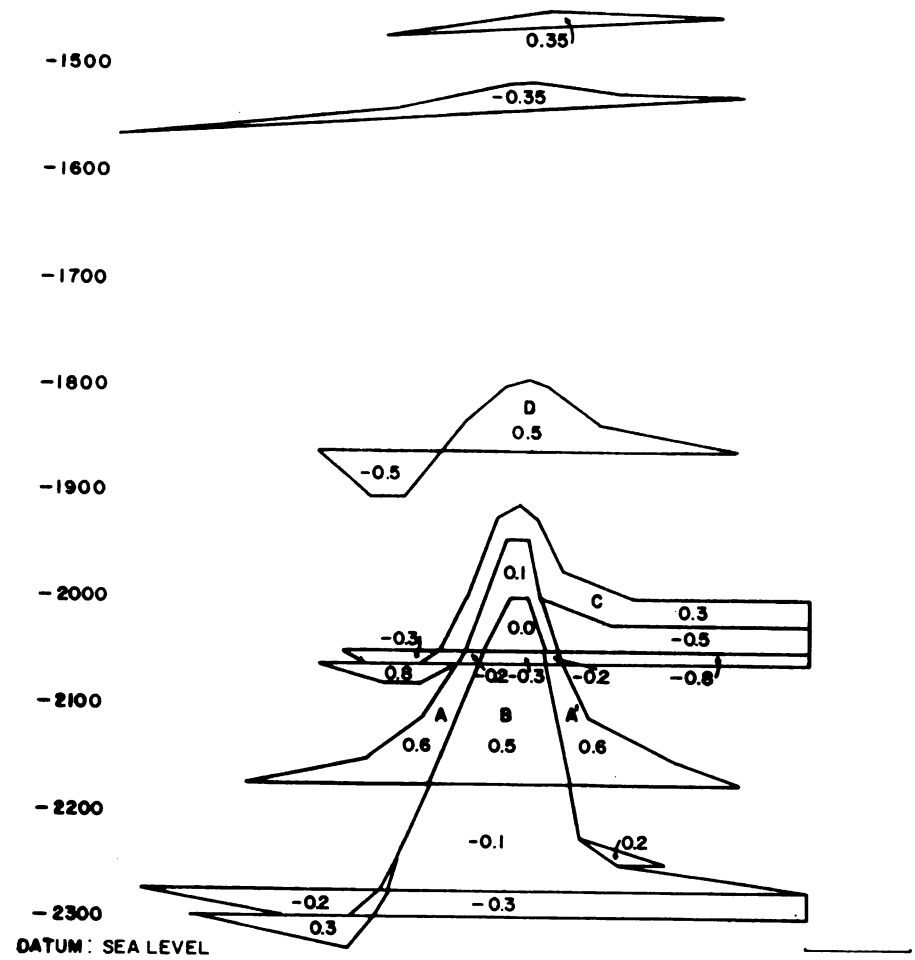

APPROXIMATION POLYGONS
FOR BIG HAND REEF STRUCTURE

FIGURE 31

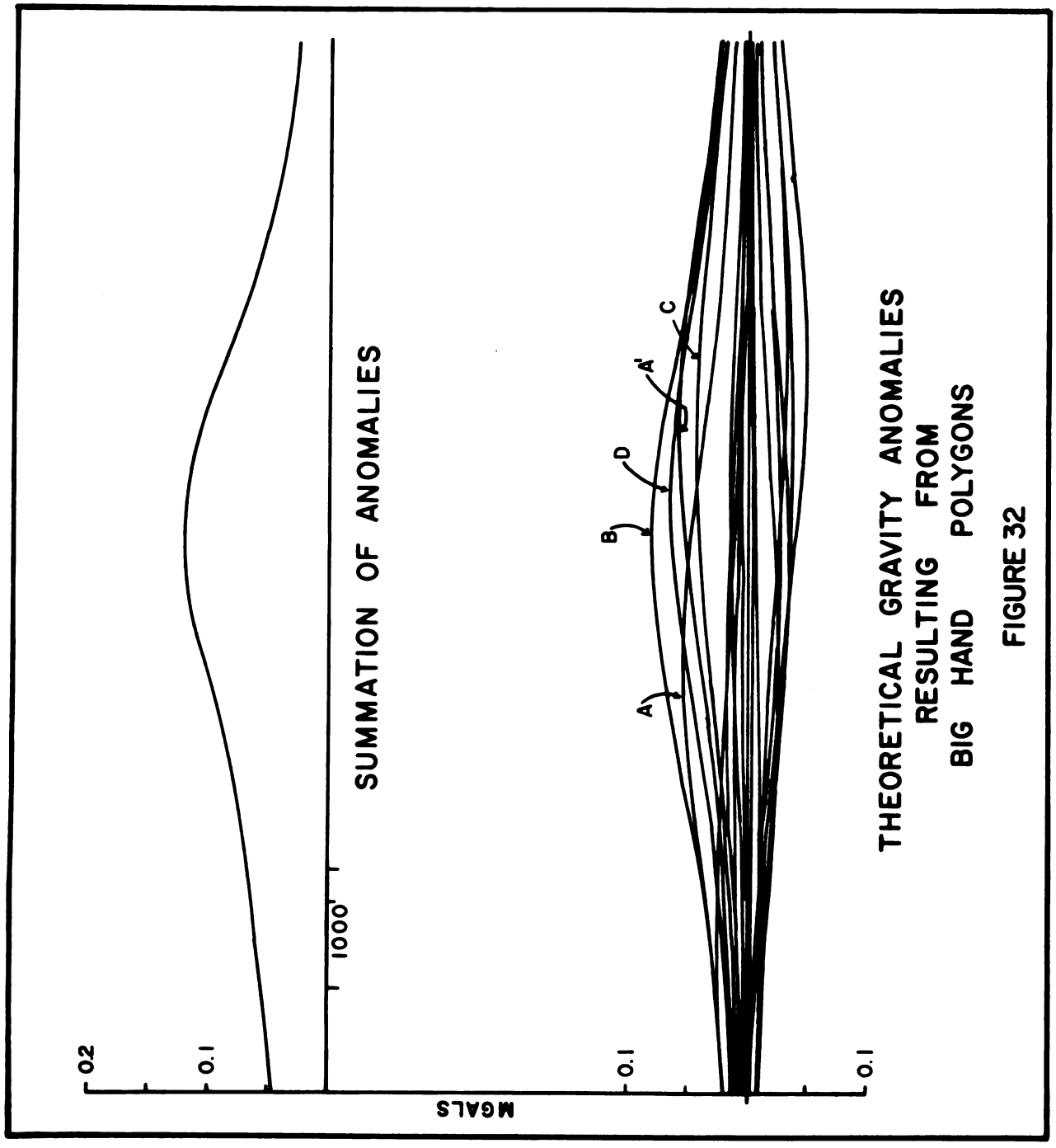
0.2
0.1
1000
SUMMATION OF ANOMALIES
MGALS
0.1
0.1
A
B
D
A'
C
THEORETICAL GRAVITY ANOMALIES
RESULTING FROM
BIG HAND POLYGONS

FIGURE 32

The magnitude of the anomaly resulting from the Columbus reef is +0.27 mgals, Figures 29 and 30. As is shown in Figures 31 and 32, the magnitude of the anomaly resulting from the Big Hand reef is +0.15 mgals. Figure 33 shows the approximation polygons for the F-salt structure and the theoretical gravity and anomaly resulting from it. The anomaly has a magnitude of -0.16 mgals. This, of course, is superimposed upon a regional anomaly caused by the sloping F-salt and G-unit interface. In Figure 34 the anomalies due to the reef structure and the F-salt structure are shown at the bottom of the diagram and the summation of these two anomalies is shown at the top. The resultant anomaly exhibits a positive 0.04 mgals on the west end of the profile and a negative 0.07 mgals on the eastern portion of the profile.

An error was introduced in the gravity calculations because the reef structures were approximated by two dimensional features. The error is about 25 per cent of the calculated value. This would reduce the magnitude of the Columbus reef anomaly to about +0.02 mg. and the Big Hand anomaly to about +0.12 mg. Because of the size of the structure on the F-salt, it is safe to approximate it as a two-dimensional feature. Therefore, the magnitude of this anomaly does not have to be reduced.

The polygons in Figure 29 which are designated by the letters A, A', B, C, and D are of primary interest. Comparing

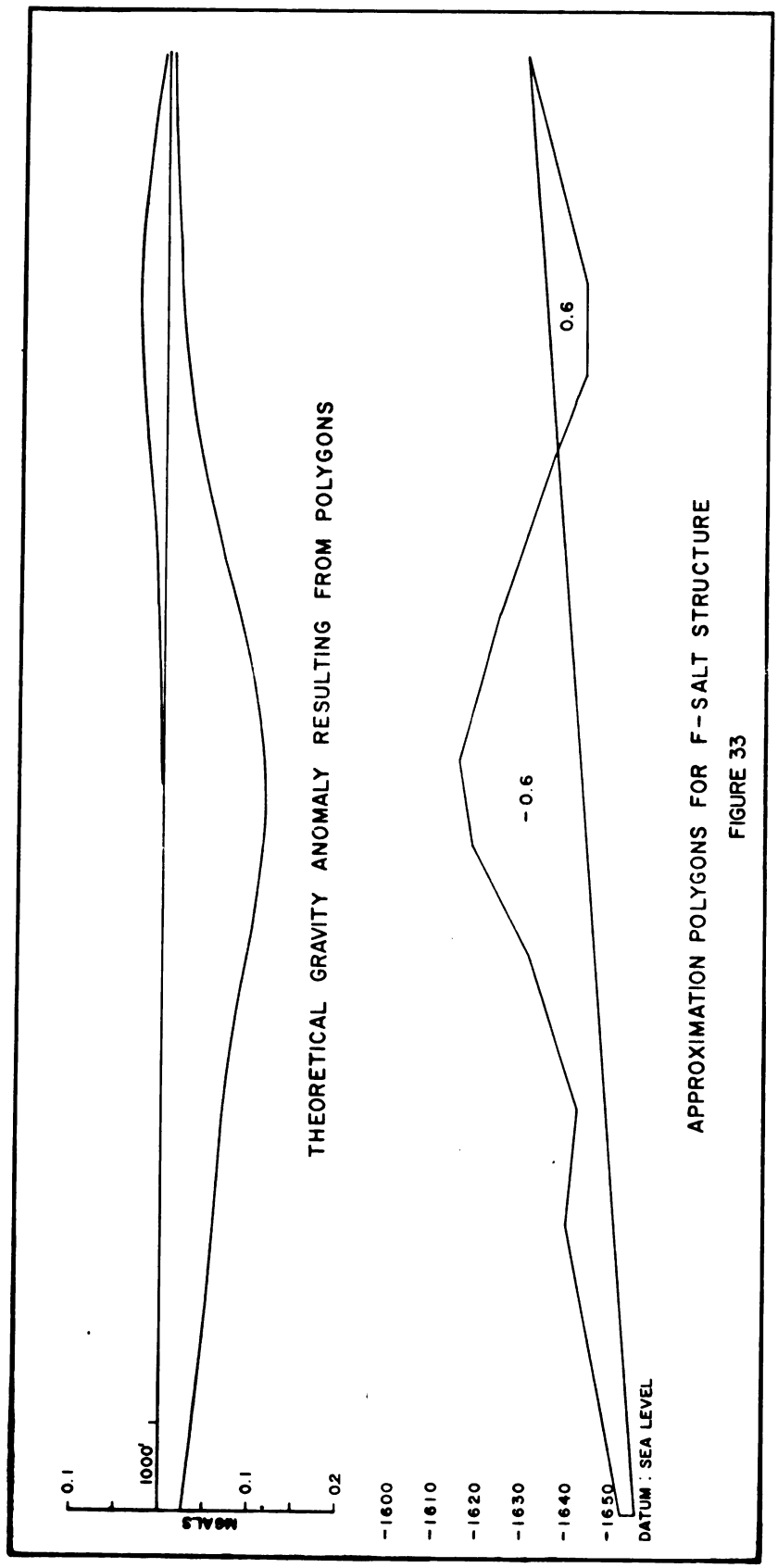
0.1
1000'
0.1
MGALS
02
-1600
-1610
-1620
-1630
-1640
-1650
DATUM : SEA LEVEL
THEORETICAL GRAVITY ANOMALY RESULTING FROM POLYGONS
0.6
-0.6
APPROXIMATION POLYGONS FOR F-SALT STRUCTURE

FIGURE 33

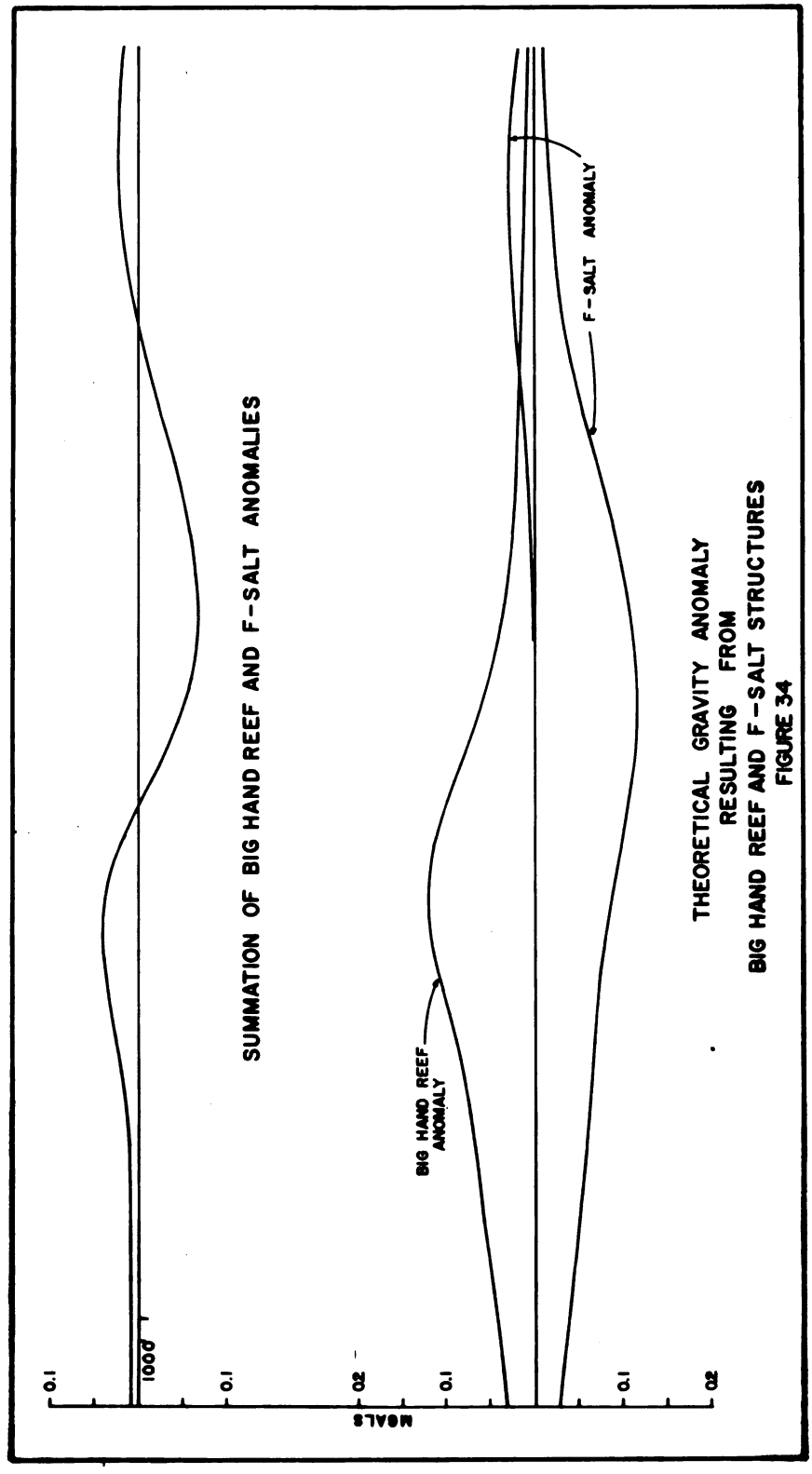

THEORETICAL GRAVITY ANOMALY
RESULTING FROM
BIG HAND REEF AND F-SALT STRUCTURES
FIGURE 34

Figure 29 with Figure 14 shows that polygons A and A' are those parts of the A-1 carbonate which constrast laterally with the A-2 salt. Polygon B is that part of the reef body which also constrasts with the A-2 salt. Polygon C approximates the portion of the A-2 anhydrite which constrasts with the A-2 carbonate. Polygon D is that portion of the A-2 carbonate which constrasts laterally with the B-salt. The curves labelled A, A', B, C, and D in Figure 30 are the theoretical gravity effects resulting from the polygons A, A', B, C, and D of Figure 29. It can be seen that the majority of the theoretical anomaly of the entire Columbus reef structure comes from that part of the reef body and the A-1 carbonate (polygons A, A', and B) which constrasts with the A-2 salt and from the structure on top of the A-2 carbonate (polygon D). As is illustrated in Figures 31 and 32, the same results were obtained for the Big Hand reef. The results of this study does not invalidate the conclusions of Servos (1965). The theoretical anomaly obtained from this study slightly underfits the observed gravity anomaly. Consideration of the effect of peripheral dolomitization could posibly account for the difference between the theoretical and observed gravity anomalies. Also, the geologic conditions in this study area and the area of Servos' study area may not be the same.

The densities used in these calculations were taken from density determinations of well samples and from formation

density logs. The formation density logs are from wells which are both in the reef structure and in the off-reef facies. These density values, shown in Table 2, agree with typical average densities for these rock types.

Table 2.--Strata densities.

Formation or Unit	Density-gm/cc
Niagaran	2.70
A-1 Evaporite	3.00
A-1 Carbonate	2.80
A-2 Salt	2.20
A-2 Anhydrite	3.00
A-2 Carbonate	2.70
B- Salt	2.20
C- Unit	2.55
D- Salt	2.20
F- Salt	2.20

Theoretical Study of the Bedrock Surface

Klasner (1964), Servos (1965), and Roth (1965) have investigated the gravitational effects of bedrock river channels. They found that river channels in the bedrock which had been filled in with low density drift material can cause negative anomalies with magnitudes as high as $^{-}0.3$ mgals.

Figure 28 is a map of the bedrock topography in this study area. There are bedrock valleys present on this map. One channel trends northeast across sections 26 and 25 and then swings northwest across section 23, where it widens

and appears to divide. One branch continues northward through section 14 and the other branch appears to continue northwestward, where it connects with a depression in section 15. There is another depression in the eastern portion of section 21. Lack of control makes it impossible to determine if this depression is only an isolated low or if it continues to the north and south.

Comparing this bedrock topographic map with the Bouguer minus the 4th degree, the cross-profile, the 3000 foot and 4000 foot downward continued and the second derivative residual gravity maps shows the correlation between the gravity lows and bedrock depressions. There is not a one to one correlation, but there definitely is a general trend. The gravity values tend to decrease over the bedrock channel which occurs in sections 26, 25, 23, and 14. The northern end of the large negative anomaly east of the Columbus reef coincides with the bedrock low in section 15. The southern end of this negative anomaly occurs along the section line between sections 22 and 23. This is where the bedrock channel appears to widen and divide. There is a noticeable lack of geologic control in the area and thus, the magnitude of this channel is not known.

The negative gravity anomaly to the west of Columbus is considerably smaller in magnitude and narrower in areal extent than the negative anomaly to the east of Columbus. This anomaly appears to coincide in section 21 with the depression

in the bedrock surface. The gravity anomaly extends both to the northwest and southwest. As has been stated previously, the extent of the bedrock depression cannot be determined because of the lack of data.

Thus, it appears that there is a general correlation between bedrock channels and negative gravity anomalies. With increased control data, the buried bedrock channels possibly would be shifted in actual position so that even better correlation would exist.

Interpretation of Observed Anomalies

A basic understanding of the types of anomalies which can be expected from various geological features has now been established. From this, it is possible to make a reasonable interpretation of the anomalies which are observable on the gravity maps.

The positive anomaly located over the Columbus reef is no doubt associated with the reef structure. The profile of the geologic cross-section along which the theoretical gravity calculations were made is located on the original minus the 4th degree least squares map, Figure 21. The observed residual gravity anomaly along this profile reaches a magnitude of about 0.22 mgals. This very closely matches the theoretical value of 0.20 mgals. For this reason, it is felt that the observed anomaly is a product of the reef structure.

A comparison of the width of the residual anomaly and width of the calculated anomaly suggests no definite conclusions. This is because the width of the residual anomaly varies with the isolation technique and the edges of the positive anomaly are masked by the negative anomalies which are believed to be the result of bedrock channels.

The negative anomolies, which flank the Columbus reef on the east and west, were first thought to be of the "sombrero" type. Yungul (1961) considered the negative "sombrero" ring to be an anomaly which is related to the reef structure. After further consideration, it is now believed that these negatives are due to bedrock river channels. There are several reasons for drawing this conclusion. First, when conducting the theoretical gravity study of the Columbus reef, no density contrasts were found in the geological sections which could cause a resultant negative anomaly of this magnitude. Secondly, gravity data to the north and south of this area indicate that these negative features do not end at the boundaries of the map. Instead, they extend to the north and south. Their shape and linear extent also are characteristic of river channels.

Finally, it has been shown, through theoretical studies of river channels in the bedrock, that they can produce negative anomalies of this magnitude and there are river channels in this area which general correlate with the negative gravity anomalies.

The gravity picture in the vicinity of the Big Hand reef is dominated by the presence of the structure on the F-salt. The negative anomaly due to this feature almost completely cancels out the positive anomaly caused by the reef structure, Figure 34. Although there is no negative closure associated with this feature, the gravity values do decrease in value. The slight increase in positive values above the northwest corner of the reef is probably due to the reef structure where it has not been completely nullified.

The positive anomaly to the west of Columbus compares favorably in magnitude with that of the anomaly caused by the Columbus reef structure. This would tend to indicate the presence of a structure which is comparably with that of the Columbus reef structure. Present drilling indicates the presence of a structure in this area. This is shown on the geological maps in Figure 4 and 12. Although a substantial number of wells have been drilled in this area, the structure probably has not been fully explored. This should prove to be an interesting area.

CHAPTER IV

CONCLUSION

In conclusion, it can be stated:

1. The Columbus reef structure produces a recognizable gravity anomaly with a magnitude of about +0.27 mgals. The width of the residual anomaly does not correspond with the width of the reef structure for the width of the residual anomaly varies with the isolation technique and the boundary of the anomaly is complicated by the flanking negative anomalies.

2. The Big Hand reef structure is estimated to produce a gravity anomaly of about +0.12 mgals, however, this positive anomaly is almost completely negated by a negative anomaly of 0.16 mgals which originates from a structure on the F-salt. This positive feature has a closure of approximately 40 feet which is not directly associated with the Big Hand reef. If this structure was not present the anomaly due to the reef could probably be isolated and recognized as resulting from a reef structure. From this, it may be concluded that in areas of known structures on the F-salt, the possibility of a reef structure occurring should not be ruled out simply because of no gravity anomaly.

3. Bedrock river channels can produce negative anomalies with a magnitude of 0.3 mgals. Bedrock river channels do exist in this study area and the negative anomalies which flank the Columbus anomaly are probably the result of such features.

4. The major source of the gravity anomaly, resulting from the Columbus and Big Hand reef structures, is probably due to that portion of the reef body and the A-1 carbonate which contrasts with the A-2 salt and the part of the A-2 carbonate which contrast with the B-salt.

5. All of the interpretation techniques successfully isolated the Columbus anomaly. It was, however, necessary to use good geological judgment in applying these techniques in order to obtain the best results. The original Bouguer surface minus the 4th degree better isolates the anomalies and for this reason it is felt that the 4th degree polynomial surface best approximates the regional gravity. In the upward and downward continuation and second derivative methods, a mesh interval of 500 feet, which is about 1/6th the depth to the reef structure, was found to be too small. A mesh interval of 1000 feet, 1/3rd the depth, gave better results. Second derivatives on the upward continued surface gave more easily interpretable results than second derivatives on the original Bouguer surface.

BIBLIOGRAPHY

BIBLIOGRAPHY

Alguire, S. L. (1962). Some geologic and economic aspects of Niagaran reefs in Eastern Michigan: Michigan Basin Geological Society Annual Field Conference, p. 30-38.

Cohee, G. V. (1948). Thickness and lithology of Upper Ordovician and Lower and Middle Silurian rocks in the Michigan Basin: U. S. Geol. Survey, Oil and Gas Invest., Preliminary Chart 33.

Cumings, E. R., and Shorck, R. S. (1928). Niagaran coral reefs of Indiana and adjacent states and their stratigraphic relationships: Geol. Soc. Amer. Bull. V. 39, p. 579-620.

Ehlers, G. M., and Keling, R. V. (1962). Silurian rocks of Michigan and their correlations: Michigan Basin Geological Society Annual Field Conference, p. 1-20.

Elkins, Thomas A. (1950). The second derivative method of gravity interpretation: Geophysics, V. XVI, Jan., no. 1:29-50.

Ells, G. D. (1964). Personal Communication.

Evans, C. S. (1950). Underground hunting in the Silurian of Ontario: Geol. Assoc. Canada Proc., V. 3, pp. 55-85.

Henderson, R. G. (1960). A comprehensive system of automatic computation in magnetic and gravity interpretation: Geophysics, Vol. 25, no. 3, p. 569-585.

Henderson, R. G., and Zietz, Isadore. (1949). The computation of the second vertical derivatives of geomagnetic fields: Geophysics, Vol. 14, p. 508-534.

Hinze, W. J. (1963). Regional gravity and magnetic maps of the Southern Peninsula of Michigan: Michigan Dept. of Conservation, Geological Survey Division, Report of Investigation 1.

Klasner, J. S. (1964). A study of buried bedrock valleys near South Haven, Michigan by the gravity method: Masters Thesis, Michigan State University.

Krumbein, W. C., and Graybill, F. A. (1965). An Introduction to Statistical Models in Geology: McGraw-Hill, New York.

Landes, K. K. (1945). The Salina and Bass Island rocks in the Michigan Basin: U. S. Geol. Surv. Oil and Gas Inv. Preliminary Map No. 40.

Landes, K. K. (1956). Petroleum Geology: John Wiley and Sons, Inc., New York, pp. 298-301.

Lowenstam, H. A. (1950). Niagaran reef of the Great Lakes area: Jour. Geology, Vol. 58, p. 430-487.

Lowenstam, H. A. (1957). Niagaran reefs in the Great Lakes area: Geol. Soc. Amer., Mem. 67, Treatise on marine ecology and paleoecology, V. 2, Paleoecology chapt. 10, p. 215-248.

Nettleton, L. L. (1940). Geophysical prospecting for oil: McGraw-Hill, New York.

Nettleton, L. L. (1954). Regional, residual, and structures: Geophysics, Vol. 19, p. 1-22.

Newcombe, R. B. (1920). Oil and gas development in Michigan: Mich. Geol. Survey Pub. 37, Series 31.

Peters, L. J. (1949). The direct approach to magnetic interpretation and its practical application: Geophysics, Vol. 14, No. 3, p. 290-319.

Pirtle, G. W. (1932). Michigan structural basin and its relationship to surrounding areas: Bull., A.A.P.G., Vol. 16, pp. 145-152.

Pohly, R. A. (1954). Gravity case history: Dawn No. 156 pool, Ontario: Geophysics, Vol. 19, p. 95-103.

Rosenbach, Otto. (1953). A contribution to the computation of the "second derivative" from gravity data: Geophysics, Vol. 18, No. 4, p. 894-912.

Roth, J. N. (1965). A gravitational investigation of fracture zones in Devonian rocks in portions of Arenac and Bay County, Michigan: Ms. Thesis, Michigan State University.

Serves, Gary Gordon. (1965). A gravitational investigation of Niagaran reefs in southeastern Michigan: Ph.D. Thesis, Michigan State University.

Talwani, M., Worzel, J., Lamar, and Landisman, M. (1959). Rapid gravity computations for two-dimensional bodies with application to the Mendocino submarine fracture zone: Jour. Geophys, Res., Vol. 64, p. 49-59.

Ver Wiebe, W. A. (1952). North American Petroleum: Edwards Brothers, Inc., Ann Arbor, Michigan pp. 58-72.

Yungul, S. H. (1961). Gravity prospecting for reefs: Effects of sedimentation and differential compaction: Geophysics, Vol. 26, No. 1, p. 45-56.

APPENDICES

APPENDIX A

FIELD METHODS

FIELD METHODS

Regional gravity coverage of the study area was obtained from interested parties. The regional coverage consists of gravity stations spaced 1/4 mile apart along the existing road network. It, therefore, was necessary only to add detailed station coverage in the near vicinity of the Columbus and Big Hand reefs. The detail coverage consists of cross-country traverses with a station spacing of 660 feet. These traverses were spaced at 1/4 mile intervals wherever it was possible.

Elevation control was obtained from U. S. Geological Survey and St. Clair County bench marks. The station elevations were established with a Zeiss self-leveling level and the distance between stations was determined by stadia interval.

The World Wide gravity meter number 45 was used to take the gravity readings. This meter has a calibration constant of 0.10093 mgal/div and a reading accuracy of 0.01 mgals.

The meter is subject to time variations. These time variations, which are called drift, are due to tidal variations, temperature changes, material fatigue and instrument handling. In order to correct for drift, it was necessary to take hourly readings at preestablished base stations. These base

stations were strategically positioned so that a minimum of time was required to reach them from all points in the survey area. If the meter drift was more than a 0.1 mgal/hr, the stations read during that hour were repeated. Each station was read until values were obtained which agreed within 0.2 of the scale division (0.02 mgal).

APPENDIX B

REDUCTION OF DATA

REDUCTION OF DATA

It is necessary to remove from the observed gravity readings those factors which are not directly related to geological conditions. This must be done for each gravity station. The value obtained after correcting for these factors is called the Bouguer gravity anomaly.

The Bouguer gravity anomaly was calculated according to the formula:

$$G_{BA} = g_o + g_{e+m} - g_\ell + g_t$$

where

G_{BA} = Bouguer gravity anomaly

g_o = observed gravity

g_{e+m} = elevation and mass correction

g_ℓ = latitude correction

g_t = terrain correction

Observed Gravity

The observed gravity values are obtained by multiplying the meter readings by the meter calibration constant and subtracting out the drift. The observed gravity values are then in milligals.

Elevation and Mass Correction

The elevation and mass correction is a combined correction involving the free-air correction and the mass correction. The free-air correction accounts for the change in the acceleration of gravity with elevation. The correction is made by first assuming an elevation datum which is common to all stations in the survey area. The difference between the station elevation and the elevation datum is multiplied by the factor 0.09406 mgals/ft. This gives the free-air correction. The elevation of the lowest station was taken to be datum. Therefore, the correction was always positive.

The material between the datum and the station obviously increases the acceleration of gravity. Therefore, a mass correction must be made to account for this increase. This is done by multiplying the difference in elevation between the datum and the station by the factor (0.01276 x material density).

Combining these two effects gives the elevation and mass correction formula:

$$g_{e+m} = (0.09406 - 0.01276\rho)h$$

where

h = elevation difference between the datum and the station

ρ = density of the material.

Servos (1965) determined that the density of the glacial in this area is 2.1 gm/cc. This is the value that was used in the elevation and mass correction.

Latitude Correction

The acceleration of gravity increases from the equator to the poles. This, of course, is due to the fact that the radius of the earth is less at the poles than at the equator and the centrifugal force decreases toward the poles. A correction is therefore necessary to account for this north-south variation in gravity.

The correction is made by first establishing a common latitude datum for the survey area and measuring the perpendicular distance from this datum to the station. This distance is then multiplied by the correction coefficient, K. The constant, K, according to Nettleton (1940) is:

$$K = 1.307 \sin 2\Phi \text{ mgals/mile}$$

where Φ is the mean latitude of the survey area. The mean latitude for this survey is 42° 52' 30". The constant, K, is therefore, equal to 0.0002474 mgal/ft.

Terrain Correction

The relief in the survey area is low enough that effects due to terrain were negligiable and therefore could be ignored. The survey stations were judiciously located, so that local elevation variations such as stream channels and ditches, did not affect the accuracy of the gravity readings.

Accuracy of Bouguer Reductions

Inaccuracies in Bouguer values result from four possible causes. These are (1) errors in observed readings, (2) errors in station elevations, (3) errors in distance measurements, and (4) errors in the density used in the mass correction.

Errors in observed readings are the results of meter drift and human error and can only be determined by repeating meter readings. A number of stations chosen at random were reread. The maximum variation in repeatability was 0.04 mgals.

The maximum allowable closure error in elevations was 0.1 of a foot per mile. The longest closed traverse loop was 4 miles. Therefore, the maximum allowable elevation error was 0.4 of a foot. But in actuality the closure error was never greater than 0.2 of a foot. This would cause an error in the combined elevation and mass corrections of 0.013 mgals, for a density of 2.1 gm/cc.

Errors in distance, of course, will cause errors in the latitude corrections, if the error is in the north-south direction. A maximum error of 50 feet was allowed in the field measurements. Another 50 feet of error was allowed in plotting the stations on the base map for a total error of 100 feet. For a latitude correction factor of 0.0002474 mgals per foot, this amounts to an error of .025 mgals.

Slight errors in the density used in the elevation and mass corrections can cause large inaccuracies in areas of

rugged topographic relief. This can be seen from the formula used in the calculation of this error. This formula is:

$$\text{Error} - 0.00128\rho h$$

where

0.00128 = magnitude of error in mgals per foot for each 0.1 gm/cc error in density

ρ = error in density in units of 0.1 gm/cc

h = maximum relief in feet

In this area the maximum relief between stations is only 10 feet. Assumming an error of 0.1 gm/cc was made in the density determination, this would lead to an error of 0.013 mgals.

Combining the effects of the errors in observed readings, station elevations, distance measurements and near surface density, would cause a maximum relative error between adjacent stations of $\pm$0.091 mgals in the Bouguer gravity. Assuming a normal distribution, the standard deviation is essentially 1/3 of the maximum error. Therefore, the standard deviation is $\pm$0.030 mgals.

APPENDIX C

ISOLATION TECHNIQUES

ISOLATION TECHNIQUES

The gravity method has been used as an exploration tool for a number of years. However, there has been a hesitancy to accept the method because of the ambiguity of the results. In recent years there has been a change in attitude toward the application and interpretation of the gravity method. This change has come about largely because the geophysicists who are now applying it have a better understanding of the geological significance of the method.

The digital computer has greatly increased the usefulness of the gravity method for it has made possible the application of interpretation techniques which prior to the advent of the computer required a tremendous amount of time.

In the following sections the theory and application of various interpretation techniques which are used in this study will be discussed.

Cross-Profile Method

One of the most common methods uded for the isolation of local anomalies is the grid method known as cross-profiling. The first step in using this method is to cover the area with a square network of profiles. The grid is positioned so that the profiles in one direction are parallel to the regional gravity trend. The profiles in

the other direction are at right angles to the regional trend. The Bouguer gravity values are plotted along these profiles. The regional gravity gradient is then estimated with a smooth curve. If the regional gradient has been estimated correctly, the points of intersection between the cross-profiles should have the same value. The regional gradient is adjusted until these intersection points agree. The final step is to subtract the regional gravity gradient from the Bouguer gravity values. This gives the residual gravity anomaly.

This method is subject to the personal bias of the interpreter. This can be an advantage if the interpreter has a good understanding of the regional geology. If he does not, it can lead to erroneous results.

Least Squares Method

The purpose of the least squares technique is to isolate residual gravity anomalies from the Bouguer gravity map.

A Bouguer gravity map describes a three-dimensional surface. The least squares method consists of approximating this three-dimensional surface with a polynomial equation. The polynomial equation is increased in degree until it roughly approximates the Bouguer surface. This rough approximation is considered to be the regional gravity trend. The residual gravity is then the difference between this approximation and the original Bouguer surface.

The degree of the polynomial, which is used to approximate the regional gravity trend, depends on the complexity of the Bouguer gravity and also depends on the personal bias of the interpretor.

The following Mathematical Treatment is taken from Krumbein and Graybill (1965).

The Bouguer value, G(x,y), at any point on a Bouguer map is a function of the x and y coordinates of that point. Thus, the Bouguer value at any point can be approximated methematically by a polynomial equation. The basic polynomial equation is:

(1) $$G(x,y)^* = \beta_{00} + \beta_{10} X + \beta_{01} Y + \ldots \beta_{pq} X^p Y^q$$

where $G(x,y)^*$ is the approximation of the Bouguer value $G(x,y)$, the p's and q's are the degree to which the term is raised and the β's are coefficients. This is the general equation for an nth degree polynomial. For instance, an equation of first degree would be:

$$G(x,y)^* = \beta_{00} + \beta_{10} X + \beta_{01} Y$$

a second degree equation would be:

$$G(x,y)^* = \beta_{00} + \beta_{10} X + \beta_{01} Y + \beta_{20} X^2 + \beta_{11} X Y + \beta_{02} Y^2$$

a third degree equation would be:

$$G(x,y)^* = \beta_{00} + \beta_{10} X + \beta_{01} Y + \beta_{20} X^2 + \beta_{11} XY + \beta_{02} Y^2 + \beta_{30} X^3 + \beta_{21} X^2Y + \beta_{12} XY^2 + \beta_{03} Y^3$$

and so on.

As was explained above, the approximation G(x,y)* is the value of the regional gravity trend at the point (x,y). It is, therefore, obvious that the regional gravity of any point on a Bouguer map can be obtained from the basic polynomial equation, simply by inserting the x and y coordinates of the point.

First, however, the values of the coefficients in the equation must be determined. One method used for determining these coefficients is the least squares method. According to the least squares method, the estimation of the coefficients will be such that the sum of the squares of the error is at a minimum. The error is the difference between the values obtained from the polynomial equation and the actual observed values.

The least squares method states that (D) must be a minimum where

$$(2) \qquad D = \sum_{1}^{n} e_i^2 = \sum_{i=1}^{n} (G_i(x,y) - G_i(x,y)^*)^2$$

$$= \sum_{i=1}^{n} (G_i(x,y) - \beta_0 - \sum_{j=1}^{K} \beta_j X_{ij})^2$$

n = number of observations and k = number of terms in the G(x,y)* equation.

The values of β_j which make (D) a minimum, are the least squares estimators of β_j. For (D) to be minimum, the partial derivative of (D) with respect to each β_i must be equal to zero. Thus,

$$\left(\frac{2D}{2\beta_0} = -2 \sum_{i=1}^{n} [G_i(x,y) - \beta_0 - \sum_{j=1}^{k} \beta_j X_{ij}] = 0\right.$$

$$\left(\frac{2D}{2\beta_1} = -2 \sum_{i=1}^{n} [G_i(x,y) - \beta_0 - \sum_{j=1}^{k} \beta_j X_{ij}] X_{i1} = 0\right.$$

$$\left(\frac{2D}{2\beta_2} = -2 \sum_{i=1}^{n} [G_i(x,y) - \beta_0 - \sum_{j=1}^{k} \beta_j X_{ij}] X_{i2} = 0\right. \quad (3)$$

$$\left(\frac{2D}{2\beta_k} = -2 \sum_{i=1}^{n} [G_i(x,y) - \beta_0 - \sum_{j=1}^{k} \beta_j X_{ij}] X_{ik} = 0\right.$$

Dividing by 2 and transposing the $G_i(x,y)$ terms, equations (3) become:

$$n\,\beta_0 + \beta_1 \sum_{i=1}^{n} X_{i1} + \beta_2 \sum_{i=1}^{n} X_{i2} + \ldots \beta_k \sum_{i=1}^{n} X_{ik} = \sum_{i=1}^{n} G_i(x,y)$$

$$\beta_0 \sum_{i=1}^{n} X_{i1} + \beta_1 \sum_{i=1}^{n} X_{i1}^2 + \beta_2 \sum_{i=1}^{n} X_{i1} X_{i2} + \ldots \beta_k \sum_{i=1}^{n} X_{i1} X_{ik} = \sum_{i=1}^{n} X_{i1} G_i(x,y)$$

$$\beta_0 \sum_{i=1}^{n} X_{i2} + \beta_1 \sum_{i=1}^{n} X_{i1} X_{i2} + \beta_2 \sum_{i=1}^{n} X_{i2}^2 + \ldots \beta_k \sum_{i=1}^{n} X_{i2} X_{ik} = \sum_{i=1}^{n} X_{i2} G_i(x,y)$$

$$\beta_0 \sum_{i=1}^{n} X_{ik} + \beta_1 \sum_{i=1}^{n} X_{ik} X_{i1} + \beta_2 \sum_{i=1}^{n} X_{ik} X_{i2} + \ldots \beta_k \sum_{i=1}^{n} X_{ik}^2 = \sum_{i=1}^{n} X_{ik} G_i(x,y)$$

These are the normal equations and they may be written in matrix form as follows:

$$\begin{bmatrix} n & \sum_{i=1}^{n} X_{i1} & \sum_{i=1}^{n} X_{i2} & \cdots & \sum_{i=1}^{n} X_{ik} \\ \sum_{i=1}^{n} X_{i1} & \sum_{i=1}^{n} X_{i1}^2 & \sum_{i=1}^{n} X_{i1} X_{i2} & \cdots & \sum_{i=1}^{n} X_{i1} X_{ik} \\ \sum_{i=1}^{n} X_{i2} & \sum_{i=1}^{n} X_{i2} X_{i1} & \sum_{i=1}^{n} X_{i2}^2 & \cdots & \sum_{i=1}^{n} X_{i2} X_{ik} \\ \sum_{i=1}^{n} X_{ik} & \sum_{i=1}^{n} X_{ik} X_{i1} & \sum_{i=1}^{n} X_{ik} X_2 & \cdots & \sum_{i=1}^{n} X_{ik}^2 \end{bmatrix} \begin{bmatrix} \beta o \\ \beta 1 \\ \beta 2 \\ \beta k \end{bmatrix} = \begin{bmatrix} \sum_{i=1}^{n} G_i(x,y) \\ \sum_{i=1}^{n} X_{i1} G_i(x,y) \\ \sum_{i=1}^{n} X_{i2} G_i(x,y) \\ \sum_{i=1}^{n} X_{ik} G_i(x,y) \end{bmatrix}$$

It is easily seen by carrying out the multiplication that this is indeed the matrix form of the normal equations.

If the previous matrixes are denoted as:

$$T = \begin{bmatrix} n & \sum_{i=1}^{n} X_{i1} & \sum_{i=1}^{n} X_{i2} & \sum_{i=1}^{n} X_{ik} \\ \sum_{i=1}^{n} X_{i1} & \sum_{i=1}^{n} X_{i1}^2 & \sum_{i=1}^{n} X_{i1}X_{i2} & \sum_{i=1}^{n} X_{i1}X_{ik} \\ \sum_{i=1}^{n} X_{i2} & \sum_{i=1}^{n} X_{i2}X_{i1} & \sum_{i=1}^{n} X_{i2}^2 & \sum_{i=1}^{n} X_{i2}X_{ik} \\ \sum_{i=1}^{n} X_{ik} & \sum_{i=1}^{n} X_{ik}X_{i1} & \sum_{i=1}^{n} X_{ik}X_{i2} & \sum_{i=1}^{n} X_{ik}^2 \end{bmatrix}$$

$$\beta = \begin{bmatrix} \beta o \\ \beta 1 \\ \beta 2 \\ \beta k \end{bmatrix} \qquad G = \begin{bmatrix} \sum_{i=1}^{n} G_i(x,y) \\ \sum_{i=1}^{n} X_{i1} G_i(x,y) \\ \sum_{i=1}^{n} X_{i2} G_i(x,y) \\ \sum_{i=1}^{n} X_{ik} G_i(x,y) \end{bmatrix}$$

then

$$T\beta = G \qquad\qquad \beta = T^{-1} G$$

where T^{-1} is the inverse of T.

This is demonstrated for the second degree polynomial equation:

$$G(x,y)^* = \beta_{00} + \beta_{10} X + \beta_{01} Y + \beta_{20} X^2 + \beta_{11} X Y + \beta_{02} Y^2$$

where

$\beta_{00} = \beta_0$; $\beta_{10} X = \beta_1 X_1$; $\beta_{01} Y = \beta_2 X2$; $\beta_{20} X^2 = \beta_3 X_3$; $\beta_{11} XY = \beta_4 X_4$ and $\beta_{02} Y^2 = \beta_5 X_5$

The normal equations for this 2nd degree equation are:

$$n\ \beta_{00} + \beta_{10} \sum_{i=1}^{n} X_i + \beta_{01} \sum_{i=1}^{n} Y_i + \beta_{20} \sum_{i=1}^{n} X_i^2 + \beta_{11} \sum_{i=1}^{n} X_i Y_i + \beta_{02} \sum_{i=1}^{n} Y_i^2 = \sum_{i=1}^{n} G_i(x,y)$$

$$\beta_{00} \sum_{i=1}^{n} X_i + \beta_{10} \sum_{i=1}^{n} X_i^2 + \beta_{01} \sum_{i=1}^{n} X_i Y_i + \beta_{20} \sum_{i=1}^{n} X_i^3 + \beta_{11} \sum_{i=1}^{n} X_i^2 Y_i + \beta_{02} \sum_{i=1}^{n} X_i Y_i^2 = \sum_{i=1}^{n} X_i G_i(x,y)$$

$$\beta_{00} \sum_{i=1}^{n} Y_i + \beta_{10} \sum_{i=1}^{n} X_i Y_i + \beta_{01} \sum_{i=1}^{n} Y_i^2 + \beta_{20} \sum_{i=1}^{n} X_i^2 Y_i + \beta_{11} \sum_{i=1}^{n} X_i Y_i^2 + \beta_{02} \sum_{i=1}^{n} Y_i^3 = \sum_{i=1}^{n} Y_i G_i(x,y)$$

$$\beta_{00} \sum_{i=1}^{n} Y_i^2 + \beta_{10} \sum_{i=1}^{n} X_i^3 + \beta_{01} \sum_{i=1}^{n} X_i^2 Y_i + \beta_{20} \sum_{i=1}^{n} X_i^4 + \beta_{11} \sum_{i=1}^{n} X_i^3 Y_i + \beta_{02} \sum_{i=1}^{n} X_i^2 Y_i^2 = \sum_{i=1}^{n} X_i^2 G_i(x,y)$$

$$\beta_{00} \sum_{i=1}^{n} X_i Y_i + \beta_{10} \sum_{i=1}^{n} X_i^2 Y_i + \beta_{01} \sum_{i=1}^{n} X_i Y_i^2 + \beta_{20} \sum_{i=1}^{n} X_i^3 Y_i$$

$$+ \beta_{11} \sum_{i=1}^{n} X_i^2 Y_i^2 + \beta_{02} \sum_{i=1}^{n} X_i Y_i^3 = \sum_{i=1}^{n} X_i Y_i G_i \ (x,y)$$

$$\beta_{00} \sum_{i=1}^{n} Y_i^2 + \beta_{10} \sum_{i=1}^{n} X_i Y_i^2 + \beta_{01} \sum_{i=1}^{n} Y_i^3 + \beta_{20} \sum_{i=1}^{n} X_i^2 Y_i^2$$

$$+\beta_{11} \sum_{i=1}^{n} X_i Y_i^3 + \beta_{02} \sum_{i=1}^{n} Y_i^4 = \sum_{i=1}^{n} Y_i^2 G_i \ (x,y)$$

The matrix form of the normal equations are shown on the following page.

The matrix for the system of linear (first degree) equations is those elements in the matrix for the second degree equation which are enclosed in the dashed lines. This is easily seen by setting up the matrix for the linear equations in the same manner in which the second degree was set up.

As a further example consider the data in Table 3.

When this data is substituted into the matrix for the system of linear equations, it becomes:

12.0	240.0	450.0	β_0	4.06
240.0	6300.0	9000.0	β_1	103.15
450.0	9000.0	21875.0	β_2	160.77

$$T\beta = G; \quad \beta = T^{-1} G$$

$$
\left[\begin{array}{c|ccc|ccc}
n & \sum_{i=1}^{n} X_i & \sum_{i=1}^{n} Y_i & \sum_{i=1}^{n} X_i^2 & \sum_{i=1}^{n} X_i Y_i & \sum_{i=1}^{n} Y_i^2 & \beta_{00} \\
\sum_{i=1}^{n} X_i & \sum_{i=1}^{n} X_i^2 & \sum_{i=1}^{n} X_i Y_i & \sum_{i=1}^{n} X_i^3 & \sum_{i=1}^{n} X_i^2 Y_i & \sum_{i=1}^{n} X_i Y_i^2 & \beta_{10} \\
\sum_{i=1}^{n} Y_i & \sum_{i=1}^{n} X_i Y_i & \sum_{i=1}^{n} Y_i^2 & \sum_{i=1}^{n} X_i^2 Y_i & \sum_{i=1}^{n} X_i Y_i^2 & \sum_{i=1}^{n} Y_i^3 & \beta_{01} \\
\hline
\sum_{i=1}^{n} X_i^2 & \sum_{i=1}^{n} X_i^3 & \sum_{i=1}^{n} X_i^2 Y_i & \sum_{i=1}^{n} X_i^4 & \sum_{i=1}^{n} X_i^3 Y_i & \sum_{i=1}^{n} X_i^2 Y_i^2 & \beta_{20} \\
\sum_{i=1}^{n} X_i Y_i & \sum_{i=1}^{n} X_i^2 Y_i & \sum_{i=1}^{n} X_i Y_i^2 & \sum_{i=1}^{n} X_i^3 Y_i & \sum_{i=1}^{n} X_i^2 Y_i^2 & \sum_{i=1}^{n} X_i Y_i^3 & \beta_{11} \\
\sum_{i=1}^{n} Y_i^2 & \sum_{i=1}^{n} X_i Y_i^2 & \sum_{i=1}^{n} Y_i^3 & \sum_{i=1}^{n} X_i^2 Y_i^2 & \sum_{i=1}^{n} X_i Y_i^3 & \sum_{i=1}^{n} Y_i^4 & \beta_{02}
\end{array}\right]
=
\left[\begin{array}{c}
\sum_{i=1}^{n} G_i(x,y) \\
\sum_{i=1}^{n} X_i G_i(x,y) \\
\sum_{i=1}^{n} Y_i G_i(x,y) \\
\hline
\sum_{i=1}^{n} X_i^2 G_i(x,y) \\
\sum_{i=1}^{n} X_i Y_i G_i(x,y) \\
\sum_{i=1}^{n} Y_i^2 G_i(x,y)
\end{array}\right]
$$

Table 3.--Gravity Data and Location Coordinates after Krumbein and Graybill.

Sample Number	X	Y	G(x,y)
1	5.0	12.5	.234
2	15.0	12.5	.205
3	25.0	12.5	.220
4	35.0	12.5	.510
5	5.0	37.5	.225
6	15.0	37.5	.212
7	25.0	37.5	.214
8	35.0	37.5	.730
9	5.0	62.5	.204
10	15.0	62.5	.202
11	25.0	62.5	.234
12	35.0	62.5	.870

$$\begin{bmatrix} \beta_0 \\ \beta_1 \\ \beta_2 \end{bmatrix} = \begin{bmatrix} 12.0 & 240.0 & 450.0 \\ 240.0 & 6300.0 & 9000.0 \\ 450.0 & 9000.0 & 21875.0 \end{bmatrix}^{-1} \begin{bmatrix} 4.06 \\ 103.15 \\ 160.77 \end{bmatrix}$$

The matrix T must first be inverted. One method of doing this is to divide each element of the matrix of cofactors by the determinant of the matrix and then transpose the results. For instance, the first element of the matrix of cofactors is 56,812,500. The determinant of T is 90,000,000. The first element of inverse matrix is 0.631250. Proceeding in a like manner, the remaining elements of the T^{-1} matrix are determined. The inverse matrix is then:

$$T^{-1} = \begin{bmatrix} 0.631250 & -0.013333 & -0.007500 \\ -0.013333 & 0.000667 & 0.00000 \\ -0.007500 & 0.00000 & 0.000200 \end{bmatrix}$$

The matrix of coefficients is then:

$$\begin{bmatrix} \beta_0 \\ \beta_1 \\ \beta_2 \end{bmatrix} = \begin{bmatrix} 0.631250 & -0.013333 & -0.007500 \\ -0.013333 & 0.000667 & 0.00000 \\ -0.007500 & 0.00000 & 0.000200 \end{bmatrix} \begin{bmatrix} 4.06 \\ 103.15 \\ 160.77 \end{bmatrix}$$

Multiplying the two matrixes on the right, the coefficient matrix becomes:

$$\begin{bmatrix} \beta_0 \\ \beta_1 \\ \beta_2 \end{bmatrix} = \begin{bmatrix} -0.0183 \\ 0.0146 \\ 0.0017 \end{bmatrix}$$

Substituting the coefficients into the polynomial equation, the predicting equation becomes:

$$G(x,y)^* = -0.0183 + 0.0146\ X + 0.0017\ Y$$

The approximation of the observed values is obtained by substituting the x and y coordinates into the predicting equation. For the data used in this example the results are as listed in Table 4.

The equations of higher degree are obtained in the same manner. The techniques for calculation of these mathematical operations have been programed for the digital computer.

Table 4.--Results Obtained from Least Squares Polynomial Equation after Krumbein and Graybill.

Sample Number	Observed Values-G(x,y)	Regional Values G(x,y)*	Residual G(x,y)-G(x,y)*
1	.2340	.0762	.1578
2	.2050	.2225	-.0175
3	.2200	.3689	-.1489
4	.5100	.5152	-.0052
5	.2250	.1188	.1062
6	.2120	.2652	-.0532
7	.2140	.4115	-.1975
8	.7300	.5578	.1722
9	.2040	.1615	.0425
10	.2020	.3078	-.1058
11	.2340	.4541	-.2201
12	.8700	.6005	.2695

Analytical Techniques

In gravity investigations, it is often desirable to know the gravitational field above or below the plane of observation (ground surface).

Many investigators have dealt with this problem including Evjen (1936), Peters (1949), Elkins (1951), Rosenbach (1953), Henderson (1960), and others. The basic problem is the same, but the manner in which it is approached has led to many different solutions.

Henderson's method was used in this study for the determination of upward and downward continuation and 2nd derivatives. This method will be outlined in the following paragraphs and an example worked out to demonstrate the use of the method.

The horizontal change in gravity on the plane of observation is represented as $\Delta\Phi(x,y,z)$, where x and y are the horizontal axes and z is the vertical axis which is positive vertically downwards. $\Delta\Phi(x,y,z)$ satisfies the Laplacian $\nabla^2[\Delta\Phi(x,y,z]=0$ and therefore, can be treated by the conventional potential theory methods.

The so-called "upward continuation integral" solves the problem of computing the gravational field above the plane of observation. The integral in polar coordinates is:

$$(1) \quad \Delta\Phi(-ma) = \int_0^\infty \frac{ma\ \Delta\bar{\Phi}\ (r)\ r\ dr}{(r^2 + m^2\ a^2)3/2}$$

$$m = 1,2,3, \ldots . n$$

where

$$\Delta\bar{\Phi} = 1/2\pi \int_0^{2\pi} \Delta\Phi\ (r,\ \theta)\ d\theta$$

is the average value of $\Delta\Phi\ (x,y,z)$ on circles of radius r about the point at which $\Delta\Phi\ (-ma)$ is to be determined. The term "a" is the distance between stations which course, must be in a square grid pattern. Using a mean value theorem over the interval $r_i \leq r \leq r_{i+1}$ for each interval, equation (1) can be approximated numerically. Equation (1) then becomes:

$$(2)\quad \Delta\Phi(-ma) \simeq \sum_{i=0}^{n-1} \left[(r_{i+1} - r_i)^{-1} \int_{r_i}^{r_{i+1}} \Delta\Phi(r)\, dr\right] ma \cdot$$

$$[r_i^2 + (ma)^2]^{-1/2} - [r_{i+1}^2 + (ma)^2]^{-1/2} + 0\ (1/rn)$$

(a) is set equal to 1 and equation (2) is successively evaluated for m = 1, 2, . . . 5. In otherwords, the gravitational field is determined for a distance a, 2a, 3a, 4a, and 5a above the observation plane. The 5 sets of coefficients are thus obtained for the upward continuation formula. These coefficients are shown in Table 5. The working equation then is:

$$(3)\quad \Delta\Phi(-m) \simeq \Sigma\ \Delta\Phi(r_i)\ K\ (r_i, m)$$

where $K\ (r_i, m)$ are the upward continuation coefficients.

Let P(x,y,0) be the point at which the upward continued values of gravity have been determined. According to equation (3), these values are at distinct points. They are at a distance of a, 2a, 3a, 4a, and 5a above P(x,y, 0). A polynomial can then be fitted to these points. Henderson uses the Lagrangian interpolation method for determining this polynomial. This polynomial is:

$$(4)\quad \Delta\Phi(Z) \simeq \Sigma\ \frac{(-1)^m\ Z(Z+a)\ (Z + 2a)\ .\ .\ .\ .\ (Z + na)}{a^n\ (Z + ma)\ (n-m)\ !\ m!}(\Delta\Phi(-ma))$$

where $\Delta\Phi(-ma)$ is equation (3). Now, to determine the gravitational field below the surface the polynomial is simply extrapolated into this region. The working formula for downward continuation is obtained by substituting equation (3)

Table 5.--Upward Continuation Coefficients after Henderson.

i	$\Delta\bar{\Phi}(r_i)$	$K(r_i,1)$	$K(r_i,2)$	$K(r_i,3)$	$K(r_i4)$	$K(r_i,5)$
0	$\Delta\bar{\Phi}(0)$	0.11193	0.04034	0.01961	0.01141	0.00742
1	$\Delta\bar{\Phi}(1)$	0.32193	0.12988	0.06592	0.03908	0.02566
2	$\Delta\bar{\Phi}(\sqrt{2})$	0.06062	0.07588	0.05260	0.03566	0.02509
3	$\Delta\bar{\Phi}(\sqrt{5})$	0.15206	0.14559	0.10563	0.07450	0.05377
4	$\Delta\bar{\Phi}(\sqrt{8})$	0.05335	0.07651	0.07146	0.05841	0.04611
5	$\Delta\bar{\Phi}(\sqrt{13})$	0.06586	0.09902	0.10226	0.09173	0.07784
6	$\Delta\bar{\Phi}(\sqrt{25})$	0.06650	0.11100	0.12921	0.12915	0.11986
7	$\Delta\bar{\Phi}(\sqrt{50})$	0.05635	0.10351	0.13635	0.15474	0.16159
8	$\Delta\bar{\Phi}(\sqrt{136})$	0.03855	0.07379	0.10322	0.12565	0.14106
9	$\Delta\bar{\Phi}(\sqrt{274})$	0.02273	0.04464	0.06500	0.08323	0.09897
10	$\Delta\bar{\Phi}(\sqrt{625})$	0.03015	0.05998	0.08917	0.11744	0.14458

$$\Delta\Phi(-m) \simeq \sum_{i=0}^{10} \Delta\bar{\Phi}\ (r_i)\ K\ (r_i,\ m).$$

into equation (4) and successively setting Z = a, 2a, 3a, 4a, and 5a. After some algebraic manipulating the equation becomes:

$$(5)\quad \Delta\Phi\ (k) \simeq \sum_{i=0}^{10} \Delta\Phi\ (r_i)\ D\ (r_i,k)$$

where $D(r_i,k)$ are the downward continuation coefficients. They are given in Table 6.

The second derivative formula can be obtained by taking the second derivative of equation (4). First equation (4) must be put in equivalent determinant form:

Table 6.--Downward Continuation Coefficients after Henderson.

i	$\Delta\bar{\Phi}(r_i)$	$D(r_i,1)$	$D(r_i,2)$	$D(r_i,3)$	$D(r_i,4)$	$D(r_i,5)$
0	$\Delta\bar{\Phi}(0)$	4.8948	16.1087	41.7731	92.5362	183.2600
1	$\Delta\bar{\Phi}(1)$	-3.0113	-13.2209	-38.2716	-89.7403	-183.9380
2	$\Delta\bar{\Phi}(\sqrt{2})$	0.0081	0.4027	1.7883	5.1388	11.8804
3	$\Delta\bar{\Phi}(\sqrt{5})$	-0.5604	- 1.9459	- 4.7820	- 9.9452	- 18.6049
4	$\Delta\bar{\Phi}(\sqrt{8})$	-0.0376	0.0644	0.5367	1.7478	4.2324
5	$\Delta\bar{\Phi}(\sqrt{13})$	-0.0689	- 0.0596	0.1798	0.8908	4.4237
6	$\Delta\bar{\Phi}(\sqrt{25})$	-0.0605	- 0.0522	0.1342	0.6656	1.7777
7	$\Delta\bar{\Phi}(\sqrt{50})$	-0.0534	- 0.0828	- 0.0560	0.0718	0.3606
8	$\Delta\bar{\Phi}(\sqrt{136})$	-0.0380	- 0.0703	- 0.0900	- 0.0890	- 0.0571
9	$\Delta\bar{\Phi}(\sqrt{274})$	-0.0227	- 0.0443	- 0.0639	- 0.0802	- 0.0921
10	$\Delta\bar{\Phi}(\sqrt{625})$	-0.0302	- 0.0600	- 0.0891	- 0.1173	- 0.1444

$$\Delta\Phi(k) \approx \sum_{i=0}^{10} \Delta\bar{\Phi}(r_i) D(r_i, k)$$

$$(4a)\quad \Delta\Phi(Z) \simeq -|V|^{-1} \begin{vmatrix} 0 & 1 & -Z/a & (Z/a)^2 & \cdots & (-Z/a)^n \\ \Delta\Phi(0) & 1 & 0 & 0 & \cdots & 0 \\ \Delta\Phi(-a) & 1 & 1 & 1 & \cdots & 1 \\ \Delta\Phi(-2a) & 1 & 2 & 2^2 & \cdots & 2^n \\ \vdots & \vdots & \vdots & \vdots & & \\ \Delta\Phi(-na) & 1 & n^2 & n^2 & \cdots & n^n \end{vmatrix}$$

where $|V|$ is the Vandermonde determinant. It is obtained be deleting the first two rows and columns of (4a).

Putting n=5 in (4a) and differentiating once with respect to z, the first derivative is obtained.

$$(6)\quad \frac{\delta\Delta\Phi(Z)}{\delta Z} \simeq -(a|V|)^{-1} \begin{vmatrix} 0 & 0 & -1 & 2(Z/a) & -3(Z/a)^2 & 4(Z/a)^3 & -5(Z/a)^4 \\ \Delta\Phi(0) & 1 & 0 & 0 & 0 & 0 & 0 \\ \Delta\Phi(-a) & 1 & 1 & 1 & 1 & 1 & 1 \\ \Delta\Phi(-2a) & 1 & 2 & 2^2 & 2^3 & 2^4 & 2^5 \\ \Delta\Phi(-3a) & 1 & 3 & 3^2 & 3^3 & 3^4 & 3^5 \\ \Delta\Phi(-4a) & 1 & 4 & 4^2 & 4^3 & 4^4 & 4^5 \\ \Delta\Phi(-5a) & 1 & 5 & 5^2 & 5^3 & 5^4 & 5^5 \end{vmatrix}$$

Then, taking the derivative again with respect to z, the second derivative is obtained:

$$(7)\quad \frac{\delta^2\Delta\Phi(Z)}{\delta Z^2} \simeq (a^2|V|)^{-1} \begin{vmatrix} 0 & 0 & 0 & 2 & -6(Z/a) & 12(Z/a)^2 & -20(Z/a)^3 \\ \Delta\Phi(0) & 1 & 0 & 0 & 0 & 0 & 0 \\ \Delta\Phi(-a) & 1 & 1 & 1 & 1 & 1 & 1 \\ \Delta\Phi(-2a) & 1 & 2 & 2^2 & 2^3 & 2^4 & 2^5 \\ \Delta\Phi(-3a) & 1 & 3 & 3^2 & 3^3 & 3^4 & 3^5 \\ \Delta\Phi(-4a) & 1 & 4 & 4^2 & 4^3 & 4^4 & 4^5 \\ \Delta\Phi(-5a) & 1 & 5 & 5^2 & 5^3 & 5^4 & 5^5 \end{vmatrix}$$

Putting z=a and substituting (3) into (6), the working equation for second derivatives is obtained:

$$\left[\frac{\delta^2(\Delta\Phi)}{\delta Z^2}\right]_{z=k} \simeq \sum_{i=0}^{10} \Delta\Phi\,(r_i)\; D''(r_i, k)$$

where $D''(r_i,k)$ are the second derivative coefficients. The coefficients are given in Table 7.

Table 7.--Second Derivative Coefficients after Henderson.

i	$\Delta\bar{\Phi}(r_i)$	$D''(r_i,0)$	$D''(r_i,1)$	$D''(r_i,2)$	$D''(r_i,3)$
0	$\Delta\bar{\Phi}(0)$	2.82994	7.08408	14.15751	24.74755
1	$\Delta\bar{\Phi}(1)$	-2.49489	-6.93715	-14.51327	-26.02351
2	$\Delta\bar{\Phi}(\sqrt{2})$	0.05173	0.36265	0.96018	1.92719
3	$\Delta\bar{\Phi}(\sqrt{5})$	-0.39446	-0.80764	- 1.42970	- 2.30269
4	$\Delta\bar{\Phi}(\sqrt{8})$	0.00932	0.13050	0.35907	0.72474
5	$\Delta\bar{\Phi}(\sqrt{13})$	-0.00732	0.07231	0.22256	0.46253
6	$\Delta\bar{\Phi}(\sqrt{25})$	0.00304	0.06502	0.17330	0.33920
7	$\Delta\bar{\Phi}(\sqrt{50})$	0.00219	0.02312	0.05501	0.09985
8	$\Delta\bar{\Phi}(\sqrt{136})$	0.00040	0.00565	0.01239	0.02070
9	$\Delta\bar{\Phi}(\sqrt{274})$	0.00004	0.00103	0.00210	0.00322
10	$\Delta\bar{\Phi}(\sqrt{625})$	0.00000	0.00043	0.00085	0.00122

A simple example will be done here to demonstrate the use of the upward continuation equation (3), the downward continuation equation (5), and the second derivative equation (8). Figure 35 is a portion of a gravity map with the stations in the necessary square grid pattern. In practice, it is usually impossible to obtain field stations in such a pattern. So, it is necessary to interpolate between the actual stations to procure a grid pattern. In this example, the distance between stations is 500 feet. A template of circles is placed over the point at which it is desired to obtain upward continuation, downward continuation, and second derivative values. Henderson

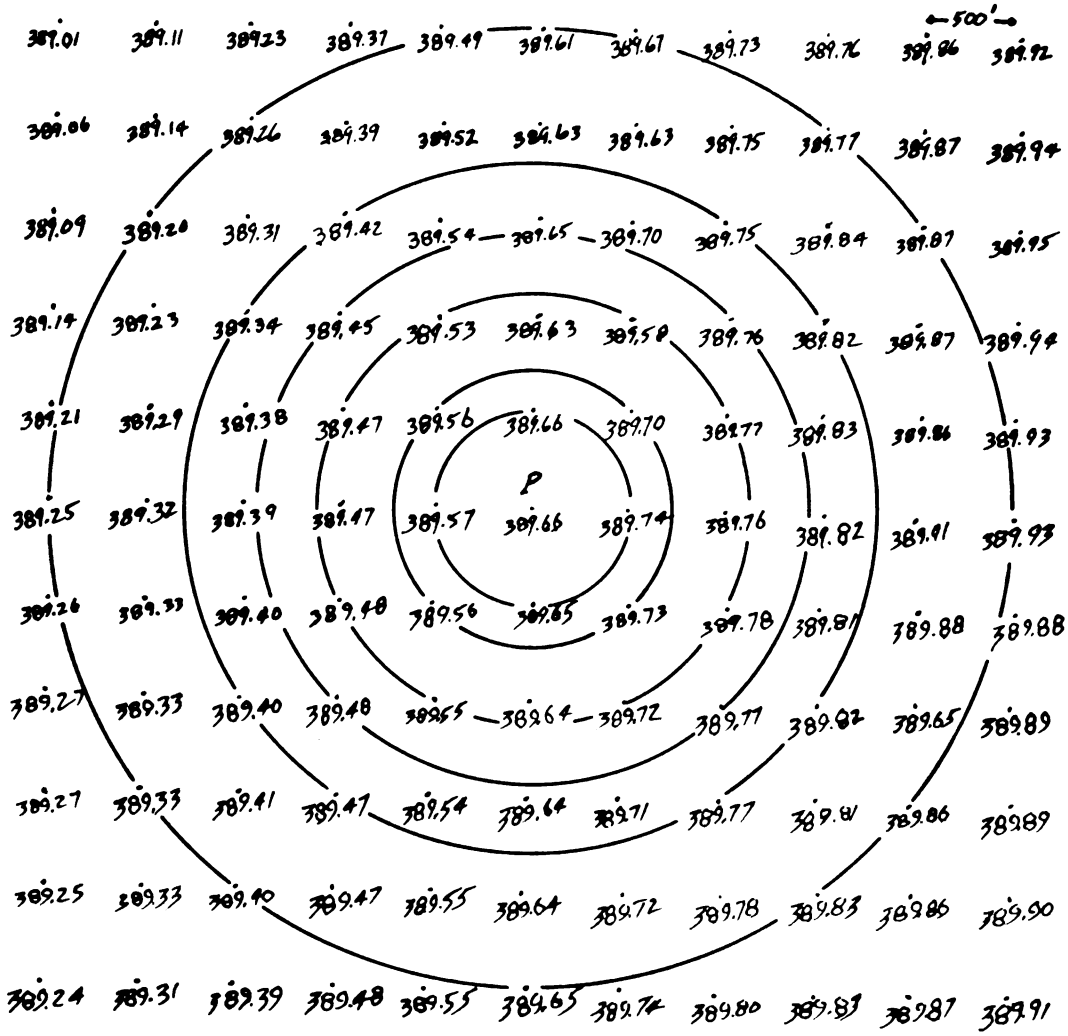

PORTION OF GRAVITY MAP
AND SIX RING TEMPLATE

FIGURE 35

has found that ten circles with radii or r=a, $a\sqrt{2}$, $a\sqrt{5}$, $a\sqrt{8}$, $a\sqrt{13}$, a5, $a\sqrt{50}$, $a\sqrt{136}$, $a\sqrt{274}$, and a 25, adequately sample the field. This is why there are 11 rows of coefficients in the tables of coefficients--one for each ring and one for the center point. It can be seen from Figure 35, where the ring template has been placed over the point P, that the number of grid points falling on the circles having the above radii, are respectively 1,4,4,8,4,8,12,12,8,8,12.

The average value of the points falling on the first 5 rings was determined and the average value was then multiplied by the appropriate coefficients. Thus, the upward continuation, downward continuation, and second derivative values were calculated for the point P. The calculations are shown in Table 8. The calculations involving the remaining 5 rings are carried out in the same manner.

Table 8.--Example of Upward and Downward Continuation and Second Derivative Calculations.

Center	1st	2nd	3rd	4th	5th
389.66	389.65	389.73	389.72	389.77	389.77
	389.74	389.70	389.78	389.76	389.82
	389.66	389.56	389.77	389.45	389.82
	389.57	389.56	389.58	389.48	389.75
			389.53		389.42
			389.47		389.34
			389.48		389.40
			389.55		389.47
389.66	1558.62	1558.55	3116.88	1558.46	3116.79
			Average Values		
389.66	389.66	389.64	389.61	389.62	389.60

1 unit or 500 ft. above original surface

389.66 (.11193) + 389.66 (.32193) + 389.64 (.0602) + 389.61 (.15206) + 389.62 (.05335) + 389.60 (.06588) =

43.61 + 125.44 + 23.62 + 59.24 + 20.79 + 25.66 = **298.36**

1 unit or 500 ft. below original surface

389.66 (4.8948) - 389.66 (-3.0113) + 389.64 (.0081) - 389.61 (.5604) - 389.62 (.0376) - 389.60 (.0689) =

1907.31 - 1173.38 + 3.16 - 218.34 - 14.65 - 26.84 = **477.26**

2500 ft. above original surface

2.89 + 10.00 + 9.78 + 20.95 + 17.96 + 30.33 + 46.70 = **138.61**

second on original surface

389.66 (2.82994) - 389.66 (2.49489) + 389.64 (.05173) -389.61 (+.39446) + 389.62 (.00932) - 389.60 (.00732) =

1102.71 - 972.16 + 20.16 - 153.69 + 3.63 - 2.85 = **2.20**